Distribution Agreement

In presenting this thesis or dissertation as a partial fulfillment of the requirements for an advanced degree from Emory University, I hereby grant to Emory University and its agents the non-exclusive license to archive, make accessible, and display my thesis or dissertation in whole or in part in all forms of media, now or hereafter known, including display on the world wide web. I understand that I may select some access restrictions as part of the online submission of this thesis or dissertation. I retain all ownership rights to the copyright of the thesis or dissertation. I also retain the right to use in future works (such as articles or books) all or part of this thesis or dissertation.

Signature:

_____ _____

Nicole E. Bowen Date

Sink or Swim:
Mechanisms of dNTP Pool Elevation by Lentiviruses and Cancer

By

Nicole E. Bowen
Doctor of Philosophy

Graduate Division of Biological and Biomedical Science
Microbiology and Molecular Genetics

_____
Baek Kim, Ph.D.
Advisor

_____
Bernardo Mainou, Ph.D.
Committee Member

_____
Gregory Melikian, Ph.D.
Committee Member

_____
Stefan Sarafianos, Ph.D.
Committee Member

_____
David Yu, Ph.D.
Committee Member

Accepted:

_____
Kimberly Jacob Arriola, Ph.D., MPH
Dean of the James T. Laney School of Graduate Studies

_____
Date

Sink or Swim:
Mechanisms of dNTP Pool Elevation by Lentiviruses and Cancer

By

Nicole E. Bowen
B.S., Boston College, 2018

Advisor: Baek Kim, Ph.D.

An abstract of
A dissertation submitted to the Faculty of the
James T. Laney School of Graduate Studies of Emory University
in partial fulfillment of the requirements for the degree of
Doctor of Philosophy
in Graduate Division of Biological and Biomedical Science
Microbiology and Molecular Genetics
2023

Abstract

Sink or Swim:
Mechanisms of dNTP Pool Elevation by Lentiviruses and Cancer

By Nicole E. Bowen

The sole utility of deoxynucleoside triphosphates (dNTPs) is to serve as substrates for DNA polymerase during DNA synthesis. Correspondingly, dNTP concentrations elevate at the G1/S phase transition to accommodate novel DNA synthesis. In contrast, non-dividing quiescent cells that lack chromosomal replication harbor consistently low dNTP pools. Appropriate intracellular dNTP levels are maintained by a delicate balance of *de* novo and salvage biosynthetic pathways and hydrolysis by dNTPase, SAMHD1. Importantly, the regulation of these pathways is tied closely to the cell cycle. Proper maintenance of dNTP levels is essential to the health of a host as abnormal dNTP levels can contribute to decreased polymerase fidelity and mutation synthesis. Lentiviruses infecting non-diving cells and fast-replicating cancer cells are faced with the barrier of insufficient dNTP pools for copying their genomes. To address this, lentiviruses such as HIV-2 and some SIVs code for Viral protein X (Vpx), which targets host SAMHD1 for proteasomal degradation and elevates intracellular dNTP levels. Similarly, cancer cells elevate dNTP levels 6-11-fold and this alteration in metabolism has been suggested as a hallmark of cancer. Therefore, SAMHD1 counteracting lentiviruses and cancer cells both elevate intracellular dNTP pools during the course of their pathogenesis. In this work, I first explore necessary determinants for Vpx-mediated dNTP elevation in non-diving cells. Here, I uncover active dNTP biosynthesis in primary non-dividing macrophages. I then find that Vpx-mediated dNTP elevation and rescue of infection in non-dividing cells after SAMHD1 depletion is dependent on this ongoing dNTP biosynthesis. In subsequent work, I identify cancer associated SAMHD1 mutants that have similar expression and stability profiles to wild type. I then used these mutants as tools to probe which functions of SAMHD1 may contribute to cancer phenotypes. Here, I find only dNTPase activity has been altered by these mutations, suggesting cancer-associated mutations in SAMHD1 can contribute to the elevated dNTP level characteristic of cancer cells. Together, this work provides mechanistic insights into the shared phenomenon of dNTP elevation during viral infection and oncogenesis.

Sink or Swim:
Mechanisms of dNTP Pool Elevation by Lentiviruses and Cancer

By

Nicole E. Bowen
B.S., Boston College, 2018

Advisor: Baek Kim, Ph.D.

A dissertation submitted to the Faculty of the
James T. Laney School of Graduate Studies of Emory University
in partial fulfillment of the requirements for the degree of
Doctor of Philosophy
in Graduate Division of Biological and Biomedical Science
Microbiology and Molecular Genetics
2023

Acknowledgements

This body of work would not exist without the support of many people, and I am immensely grateful to everyone who has contributed to this achievement. I wish to thank the Microbiology and Molecular Genetics community for creating a welcoming and collegial environment for junior scientists. I would also like to thank my esteemed committee members: Drs. Stefan Sarafianos, Gregory Melikian, Bernardo Mainou, and David Yu for their expertise and perspectives. Their guidance has helped me to think beyond my individual lab bench and has greatly contributed to my scientific growth.

I am so grateful that my career crossed paths with Dr. Baek Kim, who has been an incredible mentor and advisor. Baek has pushed me to become a better scientist, but he accomplished this with an unparalleled amount of humor and patience. Truly, he has a rare gift for knowing when to poke fun at me for a lab mishap or when I'm on the verge of tears and need to be left alone. I can't imagine most people laugh even half as much with their supervisors, but it is Baek's lighthearted nature that made failed experiments seem less like the end of the world. My favorite quality of Baek is that he is a storyteller first and a scientist second. Correspondingly, the most important lesson I have learned from Baek during my graduate work is that science is all about the story you tell and how to use data effectively. Baek, thank you for helping shape this part of my story and for giving me the tools I need to write my next one.

The Kim Lab has experienced its fair share of turnover during my graduate work, but one thing remains true: it is made up of many talented scientists who are even better people. A large part of my technical training was accomplished because of the generosity of this team. They are always teaching me something, whether it's the concentration of primer to use in an assay or the cheapest place in Atlanta to get tires. It is their comradery and friendship that make coming in everyday worth it. Lindsey, Natalie, Tzipi, Adrian, Young, Michael, Bijan, Si'Ana, Jess, Joella, T, and Caitlin, I would not be where I stand today without your support.

I am so thankful for my friends, both new and old. I have befriended a group of brilliant women in my program who just "get it" and are there to complain about the lows and celebrate the highs of graduate school. I am particularly grateful for my roommate of five years, my best friend, my biggest cheerleader, and fellow graduate student, Elizabeth Heaton. I am so lucky to have someone like her to walk this path with and I am both a better scientist and better person because of this wonderful friendship. Finally, I am so appreciative of my friends from home and from college who cheered me on from afar and reminded me that I amount to more than just a graduate student. To my dearest friends, each and every one of you has helped me stay afloat during this journey.

During the chaos of my graduate work, I met someone who felt like the calm in a storm. I can't imagine dating a graduate student is ever easy, especially in the last two years where some of the magic of science has rubbed off. He has given me the beautiful gift of a soft place to fall apart and the encouragement to get on planes (figuratively and literally) I would not otherwise have gotten on. Simply put, his belief in me has carried me on the days I have not believed in myself. Joshua Allen, I would not have crossed this finish line without you.

I would like to thank my family but simultaneously feel I will never have the words to thank them enough for their unconditional love. Thank you to my parents, Martin and Kerry Bowen, who made sacrifices throughout their lives to ensure that their children would have opportunities they did not. Thank you to my siblings, Joyce and Daniel Bowen, for their humor and for pulling me out of my own head when I need a break. Lastly, this thesis is dedicated to my nana, Eileen Nicholson. She has taught me the strength in meeting challenges with kindness and has always believed in the best in me. Without her teaching me how to count using playing cards decades ago, I imagine much of the work in this dissertation would have been impossible. To my wonderful family, I love you and you are the reason I can shine so brightly today.

Table of Contents

List of Figures and Tables

Chapter 1

Introduction

Nicole E. Bowen[1]*, Adrian Oo[1]*, Baek Kim[1,2].

Published in part as: *Interplay between HIV-1 Reverse Transcriptase Enzyme Kinetics and Host SAMHD1 Protein: Viral Myeloid-Cell Tropism and Genomic Mutagenesis.* Viruses. 2022;14(8). Epub 20220726. doi: 10.3390/v14081622. PubMed PMID: 35893688; PMCID: PMC9331428.

[1]Department of Pediatrics, School of Medicine, Emory University, Atlanta, GA 30329, USA.

[2]Center for Drug Discovery, Children's Healthcare of Atlanta, Atlanta, GA 30329, USA.

*These authors contributed equally to this work.

1.1 Intracellular dNTP pool maintenance.

Deoxynucleoside triphosphates (dNTPs) consist of a deoxyribose sugar bound to a triphosphate group at the 5′-hydroxyl and a nitrogenous base at the 1'-carbon[1, 2]. There are four canonical variations of nitrogenous bases making the canonical dNTPs deoxyadenosine triphosphate (dATP), deoxythymidine triphosphate (dTTP), deoxycytidine triphosphate (dCTP), and deoxyguanosine triphosphate (dGTP)[1, 2]. The sole utility of intracellular dNTPs is to serve as substrates for DNA polymerase during DNA synthesis[2]. As such, dNTP concentrations elevate at the G1/S phase transition to accommodate the DNA synthesis characteristic of S phase[3, 4]. In contrast, non-dividing quiescent cells harbor consistently low dNTP pools[4, 5]. In both situations, dNTP levels are maintained by a delicate balance of biosynthetic and degradation pathways, the regulation of which is tied closely to phases of the cell cycle.

There are two distinct pathways that synthesize dNTPs, the de novo synthesis pathway and the salvage pathway. The *de novo* synthesis pathway generates dNTPs from nucleoside diphosphates (NDPs) whereas the salvage pathway repurposes deoxyribonucleosides (dNs) from sources such as DNA degradation of apoptotic cells into dNTPs[6, 7]. A key enzyme in the *de novo* synthesis pathway is ribonucleotide reductase (RNR), which catalyzes the rate limiting step of reducing the 2' hydroxyl group on the sugar moiety of nucleoside diphosphate (NDP) substrates[8]. RNR consists of a heterodimeric tetramer of two distinct subunits, RNR M1 and RNR M2[9]. M1, the large subunit, binds the substrate and contains allosteric regulation sites[10, 11]. M2 generates a tyrosyl radical that is transferred to M1 and used in the reduction of NDP substrate[10, 11]. The activity of this enzyme is highly regulated by allosteric activation [12], cell cycle dependent expression [13-15], subcellular localization[16], and by DNA damage checkpoints [17]. This pathway is also dependent on nucleotide

diphosphate kinase (NDPK), which phosphorylates the resulting dNDP to form the final dNTP product. The salvage pathway is primarily composed of kinases, such as thymidine kinase 1 (TK1), that can mediate the transfer of phosphates to the dN substrate to generate dNTPs. Notably, several enzymes involved in dNTP biosynthesis are upregulated during S phase to accommodate the dNTP needs of DNA synthesis[13, 18].

Working in opposition to these dNTP synthesis pathways is sterile alpha motif and histidine-aspartate domain containing protein 1 (SAMHD1)[19]. SAMHD1 is a triphosphohydrolase that catalyzes the hydrolysis of cellular dNTPs into their dN and triphosphate components[20]. Notably, the enzymatic activity of SAMHD1 establishes low dNTP pools in non-dividing cells such as macrophages[21-23]. SAMHD1 has 626 residues is composed of three structural domains (1) an N-terminal nuclear localization tag (^{11}KRPR^{14})[24-26] followed by a SAM domain[27], (2) an HD domain that houses the conserved histidine- aspartate residues that are critical for phosphohydrolase activity[27, 28], and (3) a C-terminal regulatory domain containing the T592 residue and two cyclin-binding motifs (^{451}RXL^{453} and ^{620}LF^{621}) which are critical for regulation by the cell cycle[29-31]. SAMHD1 expression is consistent throughout the cell cycle making post-translational modifications a critical regulator of the enzyme's function[32].

1.2 Retroviruses.

The *Retroviridae* family are enveloped viruses with two copies of a positive-sense, single-stranded RNA genome[33]. A defining characteristic of retroviruses is the reverse transcriptase (RT) enzyme, which catalyzes the synthesis of DNA from the viral RNA genome[34, 35]. This generates a DNA intermediate during the viral life cycle that will integrate into the host genome[33]. From here, the integrated provirus relies on host DNA-dependent RNA polymerase II and translation

machinery to produce the next generation of viruses[33]. Lentiviruses are a genus of the Retroviral family known for their long incubation periods. Human immunodeficiency virus 1 (HIV-1), the causative agent of acquired immunodeficiency syndrome, belongs to the lentivirus genus[36, 37]. Other viruses in the lentivirus genus include HIV-2, which makes up a very small portion of the HIV epidemic[38], and SIVs, which are closely related to HIVs and infect a variety of monkey species[39]. Lentiviruses are unique among the retrovirus family as they can infect both dividing (activated $CD4^+$ T-cells) and non-dividing cell types (terminally differentiated macrophages and resting $CD4^+$ T-cells)[40].

1.3 Regulation of cellular dNTP pools is a major determinant of HIV-1 replication kinetics in target cells.

Retroviruses must utilize intracellular dNTPs in order for reverse transcriptase to generate proviral DNA from their RNA genome in infected cells. Dividing cells regularly synthesize new DNA during mitotic S phase and therefore need more abundant dNTP concentrations. In fact, dNTP concentrations are ~200 times higher in activated $CD4^+$ T cells (1–16 μM) than in macrophages (20–40 nM)[5, 41]. This dNTP concentration disparity is attributed to the high activity of host SAMHD1 in non-dividing macrophages.[22] The concentration of dNTPs in macrophages is below the K_m of RT, resulting in slowed replication kinetics and restriction by SAMHD1[42]. For this reason, viral DNA synthesis during infection of activated T-cells occurs in 12-16 hours whereas it takes up to 36 hours during macrophage infection [43]. This kinetic difference results in robust HIV-1 replication and rapid cell death of infected activated $CD4^+$ T-cells while infected myeloid cells are long-lived and persistently produce low levels of the virus[44-47]. Accordingly, after $CD4^+$ T cell depletion *in vivo* the infection is sustained by long-lived infected macrophages

marking them as an important component of the HIV-1 reservoir[45, 48]. Thus, differences in viral replication kinetics established by SAMHD1 and differential dNTP pools has a clear impact on the generation and maintenance of HIV-1 infection and reservoir.

1.4 Regulation of SAMHD1.

SAMHD1 has several layers of post-translational modifications that regulate it's dNTPase activity. First, SAMHD1 undergoes allosteric activation to form the enzymatically active tetramer[49, 50]. Each monomer contains a catalytic site and two allosteric sites, A1 and A2[51]. For activation, allosteric site 1 (A1) binds either dGTP or GTP to form the inactive dimer[52, 53]. As GTP is more abundant in the low dNTP pool environment of macrophages, GTP serves as the primary activator *in vivo*[54]. The A2 site can accommodate any dNTP, however the larger purine bases create more stable base-stacking interactions within the pocket and are therefore preferred in the order of dATP>dGTP>dTTP>dCTP[55]. Occupation of dNTPs in the A2 sites will stabilize the dimerization of dimers to form the tetramer structure[52]. In the active state, a Mg^{2+}ion bridges the phosphate groups of the dGTP/GTP of A1 and the dNTP of A2[52, 56]. Interestingly, it has been suggested that the stable tetramer can be maintained long after dNTP pools have been reduced to a level that would lead to inactivation (~10 μM)[57-59]. This property is likely essential for SAMHD1 activity in the low dNTP pool environment of non-dividing cells[5].

The catalytic site is able to accommodate any dNTP, as there is no specific interaction between the residues in the catalytic pocket and the base of the dNTP[51]. Instead, this interaction is mediated by a water network[51]. One implication of this promiscuity of the catalytic pocket is that SAMHD can hydrolyze dNTP analogues such as ddNTPs, base modified dNTPs, and cytarabine

(ara-C)[54, 60-62]. However, SAMHD1 cannot accommodate the 2' hydroxyl group of rNTPs[54] or significantly hydrolyze nucleoside reverse transcriptase inhibitors (NRTIs)[63, 64]. Recently, it has been proposed that the catalytic site of SAMHD1 contains a bi-metallic Fe–Mg center[65], similar to the HD domains of other proteins[66-68]. In their structural analysis, these two metals are bridged by a water molecule, which dissociates to form a hydroxide ion and performs an in-line nucleophilic attack on the alpha phosphate group of the substrate dNTP (P^{α}) [65].

The most extensively studied SAMHD1 post-translational modification is the cyclin dependent kinase 1/ cyclin dependent kinase 2 (CDK1/CDK2) and cyclinA2 mediated phosphorylation of residue T592[29, 30, 69, 70]. This interaction is mediated by the two cyclin binding domains of SAMHD1[30, 31] and corresponds with an increase in dNTPs before S phase[31, 71]. In non-dividing macrophages, this phosphorylation event is regulated by Raf-MEK-ERK pathway activity, which includes the Raf serine/threonine kinase, the MAPK/ERK kinase (MEK), and the extracellular signal-regulated kinase (ERK) [72]. pSAMHD1 is dephosphorylated by the protein phosphatase PP2A-$B55^{\alpha}$ holoenzyme during mitotic exit[32]. Molecular dynamics simulations indicate that the allosteric signal from the surface exposed T592 phosphorylation event are relayed to the core of the protein through critical residues N452−K455[73]. The results of this signal remain controversial. Some groups have found that pSAMHD1 destabilizes the tetramer and results in decreased triphosphohydrolase activity[56, 59, 74-76]. However, there are conflicting reports that the dNTPase activity and tetramer stability of pSAMHD1 is comparable to SAMHD1[69, 77-80]. While phosphorylation may not regulate dNTPase activity, it appears to regulate HIV-1 restriction as phosphomimic mutants lose restriction capabilities [78, 81]. With this logic, one study found success at protecting macrophages from HIV-1 infection using treatments to reduce SAMHD1 phosphorylation[82]. Most recently, it has been proposed that phosphorylation modulates SAMHD1

tetramer dynamics, allowing for ssDNA binding at the dimer-dimer interface, thus abrogating dNTPase activity specifically in cellular locations high in ssDNA[83]. Excitingly, this has the potential to bridge earlier contradictory findings and eliminate a central paradox in the field.

SAMHD1 can be acetylated at residue K405 by arrest-defective protein 1 (ARD) [84]. This post-translational modification is seen at its highest in G1 phase and results in increased dNTPase activity[84]. Increased acetylation during G1 phase may explain how SAMHD1 is able to lower dNTP pools to satisfy the G1 checkpoint and progress to S phase[19, 85]. Additionally, SAMHD1 undergoes SUMOylation at residue K595[86]. This modification is dependent on both the SUMO-consensus motif (^{592}TPQK^{595}) at the site of SUMOylation and a proximal SUMO-interacting motif (SIM) (^{488}LLDV^{501}) which can contribute to the recruitment of SUMOylation machinery[86, 87]. Inactivation of the SUMO consensus motif or the SIM suppresses HIV-1 restriction but does not impair dNTPase activity[86]. Interestingly, this was seen even when the T592 residue was dephosphorylated and SAMHD1 was expected to be antivirally active, which highlights the complexity of SAMHD1 antiviral regulation[86].

Finally, SAMHD1 can be regulated by reversible oxidation of three surface-exposed cysteine residues C341, C350, and C522. Although C522 has been shown to have the highest redox activity, several X-ray crystallography studies of SAMHD1 observe the formation of a C341-C350 disulfide bond[20, 49, 55, 88]. The Hollis group found that C522 acts as a primary sensor of redox signals and can form a disulfide bond with C341 or C350 that destabilizes tetramerization and abolishes dNTPase activity[89]. They also found that SAMHD1 is oxidized in cells in response to proliferation signals, which would allow for the accumulation of dNTPs[89]. Mutants C341A and C350A showed decreased tetramerization and dNTPase activity whereas C522A displayed phenotypes comparable to wild type[89]. The Ivanov group obtained similar biochemical results with serine

mutants, but observed wild type dNTP depletion activity *in vivo* for all mutants[90]. Interestingly, the C522S and C341S mutations lose retroviral restriction, whereas the C350S is indistinguishable from the WT protein[90]. Like the T592 phosphorylation, these data show a discrepancy between dNTPase activity, dNTP depletion, and HIV restriction. This story is further complicated by molecular dynamic simulations from the Bhattacharya group that indicate C341S and C522S mutations cause drastic disruptions to the allosteric signaling network that extend to the catalytic site[91]. More recently, their *in silico* studies have suggested a role for these redox reactions in driving affinities for allosteric regulators, thereby fine-tuning the enzyme rather than turning it off or on[92]. The Hollis group recently proposed that phosphorylation of SAMHD1 causes a higher proportion of the enzyme to localize to the nucleus, thereby protecting it from oxidization[93]. Certainly, the regulation of SAMHD1 activity involved a tight interplay between nucleic acid binding, post-translational modifications, and redox action.

1.5 HIV-1 restriction by human SAMHD1.

SAMHD1 dNTPase activity has the capacity to restrict HIV-1 at several steps in the viral life cycle. The low dNTP pool environment of macrophages established by SAMHD1 suppresses both RNA and DNA dependent proviral DNA synthesis of HIV-1[5]. In these conditions RT displays an increased strand transfer frequency and is more reliant upon the central polypurine tract to complete proviral DNA synthesis[94-96]. Additionally, these low dNTP conditions result in a 4-80 fold disparity between the rNTP/dNTP concentration ratio in macrophages compared to activated T-cells[41]. This disparity drives an increase in ribonucleoside triphosphate (rNTP) and rNTP chain terminator incorporation during RT mediated-DNA synthesis in macrophages[41, 97]. The presence

of an rNMP in the DNA template induces RT pausing which can result in mutation synthesis[51]. While enzymes such as RNase H2 are usually able to repair rNMP misincorporations, RNase H2 activity is lower in macrophages than in dividing cells [97]. Furthermore, the RNase H2 repair process requires DNA gap repair which is dependent upon dNTPs and is therefore kinetically limited in non-dividing cells [98]. This also restricts HIV-1 at the integration step, as host DNA polymerases need cellular dNTPs to repair the gap between single-stranded host DNA and partially integrated viral DNA[98, 99]. Finally, the SAMHD1 mediated low dNTP pools of macrophages restricts endogenous reverse transcription (ERT), where partial reverse transcription occurs within cell-free viral particles utilizing co-packaged dNTPs [100]. HIV-1 virions produced by non-dividing cells harbor less dNTPs, consequently limiting ERT activity [100]. Notably, SAMHD1 is able to suppress HIV-1 LTR driven gene expression in dividing cells and both the phosphorylation mutant (T592A) and catalytic site mutant lose this ability[101]. Although, this effect is more likely to be due to changes in nucleic acid binding ability than dNTPase activity, as dNTP levels are already high in these dividing cells[101]. Furthermore, the nucleic acid binding ability of SAMHD1 has recently been implicated in retroviral restriction[102].

1.6 Viral Protein X (Vpx) counteracts lentiviral restriction by SAMHD1.

HIV-2 and some SIVs can replicate rapidly even in the macrophage environment because they encode a viral accessory protein called viral protein X (Vpx), which is able to target SAMHD1 for proteasomal degradation[21, 103-105]. Vpx does this by binding to E3-ligase substrate adaptor, CUL4-associated factor 1(DCAF 1), which creates a new surface that can recognize SAMHD1[106]. This in turn complexes with DDB1, cullin 4, and ROC1/RBX1 followed by an E2 ligase in order

ubiquitinate SAMHD1 and target it for the proteasome[21, 103, 106-110]. This targeting of SAMHD1 by Vpx for proteasomal degradation occurs in the cell nucleus [24-26]. The transient degradation of SAMHD1 increases dNTP pools 10-fold in macrophages. As this is above the K_m of RT, the reverse transcription step occurs rapidly and the frequency at which noncanonical rNTPs are incorporated during proviral DNA synthesis is lower[111]. This relieves Vpx coding viruses of the various restrictions SAMHD1 poses, which allows SAMHD1 counteracting lentiviruses to replicate more efficiently in macrophages than SAMHD1 non-counteracting lentiviruses. Notably, Vpx originates from a gene dupplication of viral protein R (Vpr) in an ancestral lentivirus [112-114] and therefore some Vpr proteins are able to target SAMHD1 for proteasomal degradation[107, 115, 116].

1.7 Host and viral evolution due to the host-pathogen arms-race.

Restriction factors such as SAMHD1 are engaged in an evolutionary arms-race against the viruses they inhibit[117, 118]. Amino acids involved in the interaction between the restriction factor and its viral antagonist often display strong signatures of positive selection, where codons experience changes at a higher frequency than what would be expected by neutral drift[119-121]. In fact, old world monkey SAMHD1 displays a positive selection signature in the N-terminal domain whereas in new world monkey SAMHD1 displays a positive selection in the C-terminal domain[115, 122]. This discrepancy is dictated by the various requirements Vpx/Vpr orthologs have evolved for SAMHD1 recognition and degradation[123]. This evolutionary arms-race between SAMHD1 and lentiviruses has also impacted the evolution of reverse transcriptase (RT). Indeed, RTs from lentiviruses that cannot counteract SAMHD1 (such as HIV-1) more efficiently polymerize DNA

in macrophage conditions than RTs from lentiviruses that do counteract SAMHD1 (such as HIV-2)[42, 124]. RT's from SAMHD1 non-counteracting viruses are more efficient because they have evolved to more rapidly execute the conformational change step (k_{conf}) during the incorporation of a dNTP[125]. This increased efficiency allows the virus to by-pass SAMHD1 restriction and replicate in the low dNTP pool conditions of macrophages [125]. Furthermore, RTs from SIVmac239 Vpx- infections acquire numerous amino acid mutations that result in enhanced RT kinetics when compared to RTs from SIVmac239 Vpx + infections[126]. This suggests that the loss of Vpx during an *in vivo* SIVmac239 infection can drive RT variations to counteract the limited availability of dNTPs in macrophages[126].

1.8 SAMHD1 and the restriction of other retroviruses.

Like primate lentiviruses, ancestral lentiviruses such as equine infectious anemia virus (EIAV) and feline immunodeficiency virus (FIV), are restricted by SAMHD1 in myeloid cells[127, 128]. However, EIAV and FIV infections do not target their respective SAMHD1 proteins for degradation, despite Vpx from SIVmac239 being able to effectively target eSAMHD1 and fSAMHD1 for degradation[127, 128]. This would suggest that primate lentiviruses have evolved to more efficiently counteract SAMHD1 than ancestral lentiviruses. The beta-retrovirus Mason Pfizer monkey virus (MPMV)[128], Delta-retrovirus human T-lymphotropic virus (HTLV) [129], and Gamma-retrovirus murine leukemia virus (MLV) [27, 130, 131] are all restricted in macrophages by SAMHD1 dNTPase activity. However, MLV also experiences SAMHD1 independent inhibition of viral DNA nuclear import in this cell type[131]. Alpha retrovirus Rous Sarcoma Virus (RSV) cannot infect macrophages, an effect which is not relieved by SAMHD1 knockout or Vpx

treatment[128]. Prototype foamy virus (PFV) is not inhibited by SAMHD1 in macrophages because reverse transcription occurs late in the PFV lifecycle, resulting in some mature virions possessing nearly complete vDNA[128, 132-134].

1.9 SAMHD1 modulates host innate immunity.

Mutations in the SAMHD1 gene were first associated with Aicardi-Goutières Syndrome (AGS), a rare congenital neuropathy characterized by aberrant type 1 interferon (IFN) responses[135, 136]. AGS patients develop hyperactivation of the innate immune response in the absence of infection, which interferes with brain development and causes death at early ages[135, 137]. As proposed for other AGS-related proteins such as TREX1[138-140], RNase H2[141] and ADAR[142], SAMHD1 mutations may interrupt cellular nucleic acid metabolism, which can allow native nucleic acids to accumulate and trigger the innate immune response through pattern recognition receptors (PRRs) [143]. Another proposed mechanism for SAMHD1 mediated IFN downregulation suggests that the RNA and DNA binding properties of SAMHD1 may impede RIG-I/MDA5 and cGAS/STING mediated sensing of nucleic acids[102, 144-148]. Additionally, SAMHD1 has been observed to directly downregulate the innate immune response by reducing the phosphorylation of the NF-κB inhibitory protein, IκBα, and reducing inhibitor-κB kinase ε (IKKε) mediated IRF7 phosphorylation, thus inhibiting NF-κB and IRF7 activation [149]. In non-diving cells this downregulation appears to be dependent on the dNTPase activity of SAMHD1, however the effect is dNTPase independent in dividing cells[149, 150]. Further studies have demonstrated that SAMHD1 mediated NF-κB inhibition occurs through the TRAF6-TAK1 axis[151].

The ability of a virus to evade the innate immune response is critical to establishing a productive infection. A recent review highlights the many strategies HIV-1 employs to subvert the innate immune response, including counteracting restriction factors, disrupting signal pathway transduction, and masking pattern- associated molecular patterns (PAMPS)[152]. Some studies have proposed that the restricted replication kinetics of HIV-1 in macrophages falls below the threshold that would trigger an interferon response[49, 52]. This would suggest an evolutionarily favorable reason for HIV-1 to have lost the Vpx gene and the ability to counteract SAMHD1[153]. Interestingly, as SAMHD1 suppresses innate immune response [137, 143, 148], viruses such as SARS-CoV-2 are restricted in Vpx treated cells or SAMHD1 knock-out cells due to the hyperactivated IFN environment[154]. How Vpx-coding lentiviruses overcome this effect is under investigation. Some studies have observed that Vpx itself is able to suppress the innate immune antiviral response in monocyte derived macrophages and monocytic cell lines [155, 156]. One proposed mechanism is that Vpx is able to bind to the p65 subunit of NF-κB in order to suppress NF-κB activation[156]. This antagonism was conserved amongst Vpx proteins from distantly related lentiviruses and Vpr from SIVmon, which has SAMHD1-degradation activity[156]. This study is especially enticing considering one suggested mechanism for SAMHD1 mediated immune suppression is at the NF-κB activation level[150, 157]. Conversely, another study observed that Vpx elevated the innate immune response in macrophages independently of SAMHD1[158]. Understanding how SAMHD1 counteracting lentiviruses suppress or evade the hyperactive immune response triggered by SAMHD1 degradation is an ongoing effort and likely involves a network of mechanisms.

1.10 The role of SAMHD1 in DNA damage repair and cell cycle.

SAMHD1 also has other functions in the cell such as involvement in DNA repair, where it localizes to sites of DNA damage [159, 160]. During homologous recombination to repair double strand DNA breaks SAMHD1 interacts with CtIP in a dNTPase independent manner to stimulate the endonuclease activity of Mre11 and begin end resection[159]. Additionally, SAMHD1 deacetylation by SIRT1 promotes ssDNA binding at sites of dsDNA breaks[161]. Similarly, SAMHD1 promotes the degradation of nascent DNA at stalled replication forks by stimulating Mre11 activity[162]. Without SAMHD1, single strand DNA fragments accumulate in the cytosol and trigger the innate immune response[162]. Additionally, SAMHD1 partakes in non-homologous end-joining to repair double strand DNA breaks[163]. Here, the dNTPase activity of SAMHD1 degrades dNTP pools thereby limiting aberrant DNA resynthesis during DNA end joining[163]. This function has been shown to be important for DNA repair during antibody class switch recombination in B-cells[164]. Finally, SAMHD1 limits the accumulation harmful DNA:RNA hybrids called R loops at sites of transcription-replication conflicts where DNA replication machinery collides with the RNA polymerase[165]. As these R loops can cause replication fork stalling, this is one mechanism by which SAMHD1 protects against DNA damage[165].

SAMHD1 is also involved in cell cycle progression as SAMHD1 knockout cells accumulate in G1 phase of the cell cycle [85, 166, 167]. Additional features of these cells, such as proliferatory effects, depends on cell type. For example, SAMHD1 knock out in fibroblasts causes a senescent phenotype[166, 167], while SAMHD1 knockout in THP-1 cells results in increased proliferation and reduced apoptosis[85, 168]. However, overexpression of SAMHD1 consistently reduces cell proliferation, likely because of insufficient dNTP concentrations to synthesize DNA for replication[169-171].

1.11 SAMHD1 in cancer

It is essential for cells to regulate dNTP pools such that sufficient and balanced pools exist for DNA replication. Irregular or imbalanced dNTP pools result in lowered replication fidelity and an increase in mutation synthesis[172-175]. For example, alterations in RNR that inhibit its negative regulation results in a mutator phenotype[176, 177]. Such high or imbalanced dNTP pools increase mutagenesis by increasing the probability of a misincorporation event[178] and by increasing mismatch extension, a phenomenon known as next-nucleotide effect[179]. Aberrant dNTP pools can therefore contribute to mutation synthesis and sustain the uncontrolled/rapid cell division and higher cell population at S phase of cancer cells[85]. In fact, elevated dNTP pools serve as a biochemical marker for cancer cells as they harbor 6-to 11-fold higher dNTP levels than normal cells[180]. Interestingly, SAMHD1 mutations have been identified in a variety of cancers, including leukemias[160, 181-184], lymphomas[185-187], lung cancer[171], and colon cancer[188-190]. SAMHD1 cancer-associated mutations are found throughout the entire protein and most cause reduced SAMHD1 protein levels, likely due to issues with protein stability [160, 191]. In some instances, such as cutaneous T-cell lymphoma (CTCL) and T-cell acute lymphoblastic leukemia (T-ALL), downregulation of SAMHD1 expression is driven by promoter methylation instead of mutations[185, 192]. However, which function of SAMHD1 when downregulated contributes to a cancer phenotype remains unknown.[191] Cancer cells without SAMHD1 are susceptible to the cytotoxic effects of nucleotide accumulation or imbalance[193, 194]. Therefore, it has been suggested that PNP inhibitors such as forodesine which allow for the accumulation of dGTP, can be used to specifically target cancer cells lacking SAMHD1 function[193, 194].

Conversely, SAMHD1 expression can interfere with the anti-cancer efficacy of the triphosphorylated forms of some anti-cancer nucleoside analogues due to the enzyme's ability to hydrolyze these compounds [60, 63, 195, 196]. SAMHD1 expression has been shown to regulate the response of cancer cells to cytarabine (ara-C)[62, 197], arabinosylguanine (AraG) [192], and 2′-C-cyano-2′-deoxy-1-β-D-arabino-pentofuranosyl-cytosine (CNDAC) [198]. Additionally, SAMHD1 can inactivate the hypomethylating agent, decitabine. [199]

In the clinic, SAMHD1 is known to play a role in Ara-C response in acute myeloid leukemia (AML) patients[62]. Moreover, SAMHD1 expression is highly upregulated in AML patients with Ara-C resistance[61, 62] and several single nucleotide polymorphisms that predict the response of an AML patient to Ara-C have been identified[200]. Similarly, in chronic lymphocytic leukemia, refractory patients on average have a higher rate of SAMHD1 mutations[160] and SAMHD1 expression has been found to be a negative prognostic biomarker for Hodgkin lymphoma[201]. However, SAMHD1 has not been found to correlate with clinical outcomes in mantle-cell lymphoma (MCL) patients, where Ara-C is usually given in combination with other therapeutics[187, 202]. Several suggestions have been made to target SAMHD1 in order to improve nucleoside based anti-cancer therapies including: treatment with Vpx to degrade SAMHD1[61] and treatment with RNR inhibitors to induce dNTP pool imbalances and impede SAMHD1 allosteric activation [203]. Recently, it was found that NONO, a protein involved in DNA damage response, is overexpressed in Ara-C resistant cells and protects SAMHD1 from degradation, revealing a novel therapeutic target for resistance [204].

1.12 Framework and overview of the dissertation.

Proper maintenance of dNTP levels is essential to the health of a host. However, both lentiviruses in a non-dividing cell environment and fast-replicating cancer cells are faced with the barrier of insufficient dNTP pools for copying their genomes. To address this, HIV-1 has evolved a more efficient RT to synthesize DNA with the low amount of dNTPs available in a non-dividing cell[42, 125]. More common amongst primate lentiviruses, though, is the use of accessory proteins Vpx or Vpr to degrade host SAMHD1 and elevate intracellular dNTP levels[21, 103]. Similarly, cancer cells are known to elevate dNTP levels 6-11-fold and this alteration in metabolism has been suggested as a hallmark of cancer[180]. For this reason, several cancer therapies used in the clinic target this altered nucleotide metabolism[205]. Therefore, SAMHD1 counteracting lentiviruses and cancer cells both elevate intracellular dNTP pools during the course of their pathogenesis. This dissertation seeks to provide mechanistic insights into this shared phenomenon.

In Chapter 2, I explore what determinants are necessary for successful dNTP pool elevation in macrophages upon Vpx treatment. It is well established that Vpx targets SAMHD1 for E3 ubiquitin mediated proteasomal degradation in macrophages, resulting in increased dNTP pools[21, 103, 108]. However, it has been presumed that macrophages do not maintain dNTP biosynthesis capabilities due to the lack of chromosomal replication and low dNTP pools found in this cell type[5]. Thus, it was unclear how dNTP pools could be elevated in macrophages upon SAMHD1 depletion without active dNTP biosynthesis. Notably, we have previously published that treating macrophages with inhibitors of RNR, a dNTP biosynthesis enzyme, abrogated the effect of Vpx on dNTP levels[22]. This finding would suggest the presence of dNTP biosynthesis in macrophages and the importance of RNR for Vpx-mediated dNTP elevation. In this work, I monitored known dNTP biosynthesis enzymes during monocyte differentiation into monocyte derived macrophages (MDMs). Here I find that dNTP biosynthesis machinery is present in MDMs and is absent in

monocytes. Additionally, I report dNTP levels in monocytes are significantly lower than in MDMs and cannot be elevated by Vpx treatment. These extremely low dNTP concentrations found in monocytes impaired DNA synthesis by HIV-1 reverse transcriptase in a biochemical simulation. Furthermore, treatment of monocytes with VLPs containing Vpx failed to rescue the transduction efficiency of a HIV-1 GFP vector or elevate the copy number of reverse transcription products. Together, these data propose that Vpx is reliant upon the active dNTP biosynthesis present in macrophages to elevate dNTP levels and counteract SAMHD1.

In Chapter 3, I seek to define a contribution of SAMHD1 mutations towards a cancer phenotype. While SAMHD1 mutations were first reported in AGS patients, there has recently been a series of SAMHD1 mutations identified in cancer samples[137]. Like AGS mutations, these cancer mutations were found throughout the gene and results in decreased SAMHD1 expression levels, indicative of major structural alterations[81, 160]. As SAMHD1 has many cellular functions, major structural issues would impact several SAMHD1 activities, making it difficult to pinpoint a single contribution towards a cancer phenotype. In this work, I identify the R366C/H mutation, found in two different cancer types, as having similar stability profiles to wild type SAMHD1. I then probed which functions this mutation interferes with and determine that only dNTPase activity is abrogated by this mutation. Furthermore, I demonstrate that, in primary $CD4^+$ T-cells, Vpx-mediated reduction in SAMHD1 protein level, which also reduces overall dNTP hydrolysis capacity, can induce the elevated dNTP levels commonly seen in cancer cells. Collectively, this work suggests that loss of dNTPase activity induced by SAMHD1 cancer mutations can mechanistically contribute to the elevated intracellular dNTP pools commonly observed in cancer cells.

Finally, in Chapter 4 I summarize the findings of this dissertation, discuss implications of these results for the field, and propose future directions for understanding mechanisms of dNTP pool alteration during pathogenesis.

Chapter 2

Vpx requires active dNTP biosynthesis to effectively counteract the anti-lentivirus activity of SAMHD1 in macrophages.

Nicole E. Bowen[1], Sijia Tao[1], Young-Jae Cho[1], Raymond F. Schinazi[1,2], Baek Kim[1,2]

[1.] Center for ViroScience and Cure, Department of Pediatrics, School of Medicine, Emory University, Atlanta, Georgia, USA.

[2.] Children's Healthcare of Atlanta, Atlanta, Georgia, USA.

2.1 Abstract

Replication of HIV-1 in primary monocyte-derived macrophages (MDMs) is kinetically restricted at the reverse transcription step due to the low dNTP pool established by host dNTPase, SAM and HD domain containing protein 1 (SAMHD1). Lentiviruses such as HIV-2 and some SIVs counteract this restriction by coding for viral protein X (Vpx), which targets SAMHD1 for proteasomal degradation and elevates intracellular dNTP pools. However, it has been assumed that dNTP biosynthesis in terminally differentiated MDMs is absent due to the lack of chromosomal DNA synthesis and low dNTP concentrations observed in this cell type. Therefore, how dNTP pools increase to relieve restriction after Vpx degrades SAMHD1 in MDMs remains unclear. Notably, we have previously reported that treating MDMs with inhibitors of Ribonucleotide Reductase (RNR), a key *de novo* dNTP biosynthesis enzyme, eliminates the effect of Vpx on dNTP pools, supporting the possibility that nondividing MDMs may maintain active dNTP biosynthesis even in the absence of chromosomal DNA replication. In this study, we monitored known dNTP biosynthesis machinery during monocyte differentiation to MDMs using Western Blot and found MDMs actively express dNTP biosynthesis enzymes such as RNR, Thymidine Kinase 1 Deoxycytidine Kinase, and Nucleoside-Diphosphate Kinase. During differentiation the expression levels of several biosynthesis enzymes are upregulated, while there is an increase in inactivating SAMHD1 phosphorylation. In contrast, SAMHD1 predominantly remains active/dephosphorylated in monocytes and several key dNTP biosynthesis enzymes are not expressed. Indeed, we observed significantly lower levels of dNTPs in monocytes compared to macrophages when measured using LC-MS/MS. Additionally, unlike MDMs, the treatment of monocytes with virus like particles (VLPs) containing Vpx resulted in SAMHD1 depletion but

failed to elevate dNTPs. These extremely low dNTP concentrations found in monocytes impaired DNA synthesis by HIV-1 reverse transcriptase in a biochemical simulation. Furthermore, treatment of monocytes with VLPs containing Vpx failed to rescue the transduction efficiency of a HIV-1 GFP vector. Collectively, the data from our study suggests that MDMs harbor active dNTP biosynthesis and Vpx requires this dNTP biosynthesis to rapidly elevate cellular dNTP levels to effectively counteract SAMHD1 and relieve the kinetic block to HIV-1 reverse transcription in MDMs.

2.2 Introduction

Deoxynucleoside triphosphates (dNTPs), the molecular precursors and building blocks of DNA, are metabolically regulated in all living cells. Dividing cells harbor high dNTP pools to support novel chromosomal DNA synthesis during S phase[206, 207]. Conversely, in nondividing cells, it is energetically favorable to maintain lower dNTP pools due to the lack of chromosomal DNA replication and dNTP consumption[5]. In fact, dNTP concentrations in non-dividing/terminally differentiated macrophages (20–40 nM) are ~200 times lower than dividing/activated CD4+ T cells (1–16 μM)[5, 41]. The dNTP concentration difference between these two HIV-1 target cell types is a metabolic outcome of the tight regulation between dNTP synthesis and dNTP hydrolysis. Intracellular dNTPs are produced in the cell by two different metabolic pathways: the *de novo* dNTP biosynthesis pathway or the salvage pathway. In the *de novo* pathway, ribonucleoside diphosphates (rNDPs) are reduced by Ribonucleotide Reductase (RNR) to generate deoxyribonucleoside diphosphates (dNDPs), which are converted to dNTPs by Nucleoside-Diphosphate Kinase (NDPK)[9, 208, 209]. In contrast, a series of cellular deoxynucleoside and

deoxynucleotide kinases such as Thymidine Kinase 1 (TK1)[210], Deoxycytidine Kinase (DCK)[6], and NDPK are responsible for mediating phosphorylation events to generate dNTPs from dNs in the salvage pathway. Many of these biosynthetic enzymes are upregulated at the G1/S phase transition to supply dNTPs for DNA replication[13, 14, 18]. On the other hand, cellular dNTPs can be hydrolyzed into dN and triphosphate subcomponents by a dNTPase, SAM and HD domain containing protein 1 (SAMHD1)[20]. SAMHD1 is inactivated by phosphorylation during the G1/S phase transition by CDK1/CyclinA2 to reduce SAMHD1 activity and allow for dNTPs to accumulate for DNA synthesis[29, 31, 69, 83]. SAMHD1 is then dephosphorylated at mitotic exit by phosphatase PP2A/B55α to reinstall dNTPase activity[32]. Importantly, SAMHD1 abundantly exists in non-dividing cells such as macrophages to maintain low dNTP levels. Overall, the balance of biosynthesis and hydrolysis to regulate intracellular dNTP pools is a necessity for cells. Failure to maintain the appropriate amount and balance of dNTPs is a hallmark of cancer cells [180, 211] and can support rapid DNA synthesis and mutagenesis[85, 173-175].

Retroviruses utilize intracellular dNTPs during reverse transcription to generate a DNA copy of their RNA genome. Lentiviruses are a unique genus of this family as they replicate in both the high dNTP environment of dividing cells and the low dNTP environment of non-dividing cells[5, 212]. HIV-1 replicates rapidly in activated $CD4^+$ T-cells, whereas viral replication is kinetically restricted in macrophages[21]. The low macrophage dNTP concentration established by host restriction factor, SAMHD1, falls below the K_m of reverse transcriptase (RT) resulting in kinetically restricted reverse transcription[5, 20-22, 42]. Indeed, proviral DNA synthesis during HIV-1 infection of activated $CD4^+$ T-cells occurs in 12-16 hours whereas reverse transcription requires up to 36 hours during infection of macrophages[43]. However, HIV-2 and some SIVs can replicate rapidly even in macrophages due to their accessory protein, viral protein X (Vpx)[104, 105]. Indeed,

Vpx targets SAMHD1 for proteasomal degradation[21, 103, 106], relieving restriction in macrophages by elevating the intracellular dNTP level above the K_m of RT[23, 42, 213].

Interestingly, previous studies have reported that RNR inhibitors such as gemcitabine[213] and hydroxyurea[22] can limit Vpx-mediated dNTP pool elevation in macrophages. These findings would surprisingly imply the presence of RNR, a dNTP biosynthesis enzyme, in these non-dividing macrophages that lack chromosomal DNA replication. Extensive investigations on RNR have been made mainly in dividing cells, particularly cancer cells, and various RNR inhibitors are clinically available for anti-cancer treatments[214]. However, due to the low dNTP concentrations that we previously observed in macrophages, dNTP biosynthesis machinery has long been presumed to be unavailable in this nondividing cell type. Therefore, only the contribution of dNTP hydrolysis by SAMHD1 has been well characterized as a key mechanistic element of HIV-1 restriction in macrophages.

In this study, we first investigated the expression levels of several dNTP biosynthesis enzymes throughout differentiation of human primary monocytes into macrophages. Notably, we found dNTP biosynthesis enzymes present in macrophages and upregulated during the differentiation process. We also observed that monocytes harbor extremely low dNTP levels that cannot be elevated by Vpx due to the absence of dNTP biosynthesis machinery. Therefore, Vpx cannot rescue the block to HIV-1 reverse transcription in monocytes, which could contribute to the absence of productive lentivirus replication in monocytes. Collectively, our data support that Vpx-mediated dNTP elevation in macrophages is dependent on ongoing active dNTP biosynthesis machinery such as RNR.

2.3 Results

2.3.1 Ribonucleotide reductase is expressed in monocyte-derived macrophages.

dNTP biosynthesis, which is closely tied with cell cycling, cell division, and chromosomal DNA replication, has been presumed to be absent in nondividing cell types where DNA replication does not occur. Therefore, it remained unclear how Vpx can elevate cellular dNTP levels in terminally differentiated/nondividing macrophages where dNTP biosynthesis is supposed to be absent and chromosomal DNA replication permanently lacks. However, we previously reported that ribonucleotide reductase (RNR) inhibitors such as gemcitabine[213] and hydroxyurea[22] block Vpx-mediated dNTP elevation in human primary monocyte-derived macrophages (MDMs). This striking observation was also confirmed in this study (Figure 2.1A and 2.1B), where we show that hydroxyurea and gemcitabine can completely counteract the Vpx-mediated dNTP elevation in MDMs. Therefore, these data strongly support the possibility that the key de novo dNTP biosynthesis enzyme, RNR, is present and functional in human primary nondividing MDMs even though nondividing cells have been long presumed to lack active dNTP biosynthesis.

Active RNR is a heterodimeric tetramer of two distinct subunits, RNR M1 and RNR M2[9]. In dividing cells, M1 is expressed throughout the cell cycle, while M2 is expressed during S phase to allow dNTPs to accumulate for DNA synthesis[13, 14]. Therefore, to assess the expression of the functional RNR enzyme in macrophages, we differentiated human primary monocytes isolated and pooled from 5 healthy donors into macrophages using GM-CSF. We monitored the expression level of both RNR M1 and RNR M2 subunits at several time points during differentiation using Western Blot (Figure 2.1C). Inactive and activated $CD4^+$ T-cells (by IL-2/PHA) isolated from the same donors were used as a positive cycling cell control and showed increased levels of RNR M1

and M2 subunits during the activation of cell cycling. Notably, we detected expression of both the RNR M1 and RNR M2 subunits at days 5 and 7 post GM-CSF treatment where the cells are attached and fully differentiated into macrophages. However, little to no M1 and M2 subunits were detected in freshly isolated human monocytes (Day 0). Therefore, these data suggests that even though both monocytes and differentiated macrophages are nondividing cells, only MDMs express RNR. Furthermore, these data support the possibility that Vpx-mediated dNTP elevation in MDMs requires active biosynthesis such as RNR.

2.3.2 Macrophages, but not monocytes, express dNTP biosynthesis enzymes from the de novo and salvage pathways.

Given terminally differentiated macrophages express the dNTP biosynthesis enzyme RNR, we next sought to assess the expression levels of other dNTP biosynthesis enzymes during monocyte differentiation to macrophages. For this, we collected lysates at several time points during primary monocyte differentiation to macrophages by GM-CSF and probed for dNTP biosynthesis enzymes using Western Blot (Figure 2.2). Here, we observed that TK1 and dCK, kinases involved in the dNTP salvage pathway, are both expressed in macrophages at higher levels, compared to monocytes (Figure 2.2A, 2.2B). NDPK, which is utilized in a final phosphorylation step to generate dNTPs by both the salvage pathway and the *de novo* biosynthesis pathway[209], is also expressed in both monocytes and macrophages (Figure 2.2C). TK1 expression, similar to RNR, is not present in monocytes and is significantly upregulated during differentiation into macrophages (Figure 2.2A), whereas the dCK level only slightly increased during the differentiation (Figure 2.2B). These data propose active dNTP biosynthesis in macrophages even

though overall dNTP levels in this cell type are low. Monocytes, on the other hand, are missing key enzymes from both the *de novo* and salvage pathways such as RNR and TK1.

2.3.3 SAMHD1 in monocytes predominantly remains active/dephosphorylated, but SAMHD1 phosphorylation increases during differentiation to macrophages.

dNTP biosynthesis is counterbalanced by dNTP hydrolysis by host SAMHD1[20, 22]. The dNTPase activity of SAMHD1 is primarily regulated in dividing cells by phosphorylation at the C-T T672 residue that inactivates its dNTPase activity to supply sufficient dNTPs for chromosomal DNA replication. Therefore, we next monitored both total and phosphorylated/non-active SAMHD1 levels throughout monocyte differentiation to macrophages as well as $CD4^+$ T cell activation as a positive control. As shown in Figure 2.3A, we found SAMHD1 is abundantly present in both monocytes and macrophages, and this expression does not change during differentiation. Interestingly, there is a substantial population of pSAMHD1 in macrophage lysate, indicating a portion of the SAMHD1 present in macrophages is dNTPase inactive[59, 77]. However, no pSAMHD1 was detected in monocyte lysate, suggesting all of the SAMHD1 molecules in monocytes are active. This likely means that there is more potential for dNTP hydrolysis in monocytes than in macrophages. Therefore, the macrophage dNTP metabolism environment can be characterized as having ongoing dNTP biosynthesis coexisting with dNTP hydrolysis whereas in monocytes only dNTP hydrolysis is completely present. Importantly, freshly isolated non-activated $CD4^+$ T cells, which are non-dividing cells, also do not express the phosphorylated/non-active form of SAMHD1 (Figure 2.3A), which is consistent with our previous observation of the

low dNTP levels in this type of T cell[215]. However, SAMHD1 became phosphorylated during the IL-2/PHA mediated stimulation that leads to the activation of these cells into dividing cells.

After observing that pSAMHD1 levels increase throughout monocyte differentiation into macrophages, we next assessed levels of enzymes that regulate SAMHD1 phosphorylation and dephosphorylation during differentiation. As shown in Figure 2.3B, we observed increased amounts of the CDK1/CyclinA2 complex that mediates SAMHD1 phosphorylation[29] during the differentiation from monocytes to macrophages (Figure 2.3B)[29], which is consistent with the significant SAMHD1 phosphorylation increase during the differentiation to macrophages (Figure 2.3A). However, we also detected some increase of the PP2A B55α subunit, which is a specificity component of PP2A phosphatase that dephosphorylates SAMHD1[32], throughout monocyte differentiation to macrophages (Figure 2.3C). Overall, in monocytes, there is little to no capacity for the phosphorylation of SAMHD1 while dephosphorylation machinery is present in monocytes, accounting for the lack of pSAMHD1 in monocytes. On the other hand, in macrophages, phosphorylation and dephosphorylation of SAMHD1 are both occurring, resulting in a mixed population of pSAMHD1 and SAMHD1. However, it is still likely that macrophages express significant levels of active/dephosphorylated SAMHD1 protein as indicated by the strong expression of PP2A B55α (Figure 3C), which is responsible for the low dNTP level and HIV restriction capability of macrophages.

2.3.4 Monocytes enter a G1/S phase-like state during differentiation to macrophages.

Noncycling cells are thought to exist in G0, a phase that exists outside of the cell cycle[216]. Even so, we have observed macrophages express TK1[18], RNR M2[13], and several other dNTP

biosynthesis enzymes that are normally upregulated at the G1/S transition in cycling cells. Therefore, we investigated levels of G1/S phase transition markers throughout monocyte differentiation into macrophages (GM-CSF treatment). For this, we monitored the protein levels of E2F-1, a master transcription factor regulating genes required for cell cycle progression to S phase[217], and CDK2, the cyclin dependent kinase that phosphorylates numerous downstream target proteins involved in the transition to S phase [218]. As shown in Figure 2.4A, both E2F-1 and CDK2 are not expressed in monocytes, indicating that monocytes exist at G0-like status. However, these master cell cycle regulators are upregulated during differentiation, supporting the G1/S phase-like state status of macrophages.

Since macrophages express G1/S transition markers, we next assessed if macrophages were entering S phase by measuring genomic DNA synthesis, the hallmark of S phase[219]. To do this, we employed an EdU assay to fluorescently label cells synthesizing DNA, followed by flow cytometry. While 27% of 293T cells, the positive cycling cell control, were synthesizing new DNA under our experimental conditions, we observed little to no DNA synthesis in both primary monocytes and macrophages (Figure 2.4B). Therefore, similar to previous reports[72], we conclude that macrophages enter a "G1/S-like state" during differentiation but are not entering into S phase.

Next, we also investigated if dNTP biosynthesis machinery was being upregulated to support mitochondrial DNA synthesis during 7-day monocyte differentiation to macrophages. Here, we extracted total DNA at several time points during monocyte differentiation or $CD4^+$ T-cell activation as a positive cycling cell control. We then used qPCR to measure mitochondrial DNA copy number normalized to nuclear DNA copy number. Here we observed an increase in mitochondrial DNA copy number during T-cell activation by day 5, but not during monocyte differentiation into macrophages even at 7 days post differentiation (Figure 2.4C). Thus, the

upregulation of dNTP biosynthesis enzymes during differentiation does not appear to function as a support for DNA synthesis, either genomic or mitochondrial.

2.3.5 Monocytes have extremely low dNTP levels that cannot be raised by Vpx.

We hypothesized that macrophages have higher dNTP levels than monocytes due to the upregulation of dNTP biosynthesis machinery and increased SAMHD1 phosphorylation/inactivation during differentiation. To test this hypothesis, we measured dNTP levels in monocytes and macrophages using LC-MS/MS [220]. Indeed, monocyte dNTP levels are significantly lower than the already low dNTP levels of macrophages (Figure 2.5A).

Next, we tested whether Vpx, which elevates dNTP levels in macrophages[22], can also elevate dNTP levels in monocytes. Here, we predicted that Vpx would be unable to elevate dNTP pools in monocytes due to the absence of dNTP biosynthesis machinery. For this test, first, we treated monocytes and macrophages with Vesicular Stomatitis Virus (VSV-G) psuedotyped VLPs Vpx+ or VLPs Vpx-, as a negative control, and confirmed SAMHD1 depletion in VLPs Vpx+ treated cells (Supporting Figure 2.1A). Next, dNTP levels in these cells were measured using LC-MS/MS. As shown in Figure 2.5B, we observed an increase in dNTP level in macrophages treated with VLPs Vpx+ when compared to macrophages treated with VLPs Vpx-. In contrast, despite SAMHD1 depletion in monocytes treated with VLPs Vpx+, we observed no significant change in dNTP levels in these cells compared to monocytes treated with VLPs Vpx- (Figure 2.5B). These data demonstrate that SAMHD1 depletion is not sufficient for Vpx-mediated dNTP elevation in monocytes and further support that Vpx-mediated dNTP elevation requires active dNTP biosynthesis as seen in macrophages.

2.3.6 dNTP concentrations found in monocytes block efficient reverse transcription.

It has been reported that HIV-1 infection in monocytes is limited even though monocytes express the appropriate CD4 receptor and coreceptors[221, 222]. Moreover, it has been proposed that the block to HIV-1 infection in monocytes occurs at a step post-entry[221, 223]. Therefore, we hypothesized that the extremely low dNTP pool of monocytes impairs the reverse transcription reaction, thus serving as a major replicative block in this cell type. To test this, we ran a biochemical simulation of HIV-1 reverse transcription in $CD4^+$ T-cell, macrophage, and monocyte dNTP concentrations using a primer extension assay. First, we calculated the dNTP concentration of macrophages and monocytes using previously mentioned dNTP levels (Figure 2.5A) and cell volume determined by confocal microscopy. The cell volumes of the monocytes and macrophages were found to be 1108 μM^3 and 3063 μM^3, respectively, comparable to our previous publication [5] (Supporting Figure 2.2A). Therefore, the dNTP concentration of monocytes is up to 20-fold lower than macrophages, with the rate limiting nucleotide being dATP (Figure 2.6A and 2.6B). For the biochemical simulation, a 5′ ^{32}P- labeled 17-mer RNA primer annealed to a 40-mer DNA template was extended by purified HIV-1 RT protein under reaction conditions that contained dNTP concentrations present in activated CD4+ T cells (4 μM), macrophages treated with Vpx (500 nM), macrophages without Vpx (40 nM), and monocytes (2 nM) (Figure 2.6C). In this primer extension assay, the full extension of the primer (P) by HIV-1 RT produces the 40-mer DNA product (F). We conducted the primer extension reactions at the dNTP concentrations found in activated CD4+ T cells with three different HIV-1 RT protein amounts (4x, 2x and 1x, Figure 2.6C), which generated three different amounts of the fully extended product, validating that the reactions were

in the linear range under our experimental conditions. When these reactions were repeated with the dNTP concentrations found in macrophages, there was a significant reduction of fully extended primer and the exacerbation of a pause site, indicative of replicative stress. However, this restricted DNA synthesis was rescued when the same reactions were conducted at the dNTP concentrations found in the Vpx treated macrophages, which biochemically validates the anti-SAMHD1 function of Vpx. By contrast, in monocyte dNTP conditions we observed no fully extended primer and only the generation of new early pause sites. This biochemical simulation suggests that efficient reverse transcription cannot occur under monocyte dNTP concentrations, posing a significant block to HIV-1 infection in this cell type.

2.3.7 Vpx requires ongoing dNTP biosynthesis to accelerate reverse transcription and rescue HIV-1 transduction.

The low dNTP pool of macrophages restricts HIV-1 infection at the reverse transcription step [5, 20, 42] . However, Vpx overcomes this restriction in macrophages by raising intracellular dNTP pools[21, 103]. As Vpx cannot elevate intracellular dNTP levels in monocytes due to the absence of ongoing dNTP biosynthesis, we next tested the hypothesis that Vpx cannot relieve the block to reverse transcription and rescue HIV-1 infection in monocytes. For this test, we treated monocytes and macrophages with VSV-G pseudotyped VLPs Vpx+ or VLPs Vpx- for 24 hours and SAMHD1 depletion was confirmed with Western Blot (Supporting Figure 2.1B). Cells were then transduced with VSV-G pseudotyped D3-HIV-GFP vector that encodes the entire NL4-3 HIV-1 sequence except the *env* gene is deleted and the *nef* gene is replaced with GFP. At 72 hours post D3-HIV-GFP transduction, the cells were assessed for transduction efficiency using flow cytometry. As

shown in Figure 7A, while Vpx was able to rescue D3-HIV-GFP transduction in macrophages with 13% of the population transduced, Vpx failed to rescue pD3-HIV-GFP transduction in monocytes to more than 0.5%. Together, these data support that despite SAMHD1 depletion, Vpx cannot rescue HIV-1 infection in monocytes as it is unable to elevate intracellular dNTP pools to accelerate reverse transcription in the absence of ongoing dNTP biosynthesis.

2.4 Discussion

Unlike rNTPs that function in multiple biological processes such as RNA synthesis, energy carriers (ATP), and cell signaling regulation (ATP and GTP), cellular dNTPs serve one vital function, to support DNA synthesis. Therefore, dNTP biosynthesis is tightly regulated to the S phase of the cell cycle[4, 206, 207]. The fidelity of this regulation is critical for proper cell replication as exemplified by cancer cells, which upregulate dNTP metabolism to support rapid and uncontrolled cell division[3, 85, 180, 211]. This elevation in turn increases mutation synthesis during DNA replication and furthers genomic instability[173, 174]. RNR has long been recognized as a cancer therapeutic target, with inhibitors such as gemcitabine used to treat pancreatic, bladder, and lung cancers in the clinic[214]. Therefore, the regulation of dNTP biosynthesis in dividing cells and how this regulation is altered by cancer cells has been extensively studied. On the other hand, dNTP metabolism in non-dividing cells such as macrophages has been presumed to be non-existent due to their low dNTP levels and absence of chromosomal DNA synthesis for cell division. Although, with this assumption, it remained unclear how Vpx could rapidly elevate dNTP levels in macrophages, as in the absence of active dNTP biosynthesis, intracellular dNTP levels should remain low even after SAMHD1 depletion.

In this study, we confirmed the observation that inhibiting RNR activity counteracts Vpx-mediated dNTP elevation in primary monocyte-derived macrophages (MDMs)[22, 213]. Moreover, we found RNR and other dNTP biosynthesis enzymes including NDPK, TK1, and DCK are expressed in macrophages. In comparison, we observed little to no expression of RNR and TK1 in monocytes, the nondividing precursors of macrophages. As RNR and TK1 participate in early events in their respective biosynthesis pathways, their absence in monocytes likely impairs dNTP biosynthesis in this cell type regardless of the expression of enzymes that act later such as NDPK. Overall, we observed upregulation of dNTP biosynthesis enzymes during monocyte differentiation in macrophages. However, it is possible that in non-dividing cells, the relative contributions from enzymes in the *de novo* synthesis and salvage pathways are different from what is observed in dividing cells.

While the expression levels of dNTP biosynthesis enzymes were upregulated during monocyte differentiation into macrophages, we observed an increase in the population of pSAMHD1 (enzymatically inactive form). Concurrently, there was an upregulation of CDK1/CyclinA2, the complex responsible for phosphorylating SAMHD1[29], accounting for the increase in pSAMHD1 during differentiation. Furthermore, we observed G1/S phase transition markers E2F-1 and CDK2 in macrophages without evidence of DNA synthesis. This supports the idea that macrophages can enter a "G1/S transition-like state" during differentiation, agreeing with a previous report that proposed a G1-like state in macrophages [72]. Mechanistically, existing in this "G1/S transition-like state" would allow for macrophages to upregulate dNTP biosynthesis and turn down dNTP hydrolysis, thus accumulating more dNTPs than monocytes. Although, macrophages have much lower dNTP levels than dividing cells due to the coexistence of dNTP biosynthesis with dNTP hydrolysis in macrophages[5].

Indeed, our data demonstrate that macrophages have higher dNTP levels than monocytes even though macrophage dNTP levels are still much lower than dNTP levels in activated $CD4^+$ T cells. Additionally, Vpx treatment did not significantly elevate dNTP levels in monocytes, despite depletion of SAMHD1, which implies Vpx cannot elevate dNTP pools without ongoing dNTP biosynthesis. Also, no detection of the phosphorylated form of SAMHD1 in monocytes indicates that most of the SAMHD1 molecules are highly active and can constantly degrade dNTPs, which likely contributes to the extremely low dNTP levels observed in monocytes. These extremely low dNTP concentrations found in monocytes inhibited efficient reverse transcription in our biochemical simulation. Furthermore, this block to reverse transcription in monocytes cannot be relieved by Vpx due to the inability of Vpx to raise intracellular dNTP pools in this cell type. Therefore, Vpx fails to accelerate reverse transcription and rescue transduction efficiency by an HIV-1 vector in monocytes. Collectively these data suggest that Vpx requires ongoing active dNTP biosynthesis for effectively counteracting the anti-lentivirus activity of SAMHD1 in macrophages. More broadly, this study proposes the idea that non-dividing cell subtypes may have differences in their dNTP metabolism and this in turn can impact HIV-1 infection. HIV-1 infection is also restricted by SAMHD1 and enhanced by Vpx in monocyte-derived dendritic cells and quiescent $CD4^+$ T-cells, two non-dividing cell types [21, 224]. Based on the results of this study, it is possible these cell types also have some level of active dNTP biosynthesis potential that Vpx utilizes to enhance HIV-1 infection.

2.5 Experimental Procedures

2.5.1 Cell culture.

293T cells were cultured in Dulbecco's modified Eagle's medium (Gibco) supplemented with 10% (v/v) fetal bovine serum (FBS) (Omega) and 1% (v/v) penicillin/streptomycin (Gibco). Primary human monocytes were isolated from peripheral blood buffy coats of three to five donors (New York Blood Center, New York City, New York) as previously described[5]. Briefly, peripheral blood mononuclear cells (PMBCs) were collected using Ficoll density gradients (Accu-Prep, Accurate Chemicals & Scientific) in SepMate-50 conicals (Stemcell Technologies). PBMCs were incubated for 30 minutes with 150 µL of CD14 antibody conjugated magnetic beads (Miltenyi) and monocytes were isolated using positive immunomagnetic selection. Primary human CD4+ T cells were then isolated from monocyte-depleted PBMCs by positive selection using anti-CD4 antibody–conjugated magnetic beads (Miltenyi). Purified human monocytes were differentiated into macrophages by culturing in RPMI (Gibco) supplemented with 10% (v/v) FBS (Omega), 1% (v/v) penicillin/streptomycin (Gibco), and 15 ng/mL GMC-SF (Miltenyi) for 5 days and incubated for an additional two days in the absence of GMC-SF. $CD4^+$ T cells were activated by culturing in RPMI (Gibco) supplemented with 10% (v/v) FBS (Omega), 1% (v/v) penicillin/streptomycin (Gibco), 5 µg/ml PHA (Sigma), and 5 ng/ml IL-2 (Miltenyi) for 2 days and were incubated for an additional two days without PHA.

2.5.2 Vectors.

VLPs Vpx+ and Vpx- were generated as previously described[225]. 80% confluent T225 flasks (Falcon) of 293T cells were transfected with 40 µg of $pSIV3^+$ or $pSIV3^+$ ΔVpx (obtained from Dr Nathaniel Landau, New York University) and 20 µg of pVSV-G using PEI. Culture media

was changed 16 hr post transfection. Culture media was then collected on days 2 and 3 post-transfection and centrifuged (1500rpm for 10 minutes) to clear cellular debris. VLPs were concentrated by ultracentrifugation (23,000rpm, for 2hr, at 4 °C) over a 25% sucrose cushion (25% sucrose, 25 mM Tris–HCl, pH 7.5, 150 mM NaCl, and 5 mM EDTA). The resulting pellet was resuspended in serum-free RPMI (Gibco) and aliquoted. Aliquots were flash frozen and stored at −80 °C unless otherwise indicated.

D3-HIV-GFP production was modified from a previous protocol[85] to obtain a plasmid-free preparation. T225 flasks of 80% confluent 293T cells were given serum-free DMEM (Gibco). Cells were transfected with 30 μg pD3HIV-GFP, which encodes the full HIV-1 NL4-3 genome with an envelope gene deletion and the nef gene replaced by an eGFP gene[5], and 5 μg pVSV-g using PolyJet (SignaGen Laboratories; SL100688). 5 hr post-transfection, the transfection media was replaced by culture media. 48 hr post-transfection culture media was harvested, centrifuged at 1500 rpm for 20 minutes and filtered through a 0.45 μm filter to remove cell debris. Cleared media was ultracentrifuged (23,000 rpm for 2 hr at 4 °C) and the pellet was resuspended in Hanks' Balanced Salt Solution (HBSS) (Gibco). This concentrated vector was treated with Turbo DNase (Invitrogen; AM2238) for 1 hr at 37 °C, aliquoted, flash frozen, and stored at -80 °C. To test that the vector no longer contains plasmid contamination, 293T cells were transduced with D3-HIV-GFP. 24 hr later DNA from these transduced cells was harvested using the Wizard SV Genomic DNA Purification System (Promega; A2360). Quantitative polymerase chain reaction (qPCR) was conducted to compare the copy number of the beta-lactamase gene, found only on the plasmid, to the copy number of late RT-products, a region downstream of the primer binding site during RT[100]. qPCR was conducted in LightCycler 480 Multiwell Plate 96 plates (Roche; 04729692001) using a Roche LightCycler 480 Instrument. The beta-lactamase primers used were

5’-GATGCTGAAGATCAGTTGGGTG-3’ and 5’-CTCAAGGATCTTACCGCTGTTGA-3’. The beta-lactamase probe used was 56-FAM/AGTGGGTT A/ZEN/CATCGAAC/3IABkFQ-3’. The late RT primers used were 5′-TGTGTGCCCGTCTGTTGTGT-3′ and 5′-GAGTCCTGCGTCGAGAGATC-3′. The late RT probe used was 5′-/56-FAM/CAGTGGCGC/ZEN/CCGAACAGGGA/3lABkFQ-3’. Copy number curves were generated using known amounts of the pD3-HIV-GFP plasmid in the LightCycler® 480 Software (Roche) which allowed us to determine copy number in the samples.

2.5.3 RNR Inhibitor Treatment.

Primary macrophages were pre-treated with either no drug, 1 mM Hydroxyurea (MedChem Express), 2 mM Hydroxyurea, 40 nM of Gemcitabine (MedChem Express), or 100 nM of gemcitabine for 2 hours before treatment with VLPs Vpx - or Vpx +. 24 hours post VLP transduction macrophages were trypsinized with Trypsin-EDTA (0.25%), phenol red (Gibco) for counting or lysed in the plate for Western Blot and dNTP measurements.

2.5.4 Western Blot.

Cells were lysed in ice cold radioimmunoprecipitation (RIPA) buffer (50 mM Tris–HCl, pH 8, 0.1% SDS, 150 mM NaCl, 0.25% deoxycholic acid, 1 mM EDTA, and 1% NP-40) supplemented with 1:500 (v/v) protease inhibitor cocktail (Sigma). Lysates were centrifuged (13,000 rpm for 10 min at 4 °C) and the cleared lysates were diluted with Laemmli buffer (Bio-Rad). Lysates were resolved on a 4-15% gradient SDS-PAGE gel (BioRad), transferred onto a

nitrocellulose membrane (BioRad), and probed with the indicated primary antibodies and corresponding secondary antibodies. Proteins were visualized using SuperSignal West Femto Maximum Sensitivity Substrate (ThermoFisher Scientific) and a BioRad ChemiDoc MP Imaging System. Primary antibodies used in this study in order of appearance: SAMHD1 (abcam; 67820), GAPDH (Cell Signaling; 14C10), RNR M1 (abcam; 137114), RNR M2 (abcam; 172476), Thymidine Kinase 1 (abcam; 76495), dCK (abcam; 96599), Nucleoside Diphosphate Kinase (abcam; 241162), p-SAMHD1 (Cell Signaling; 89930S), PP2A B55α (Cell Signaling; 4953T), CDK1 (abcam; 133327), Cyclin A2 (abcam; 181591), E2F-1 (Cell Signaling; 3742S), and CDK2 (abcam; 32147). Secondary antibodies used in this study: anti-mouse (Cytiva; NA931V) and anti-rabbit (Cytiva; NA934V).

2.5.5 dNTP Extraction

Cells were lysed in the plate with cold 65% methanol, vortexed for 2 min, incubated at 95 °C for 3 min, and centrifuged at 14,000 rpm for 3 min. The supernatant was transferred to a clean Eppendorf tube and dried using a speed vac.

2.5.6 RT-based Cellular dNTP Measurement.

Intracellular dNTP levels were measured by our HIV-1 RT-based dNTP assay as previously described[5]. Dried dNTP extracts were resuspended in 20 μL of water and further diluted until the samples were within the linear range of the assay. 5′ 32P-end-labeled 18-mer DNA primer (5′-GTCCCTCTTCGGGCGCCA-3′; Integrated DNA Technologies) was annealed to four

different 19-mer DNA templates (3′-CAGGGAGAAGCCCGCGGTX-5′; Integrated DNA Technologies), where X represents one of the four nucleotides. 2 µL of diluted extract was incubated with 200 fmol template/primer, 4 µl of purified RT (HIV-1 HXB2), 25 mM Tris–HCl, pH 8.0, 2 mM dithiothreitol, 100 mM KCl, 5 mM $MgCl_2$, and 10 µM oligo (dT) in a 20 µL reaction at 37 °C for 5 min. Water or 0.5 mM dNTP mix replaced the diluted dNTP extract for a negative and positive control, respectively. Reactions were stopped by adding 10 µl 40 mM EDTA and 99% (v/v) formamide and incubating at 95 °C for 2 min. Reactions were resolved on a 14% urea-PAGE gel (AmericanBio, Inc) and imaged using an Amersham Typhoon (Cytiva). ImageQuant TL (Cytiva) was used to quantify single-nucleotide extensions products which is used to determine the amount of dNTP present in the extract.

2.5.7 Edu Assay.

The EdU assay to measure genomic DNA synthesis was conducted using the EdU Assay / EdU Staining Proliferation Kit (iFluor 488) (abcam; 219801) following the manufacturer's protocol. Briefly, monocytes, macrophages, and positive control 293T cells were incubated with EdU for 2 hours. Cells were fixed with 4% PFA for 15 minutes, permeabilized, and labeled with the iFluor 488 dye. Unstained cells and cells that were fixed prior to EdU incubation were used as a control for fluorescent background. Flow cytometry was conducted using a FACSymphony A5 (BD Biosciences) and analyzed using FlowJo software (BD Bioscience) . Cell debris and doublets were excluded from iFluor 488 analysis. iFluor 488 gating was established on unstained cell populations.

2.5.8 Mitochondrial DNA Copy Number qPCR.

Mitochondrial DNA copy number was calculated as previously published[226]. Total DNA was extracted from activated $CD4^+$ T-cells, monocytes, and macrophages at indicated time points using the Wizard SV Genomic DNA Purification System (Promega; A2360) following the manufacturer's protocol. Quantitative polymerase chain reaction (qPCR) was performed in LightCycler 480 Multiwell Plate 96 plates (Roche; 04729692001) using a Roche LightCycler 480 Instrument. Each well contained a VIC-labeled assay for a mitochondrial DNA gene (ND1) (ThermoFisher; Assay ID Hs02596873_s1) and a FAM labeled assay for a nuclear gene (RPPH1) (ThermoFisher; Assay ID Hs03297761_s1). Each biological replicate was run in triplicate. Ct values were obtained from the LightCycler® 480 Software (Roche) and Ct values across technical replicates were averaged. ΔCt was calculated by subtracting the mitochondrial Ct value from the nuclear Ct value. Relative mitochondrial DNA content was calculated as $2 * 2^{\Delta Ct}$.

2.5.9 LC-MS/MS based dNTP measurement.

To quantify the intracellular dNTPs, an ion pair chromatography-tandem mass spectrometry method was applied as previously published [220]. Briefly, dNTPs were extracted from approximately 6 million cells per replicate. Dried dNTP extracts were resuspended in 100 µL of mobile phase A (2 mM of ammonium phosphate monobasic and 3 mM of hexylamine), and macrophage samples were further diluted five times. Samples were centrifuged at 12,000 rpm for 10 min and 45 µL of the resulting supernatant was mixed with 5 µL of ^{13}C and ^{15}N labeled dNTPs to serve as internal standards. Calibration curves were generated from standards by serial dilutions

in mobile phase A (0.2 – 500 nM). Chromatographic separation and detection was performed on a Vanquish Flex System (Thermo Scientific, Waltham, MA) coupled with a TSQ Quantiva triple quadrupole mass spectrometer (Thermo Scientific, Waltham, MA). Samples were separated on a Kinetex EVO-C18 column (100 X 2.1 mm, 2.6 µm) (Phenomenex, Torrance, CA). The gradient increased from 8% to 35% of mobile phase B (acetonitrile) in 5 min then returned to 8% mobile phase B. Thermo Xcalibur 3.0 software was used for data collection and processing. Selected reaction monitoring in both positive and negative modes was used to detect the four dNTPs: dATP (492→136, pos), dGTP (508→152, pos), dCTP (468→112, pos), TTP (481→158.9, neg).

2.5.10 VLP Vpx treatment of monocytes and macrophages.

Freshly isolated monocytes were concentrated to 500,000 cells per 200 µL in a 48-well plate and treated with 50 µL freshly harvested VLP Vpx- or Vpx+ for 24-hours. Fully differentiated macrophages in 24-well plates were treated with 25 µL freshly harvested VLP Vpx- or Vpx+ for 24-hours. Approximately 6 million cells were used per replicate. Cells were washed thoroughly with saline before dNTP extraction and reserved wells were used for counting and Western Blot. dNTP measurement was conducted using mass spectrometry.

2.5.11 Cell Volume of Monocytes and Macrophages.

Glass bottom chambered coverslips (ibidi; 80807) were treated with 0.1 mg/mL poly-D-lysine overnight, washed with PBS, and air dried. 200,000 monocytes were loaded with CellTracker Green CMFDA Dye (ThermoFischer; C7025) for 30 minutes. Cells were washed,

resuspended in 200 uL of PBS, and plated onto the chambered coverslips. Cells were incubated for 2hr covered at room temperature to allow cells to settle onto the coverslip. Supernatant was gently aspirated, and cells were fixed to the coverslip using 4% PFA for 15 minutes. Cells were washed, coated in VECTASHIELD Antifade Mounting Medium (Vector Laboratories; H-1000-10), and stored at 4 °C until imaging. Macrophages were differentiated and cultured on the treated chamber coverslips. Fully differentiated macrophages were loaded with CellTracker Green CMFDA Dye, fixed with 4% PFA, washed, covered with VECTASHIELD and stored at 4 °C until imaging. Cells were imaged using a 60x objective on a Nikon Spinning Disk Confocal Microscope where Z-stacks were taken with 0.2 μM steps. 10 fields of vision were captured per sample. Volume for each cell in a field was determined using the surface tool in Imaris software (Oxford Instruments; Version 9.9.0). Touching objects were split morphologically and cells on the border of the image were excluded. Volume was calculated for over 200 cells per cell type. Median cell volume was obtained per field. Final volume is reported as a weighted average of median cell volume per field based on cell count per field.

2.5.12 Monocyte and macrophage dNTP Concentration.

Monocyte and macrophage dNTP concentration was calculated using the mean value from the measurement of each dNTP and the reported cell volumes.

2.5.13 Primer Extension Assay.

The primer extension assay was modified from previous publications [5, 124]. A 5′ ^{32}P-labeled 17-mer DNA primer (5′-CGCGCCGAATTCCCGCT-3′, Integrated DNA Technologies) was annealed to a 40-mer template RNA (5′AAGCUUGGCUGCAGAAUAUUGCUAGC GGGAAUUCGGCGCG-3′, Integrated DNA Technologies) in the presence of 3-fold excess template. Reactions (20uL) contained 10nM annealed primer/template, 25 mM Tris–HCl, pH 8.0, 2 mM dithiothreitol, 100 mM KCl, 5 mM $MgCl_2$, 10 μM oligo (dT), indicated dNTP concentrations, and a variety of concentrations of HIV-1 RT (from HXB2). Reactions were incubated 37 °C for 5 min and stopped by adding 10 μl 40 mM EDTA and 99% (v/v) formamide followed by incubation at 95 °C for 2 min. This allows for multiple rounds of extension of the DNA primer. A variety of HIV-1 RT concentrations were used to ensure the reactions were conducted in the linear range. Reactions were resolved using a 14% urea-PAGE gel (AmericanBio, Inc) and imaged using an Amersham Typhoon (Cytiva).

2.5.14 HIV-vector and VLP Vpx treatment of monocytes and macrophages.

Freshly isolated monocytes were concentrated to 500,000 cells per 200 μL in a 48-well plate and treated with 50 μL freshly harvested VLP Vpx- or Vpx+ for 24 hr. Fully differentiated macrophages in 24-well plates were treated with 25 μL freshly harvested VLP Vpx- or Vpx+ for 24 hr. After 24 hr monocytes and macrophages were transduced with 40 μL and 20 μL, respectively, of D3HIV-GFP. Cells not transduced with either vector were used as a negative control. After 72 hr cells were harvested for Western Blot and flow cytometry. Western blot was used to measure SAMHD1 expression levels at the time of sample harvest. Flow cytometry was used to measure transduction efficiency by measuring GFP+ cell populations. For flow cytometry

cells were fixed with 4% PFA and assessed for GFP using a FACSymphony A5 (BD Biosciences). Cell debris and doublets were excluded from GFP analysis and GFP gating was established on the untransduced negative control cell populations. Samples were analyzed using FlowJo software (BD Bioscience).

2.5.15 Statistical Analyses.

All experiments in this study were conducted in triplicate (n = 3). Individual values are reported in each figure and the mean of these replicates is reflected by the bars on the graphs. Error bars in each figure represent standard deviation. All statistical analyses were conducted using two-tailed and unpaired Welch's *t* tests in Prism (Graphpad) and the resulting p-values are included in each figure. A p-value < 0.05 was considered to be statistically significant.

2.6 Data Availability

All data generated and analyzed during this study are included in this chapter.

2.7 Funding

This study was supported by the NIH F31 AI157884 (to N.E.B.), and AI136581 and AI162633 (to B.K.). The content is solely the responsibility of the authors and does not necessarily reflect the official views of the National Institute of Health.

2.8 Author Contributions

N.E.B.: Acquisition of data, analysis and interpretation of data, drafting and editing manuscript, and funding acquisition. S.T.: Acquisition of data, analysis and interpretation of data. Y-J.C.: Acquisition of data. R.F.S.: Conception and funding acquisition. B.K.: Conception, supervision, editing and finalizing manuscript, and funding acquisition.

2.9 Conflict of Interest Statement

The authors declare they have no conflicts of interest.

2.10 Acknowledgements

This study was supported in part by the Emory Flow Cytometry Core (EFCC), one of the Emory Integrated Core Facilities (EICF) and is subsidized by the Emory University School of Medicine. Additional support was provided by the National Center for Georgia Clinical & Translational Science Alliance of the National Institutes of Health under Award Number UL1TR002378. Research reported in this publication was also supported in part by the Emory University Integrated Cellular Imaging Core and Children's Healthcare of Atlanta. The content is solely the responsibility of the authors and does not necessarily reflect the official views of the National Institute of Health.

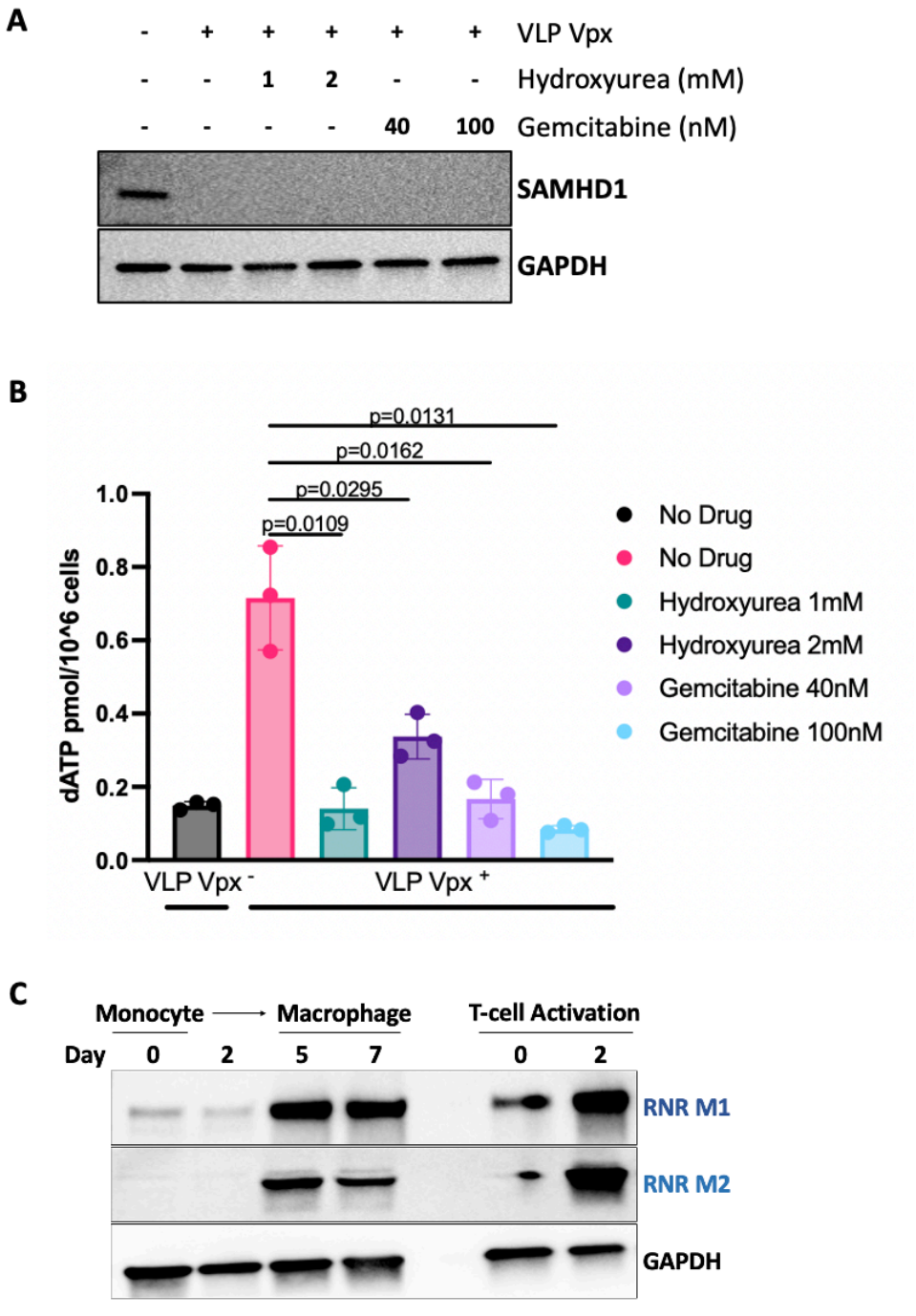

Figure 2.1: Effect of RNR inhibition on Vpx-mediated dNTP elevation in macrophages. Primary human monocytes were isolated and pooled from 5 independent healthy donors and differentiated into monocyte-derived macrophages (MDMs) using GM-CSF. $CD4^+$ T-cells were isolated from the same donors and activated with PHA and IL-2. Fully differentiated macrophages

were pretreated with indicated drug concentration and transduced using VLP Vpx+ or VLP Vpx- as a negative control. **A)** Cellular SAMHD1 expression was evaluated using Western Blot with GAPDH as a loading control. **B)** Intracellular dATP levels were determined by RT-based dNTP assay. Data are the mean of three replicates and error bars reflect standard deviation from the mean. P-values were determined using two-tailed, unpaired Welch's t-test to the no drug, VLP Vpx+ condition. **C)** Samples were collected at indicated time points during primary monocyte differentiation into MDMs. Samples from the indicated time points during $CD4^+$ T-cell activation were used as a positive cycling cell control. Cellular expression levels of the RNR M1 and RNR M2 subunits were evaluated using Western Blot with anti-RNR M1 and anti-RNR M2 antibodies, respectively. GAPDH expression was used as a loading control.

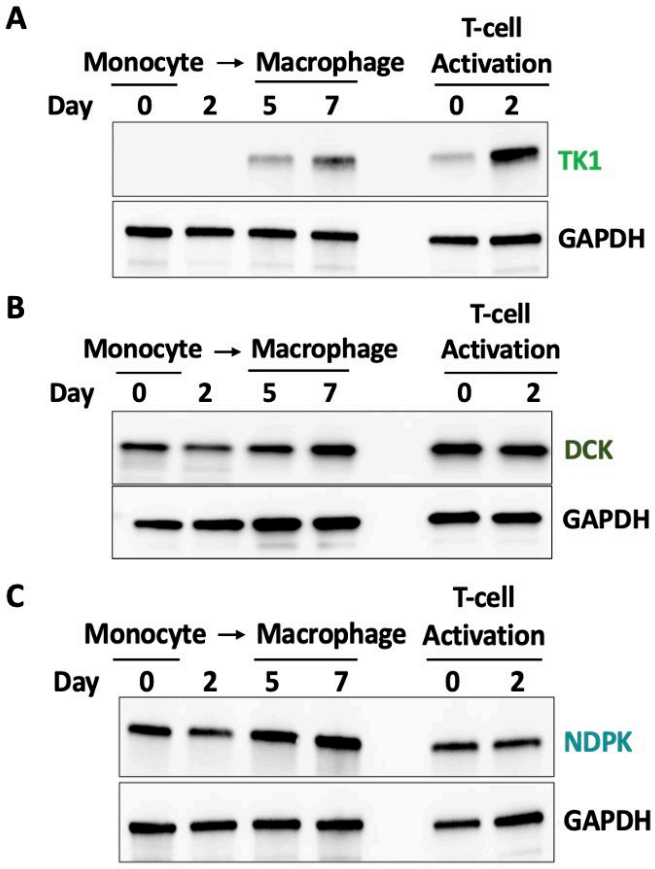

Figure 2.2: Expression of dNTP biosynthesis enzymes throughout monocyte differentiation to macrophages. Primary human monocytes were isolated from 5 healthy independent donors and differentiated into monocyte derived macrophages (MDMs) using GM-CSF. $CD4^+$ T-cells isolated from these same donors and were activated using PHA and IL-2 as a dividing cell control. Samples were collected for Western Blot at indicated time points. Cellular expression levels of **A)** Thymidine Kinase 1 (TK1), **B)** Deoxycytidine Kinase (DCK), and **C)** Nucleoside Diphosphate Kinase (NDPK) were assessed using respective primary antibodies. GAPDH expression was evaluated using an anti-GAPDH antibody as a loading control.

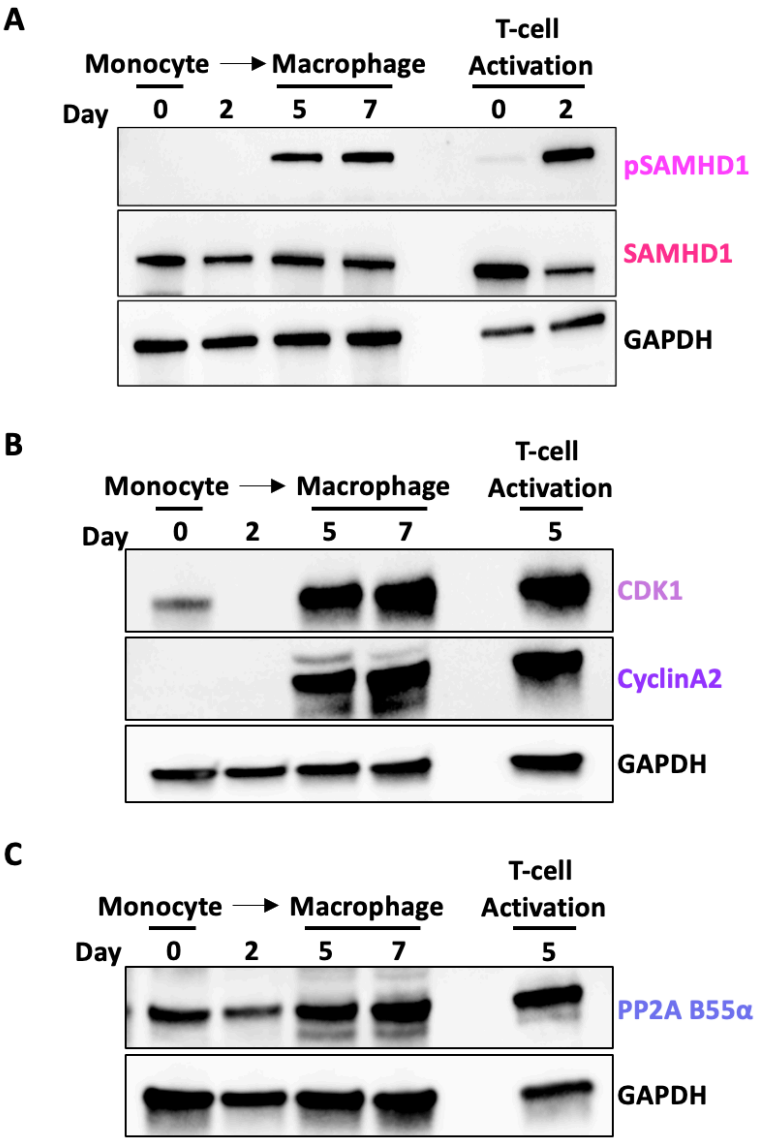

Figure 2.3: Expression of SAMHD1 and SAMHD1 dephosphorylation/ phosphorylation enzymes throughout monocyte differentiation to macrophages. Primary human monocytes were isolated from 5 healthy independent donors and differentiated into monocyte derived macrophages (MDMs) using GM-CSF. $CD4^+$ T-cells isolated from these same donors and were activated using PHA and IL-2 as a dividing cell control. Samples were collected for Western Blot at indicated time points. Cellular expression levels of **A)** T592 phosphorylated SAMHD1 (pSAMHD1) and total SAMHD1 **B)** Cyclin Dependent Kinase 1 (CDK1) and CyclinA2 **C)** Protein

Phosphatase2A B55α subunit (PP2A B55α) were assessed using respective primary antibodies. GAPDH expression was evaluated using an anti GAPDH antibody as a loading control.

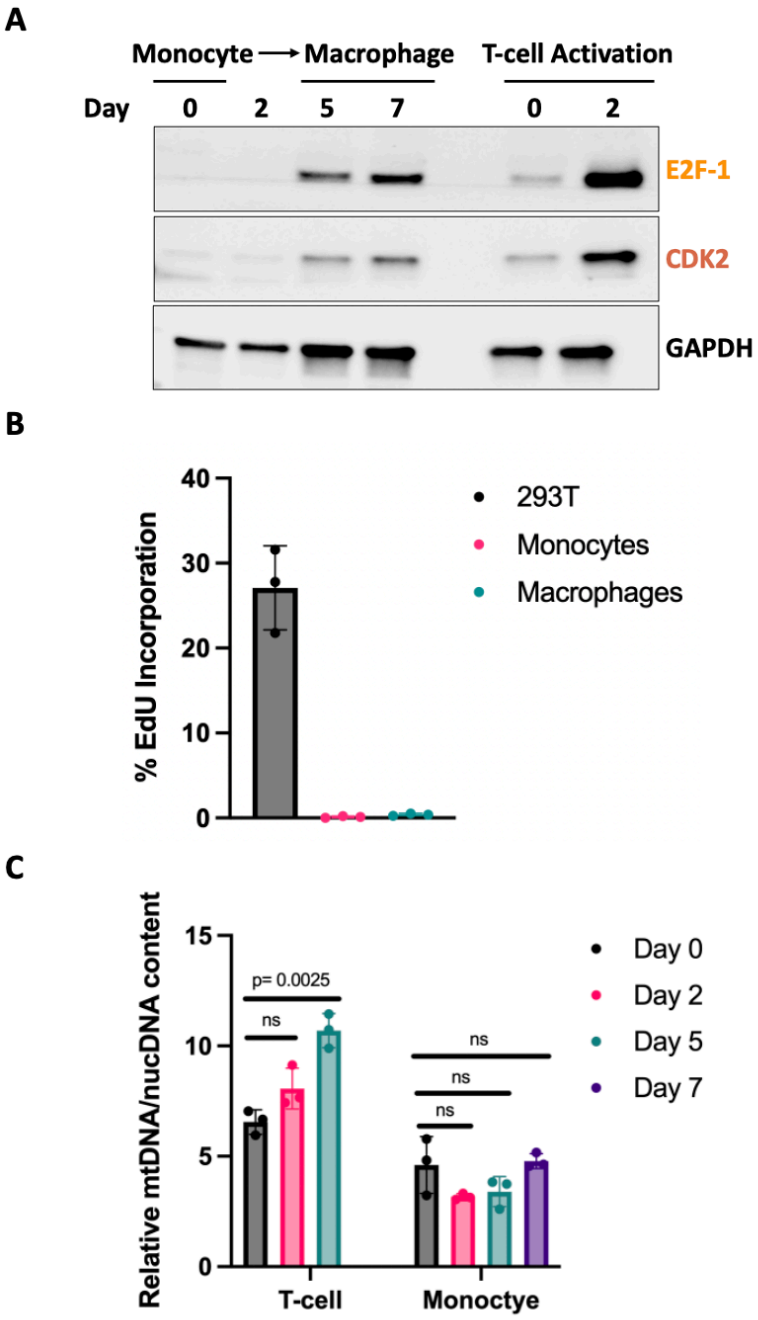

Figure 2.4: Cell cycle state during monocyte differentiation to macrophages. Primary human monocytes were isolated from **A)** 5 and **B,C)** 3 healthy independent donors and differentiated into monocyte derived macrophages (MDMs) using GM-CSF. $CD4^+$ T-cells isolated from these same donors and were activated using PHA and IL-2 as a dividing cell control. **A)** Samples were collected for Western Blot at indicated time points. Cellular expression levels of transcription

factor E2F1 and Cyclin Dependent Kinase 2 (CDK2) were assessed using respective primary antibodies. GAPDH expression was evaluated using an anti-GAPDH antibody as a loading control. **B)** Genomic DNA synthesis was evaluated using an EdU incorporation assay. Primary monocytes without GM-CSF exposure and fully differentiated MDMs were incubated with EdU for 2 hours followed by EdU labelling with an iFluor 488 florescent azide. 293T cells were used as a dividing cell control. iFluor 488 labeled EdU incorporation was determined using flow cytometry. **C)** Mitochondrial DNA copy number was measured at indicated time points throughout $CD4^+$ T-cell activation and monocyte differentiation using qPCR. Genomic DNA copy number was measured using qPCR within the same samples to normalize the mitochondrial DNA copy number. Data are the mean of three replicates and error bars reflect standard deviation from the mean. P-values were determined using two-tailed, unpaired Welch's t-test to the day 0 time point for T-cells or monocytes.

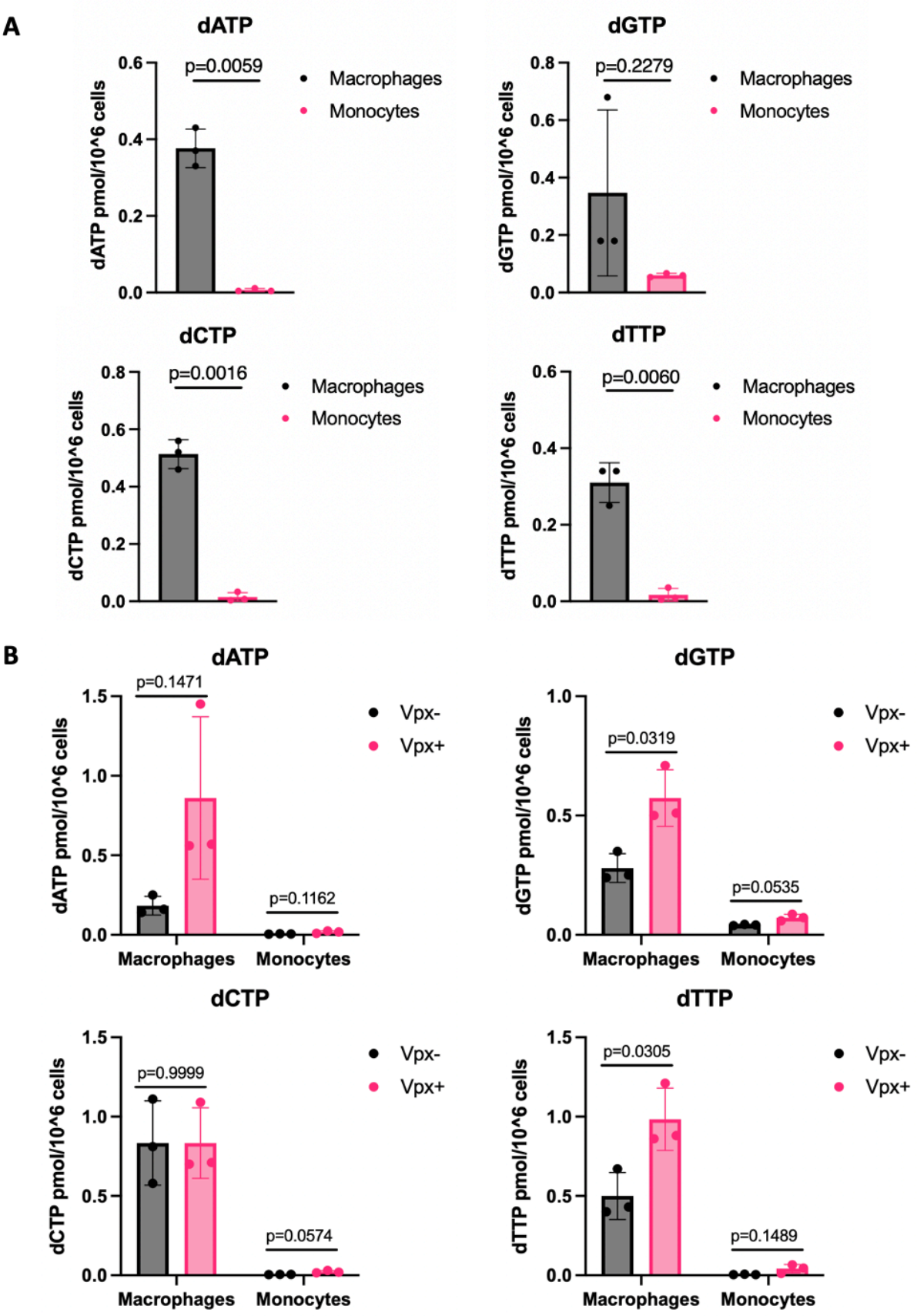
A
dATP
p=0.0059
Macrophages
Monocytes
dATP pmol/10^6 cells
0.0
0.2
0.4
0.6
dGTP
p=0.2279
dGTP pmol/10^6 cells
0.0
0.2
0.4
0.6
0.8
dCTP
p=0.0016
dCTP pmol/10^6 cells
dTTP
p=0.0060
dTTP pmol/10^6 cells
B
dATP
p=0.1471
p=0.1162
Vpx-
Vpx+
dATP pmol/10^6 cells
0.0
0.5
1.0
1.5
Macrophages
Monocytes
dGTP
p=0.0319
p=0.0535
dGTP pmol/10^6 cells
dCTP
p=0.9999
p=0.0574
dCTP pmol/10^6 cells
dTTP
p=0.0305
p=0.1489
dTTP pmol/10^6 cells

Figure 2.5: Effect of Vpx on dNTP levels in primary monocytes and macrophages. Primary human monocytes were isolated from 3 healthy independent donors and differentiated into monocyte derived macrophages (MDMs) using GM-CSF. **A)** Cellular dNTP levels of fully differentiated macrophages and monocytes without GM-CSF exposure were analyzed using LC-MS/MS. **B)** Fully differentiated macrophages and monocytes without GM-CSF exposure were treated with VLPs Vpx+ for 24 hours. Treatment with VLPs Vpx- was used as a negative control. dNTP levels were measured using LC-MS/MS. Data are the mean of three replicates and error bars reflect standard deviation from the mean. P-values were determined using two-tailed, unpaired Welch's t-test to A) macrophages and B) VLPs Vpx- treated macrophages or monocytes.

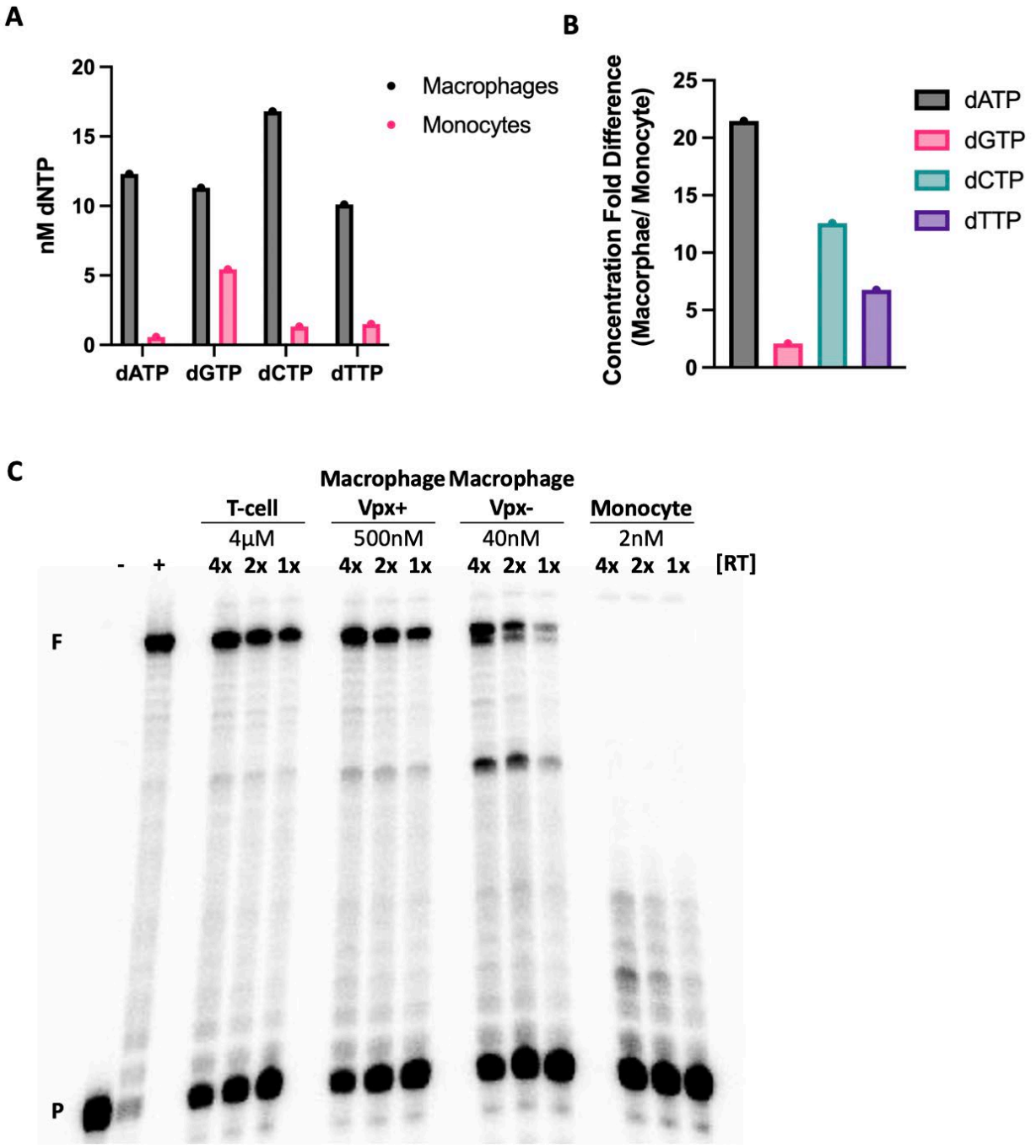

Figure 2.6: HIV-1 Reverse transcription biochemical simulation in monocyte dNTP concentrations. A) Monocyte and macrophage dNTP concentrations using dNTP levels from Figure 2.5A. **B)** dNTP concentration fold differences between monocytes and macrophages. **C)** A primer extension reaction using 5′ ^{32}P-labeled 17-mer DNA primer (P) annealed to 40-mer

template RNA, purified HIV-1 reverse transcriptase (RT), and dNTP concentrations found in primary activated CD4+ T-cells, macrophages treated with VLPs Vpx+, macrophages treated with VLPs Vpx-, and monocytes. A variety of RT was utilized to ensure the reactions were in the linear range. -: Negative control using water in place of dNTPs. +: Positive control using 5 μM dNTPs and undiluted RT. P: 17-mer unextended primer. F: 40-mer fully extended primer.

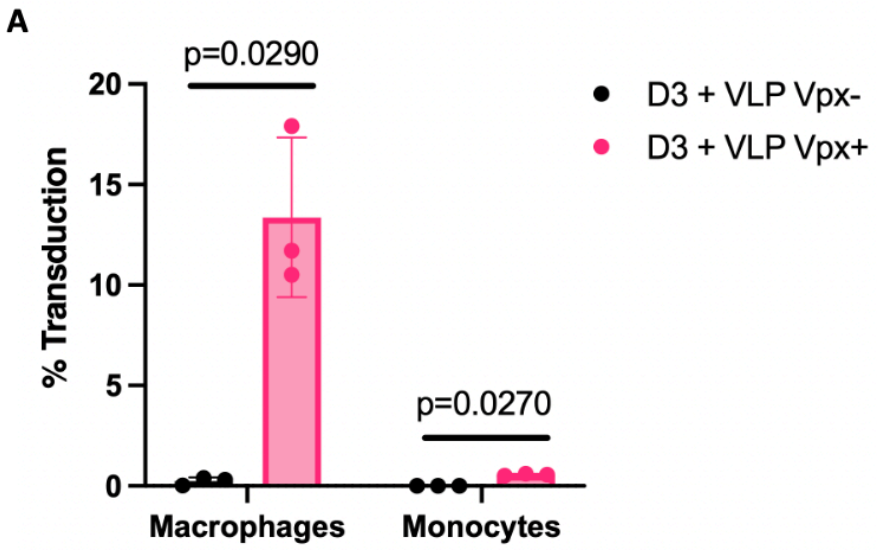

Figure 2.7: Effect of Vpx on HIV-1 vector transduction of monocytes and macrophages: A) Primary human monocytes were isolated from 3 healthy independent donors and differentiated into monocyte derived macrophages (MDMs) using GM-CSF. Fully differentiated macrophages and monocytes without GM-CSF exposure were treated with VLPs Vpx+ for 24 hours. VLPs Vpx- treatment was used as a negative control. Cells were then transduced with a VSV-G pseudotyped and GFP labelled HIV-1 vector. 72 hours later cells were harvested, and transduction efficiency was measured using flow cytometry. Data are the mean of three replicates and error bars reflect standard deviation from the mean. P-values were determined using two-tailed, unpaired Welch's t-test to VLPs Vpx- treated macrophages or monocytes.

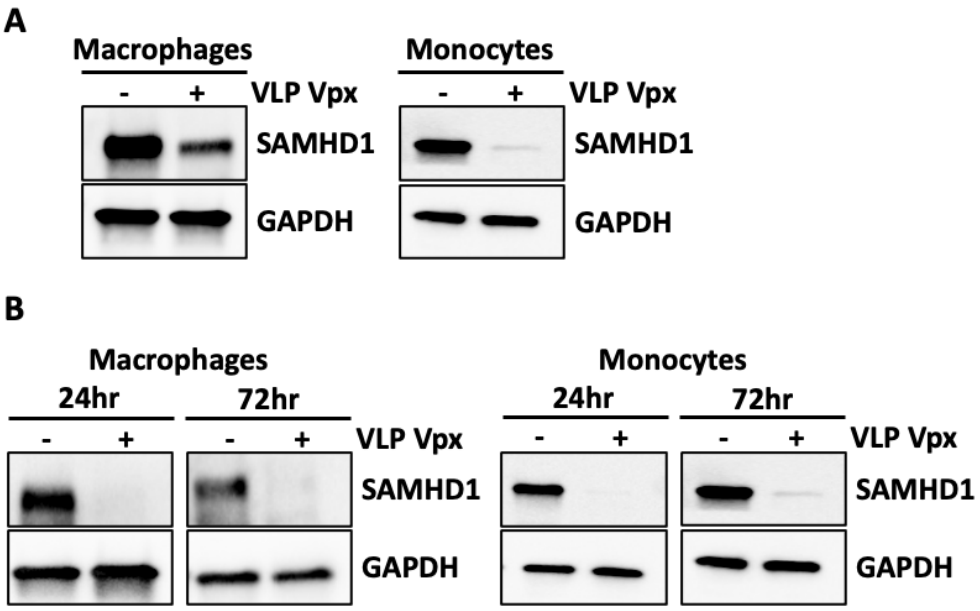

Supporting Figure 2.1: SAMHD1 expression in macrophages and monocytes treated with VLPs: Western Blots for cellular SAMHD1 in macrophages and monocytes treated with VLPs Vpx- or VLPs Vpx+ for **A)** dNTP measurements (Figure 2.5B) and **B)** 24 and 72 hours post HIV-1 vector transduction (Figure 2.7A). Western Blot for GAPDH was used as a loading control.

A

	Monocyte	Macrophage
Total Cell Count	213	239
Fields of Vision	9	4
Minimum Field Median Volume (µM^3)	672.71	2837.35
Maximum Field Median Volume (µM^3)	1776.59	3264.22
Weighted Average of Field Medians Volume (µM^3)	1108.95	3063.29

Supporting Table 2.1: Monocyte and Macrophage Cell Volume Statistics.

Chapter 3

Elevation of intracellular dNTP Levels: A mechanistic role of SAMHD1 cancer mutations.

Nicole E. Bowen[1*], Joshua Temple[2*], Caitlin Shepard[1], Adrian Oo[1], Fidel Arizaga[2], Priya Kapoor-Vazirani [3], Mirjana Persaud[4], Corey H. Yu [5], Dong-Hyun Kim[6], Raymond F. Schinazi[1], Dmitri N. Ivanov[5], Felipe Diaz-Griffero[4], David S. Yu[3], Yong Xiong[2,] Baek Kim[1,7,]

Published in part as: *Structural and functional characterization explains loss of dNTPase activity of the cancer-specific R366C/H mutant SAMHD1 proteins.* J Biol Chem. 2021;297(4):101170. Epub 2021/09/08. doi: 10.1016/j.jbc.2021.101170. PubMed PMID: 34492268; PMCID: PMC8497992.

[1.] Department of Pediatrics, School of Medicine, Emory University, Atlanta, GA USA.

[2.] Department of Molecular Biophysics and Biochemistry, School of Medicine, Yale University, New Haven, CT USA.

[3.] Department of Radiation Oncology, School of Medicine, Emory University, Atlanta, GA USA.

[4.] Department of Microbiology and Immunology, Albert Einstein College of Medicine, Bronx, NY USA.

[5.] Department of Biochemistry and Structural Biology, University of Texas Health San Antonio, San Antonio, TX USA.

[6.] School of Pharmacy, Kyung-Hee University, Seoul, South Korea.

[7.] Children's Healthcare of Atlanta, Atlanta, GA USA.

[*]These authors contributed equally to this work.

3.1 Abstract

Elevated intracellular levels of deoxy-nucleotide triphosphates (dNTPs) have been shown to be a biochemical marker of cancer cells. Recently, a series of mutations in the multi-functional dNTPase, SAMHD1, have been reported in various cancers. Here we investigated the structure and functions of SAMHD1 R366C/H mutants, found in colon cancer and leukemia. Unlike many other cancer-specific mutations, the SAMHD1 R366 mutations do not alter cellular protein levels of the enzyme. However, R366C/H mutant proteins exhibit a loss of dNTPase activity, and their X-ray structures demonstrate the absence of dGTP substrate in their active site, likely due to loss of interaction with γ-phosphate of the substrate. The R366C/H mutants failed to reduce intracellular dNTP levels and restrict HIV-1 replication, functions of SAMHD1 that are dependent on the ability of the enzyme to hydrolyze dNTPs. However, these mutants retain dNTPase-independent functions, including mediating double-stranded DNA break repair, interacting with CtIP and Cyclin A2, and suppressing innate immune responses. Finally, SAMHD1 degradation in human primary activated/dividing CD4+ T cells further elevates cellular dNTP levels. This study suggests that the loss of SAMHD1 dNTPase activity induced by R366 mutations can mechanistically contribute to the elevated dNTP levels commonly found in cancer cells.

3.2 Introduction

Sterile alpha motif (SAM) domain and histidine-aspartic acid (HD) domain containing protein 1 (SAMHD1) is a dNTP triphosphohydrolase (dNTPase) that hydrolyzes dNTP substrates into their deoxynucleotide (dN) and triphosphate (TP) subparts[19, 20, 53]. Mutations in SAMHD1

were first reported in patients with a rare genetic neuro-immunological disorder, Aicardi-Goutières Syndrome (AGS)[137]. AGS patients develop hyperactivation of the innate immune response in the absence of infection, which interferes with brain development and causes death at early ages[135]. As proposed for other AGS-related proteins such as TREX1[138], RNase H2[141] and ADAR[142], SAMHD1 mutations may interrupt cellular nucleic acid metabolism, which can trigger hyper-interferon responses[143]. In addition, SAMHD1 dNTPase activity restricts HIV-1 infection in nondividing myeloid cells[21, 103]. SAMHD1 mediated intracellular dNTP depletion kinetically suppresses the reverse transcription step of HIV-1, which consumes intracellular dNTPs during proviral DNA synthesis[22, 23]. SAMHD1 also inhibits the replication of other viruses[27, 127, 157, 225, 227] as well as retrotransposons[228, 229].

SAMHD1 harbors additional biological activities that are independent of the enzyme's dNTPase capability. First, SAMHD1 is involved in dsDNA break repair, which requires interaction with CtlP in order to promote DNA end resection and homologous recombination during repair[159]. Next, SAMHD1 promotes cellular DNA replication by facilitating the removal of nascent DNAs at stalled replication forks by enhancing Mre11 nuclease[162]. This process appears to reduce the synthesis of cellular nucleic acid products that can induce innate immunity activation[162]. Additionally, SAMHD1 suppresses the innate immune response by inhibiting NF-κB and IRF7 activation by reducing the phosphorylation of the NF-κB inhibitory protein, IκBα, and reducing inhibitor-κB kinase ε (IKKε) mediated IRF7 phosphorylation, respectively[148, 150]. SAMHD1 also blocks LTR-mediated HIV-1 transcription,[101] a process known to require NF-κB[230]. Finally, SAMHD1 binds single-stranded nucleic acids, primarily when in the monomeric form[102, 144].

SAMHD1 activity is regulated at multiple levels. First, the enzymatically active SAMHD1 tetramer is formed when dGTP/GTP and dNTPs bind to two allosteric sites of SAMHD1, A1 and A2, respectively[51, 52, 54]. Second, the phosphorylation of SAMHD1 residue T592 at the enzyme's C-terminal tail by Cyclin A2/CDK1/CDK2 regulates HIV-1 restriction activity[69]. However, phosphorylated inactive SAMHD1 becomes dephosphorylated by cellular PP2A-B55a phosphatase during mitotic exit of dividing cells[32]. Finally, while SAMHD1 restricts HIV-1 replication in nondividing myeloid cells such as macrophages and microglia, HIV-2 and some SIV strains effectively escape from SAMHD1 restriction by employing their accessary proteins , Vpx or Vpr, to proteasomally degrade SAMHD1 and elevate dNTP levels[21, 103, 115], which enables these lentiviruses to replicate rapidly even in nondividing myeloid cells[23, 105].

Cancer cells harbor 6-11-fold higher intracellular dNTP levels than normal cells and this dNTP elevation is a biochemical marker of cancer cells[180]. Elevated intracellular dNTP level is mechanistically tied with uncontrolled/rapid cell division and higher cell population at S phase of cancer cells where dNTP biosynthesis is activated[85]. Recently, a series of SAMHD1 mutations have been reported in various cancer cells including leukemias[160, 181-184], lymphomas[185, 186], lung cancer[171], and colon cancer[188-190]. However, it is unclear how these SAMHD1 mutations mechanistically contribute to cancer cell phenotypes. Importantly, as observed for SAMHD1 mutations in AGS cells[81, 135], SAMHD1 cancer-associated mutations are found throughout the entire protein and most cause reduced SAMHD1 protein levels[160]. These low protein levels could be indicative of their structural alterations, which makes it difficult to investigate the mechanistic and functional alternations made by the SAMHD1 cancer mutations. In this report, we structurally and functionally investigated R366C/H SAMHD1 mutations, found in leukemia[184] and colon cancer[188, 189], but not in AGS. Notably, the R366C/H mutants possess protein stability profiles

comparable to wild type and retained all functions tested except dNTPase activity. This study suggests that SAMHD1 mutations can contribute to the intracellular dNTP level elevation commonly observed in cancer cells.

3.3 Results

3.3.1 R366C/H mutants are cancer-associated mutants with wild type protein expression level.

To investigate the impact of cancer-associated mutations on SAMHD1 functions, we searched for SAMHD1 mutants showing wild type level cellular protein stability. For this, we conducted a screen of multiple SAMHD1 mutants for their cellular stability in 293T cells transfected with an equal amount of SAMHD1 expression plasmids (Figure 3.1A). SAMHD1 mutants selected for the screen include Leukemia-associated mutants[160], R145Q, Y155C, P158S, and R451C, which are located in the allosteric sites of the enzyme (Figure 3.1B). R366C, found in both colon cancer[189] and leukemia[184], and R366H, found in colon cancer[188], are located in the enzyme's catalytic site (Figure 3.1B). Notably, the R366 residue coordinates the γ-phosphate group of the dNTP substrate in the catalytic pocket. Finally, I201N, found in leukemia[160] is located outside of both of these functional domains (Figure 3.1A). As shown in an immunoblot assay with the transfected 293T cells (Figure 3.1C), R145Q, Y155C, P158S, I201N, and R451C displayed a marked reduction in expression level when compared to wild type SAMHD1, suggesting their cellular protein instability. This finding is consistent with previous reports which show decreased SAMHD1 expression in primary cells harboring SAMHD1 mutations isolated from Leukemia patients[160]. Importantly, the R366C/H mutants show similar expression levels to wild type

SAMHD1. Mutants from this initial screen that have poor cellular expression profiles likely possess several functional impairments due their general protein instability. However, the unaltered cellular expression of R366C and R366H allowed us to use these mutants as a tool for investigating which functions of SAMHD1 may be implicated in the enzyme's role in cancer cells.

3.3.2 Biochemical analyses of protein stability and structural integrity of R366C/H mutants.

In order to further probe the overall protein stability changes induced by the R366C/H mutations, we overexpressed wild type and mutant SAMHD1 proteins in *E. coli* and purified these proteins for several biochemical and biophysical analyses. First, we employed a thermal shift assay to monitor the temperature-dependent stability of the SAMHD1 proteins. For this, each protein was incubated with activator dGTP and Sypro Orange, and denaturation was monitored by increased relative fluorescence, as a function of temperature (Figure 3.2A). Y155C, which displayed reduced cellular expression levels in 293T cells (Figure 3.1C), exhibited an altered thermal shift curve and melting temperature (T_m). Conversely, R366C and R366H displayed only minor alterations in thermal shift curves and melting temperatures. These minor alterations are not sufficient to induce changes in cellular protein level (Figure 3.1C). As mutants that showed altered cellular protein stability had alterations in the allosteric site residues, it is possible that these stability changes are due to an inability to form the more stable tetramer conformation. To understand how differences in ability to form tetramers might underpin the stability changes provoked by these mutations we utilized a cross-linking assay[50]. Purified proteins were incubated with activator dGTP in order to induce tetramerization and formaldehyde cross-linked products were analyzed using SDS-PAGE (Figure 3.2B). The two stable R366C/H mutants were able to

form tetramers comparable to wild type SAMHD1. However, Y155C, representative of an unstable mutant, was unable to form tetramers. This suggests that the ability to form tetramers in the presence of dGTP activator may lead to the instability displayed by some cancer mutants. However, these data would suggest that the R366C/H mutations do not impair oligomerization, further supporting the intact structural integrity of the two R366C/H mutant proteins.

HIV-2 and SIV code for Viral Protein X (Vpx) which targets SAMHD1 for proteolytic degradation, thus relieving restriction in non-dividing cells[21, 103, 108]. As the Vpx binding site on SAMHD1 is dependent on the protein's three-dimensional structure[106], we utilized a Vpx degradation assay to further probe changes in structure[127]. For this test, we transiently co-overexpressed Vpx with wild type or R366C/H SAMHD1 in 293T cells and monitored SAMHD1 degradation using immunoblot (Figure 3.2C). Wild type SAMHD1 was successfully degraded by Vpx and R366C/H was comparably degraded. Overall, the multiple biochemical and cellular analyses validate that the three-dimensional structure of these R366C/H mutants is relatively preserved.

3.3.3 Cancer-associated SAMHD1 mutants have significantly reduced dNTPase activity.

SAMHD1 is a dNTP triphosphohydrolase that degrades dNTPs into their deoxynucleotide and triphosphate components[19, 20, 53]. As dNTP levels in cancer cells are 6-11-fold higher than that of normal cells[180], we hypothesized that cancer-associated SAMHD1 mutants would have reduced dNTPase activity, ultimately elevating intracellular dNTP levels. To test the dNTPase activity of SAMHD1 cancer mutants, we purified the catalytic core HD domain (residues 113-626) of some SAMHD1 mutants including R366C/H. We then incubated the purified enzymes with [α-^{32}P]dGTP

in the presence of an excess unlabeled dGTP[54]. dGTP not only binds to the two allosteric sites of SAMHD1 for activation but also serves as a substrate[20, 53]. Production of labeled triphosphate product (PPP) was monitored by TLC-based dNTPase assay (Figure 3.3A). A no-enzyme control (*NE*) and a calf intestinal phosphatase control (*CIP*) were used to detect [α-^{32}P]dGTP substrate and monophosphates (*P*), respectively. Incubation times were chosen such that product formation was in the linear range under saturating dNTP concentrations. Percent dGTP hydrolysis was calculated by dividing the triphosphate product by the lane total (Supporting Figure 3.1). Relative dGTPase activity was calculated by subtracting the no enzyme control condition from percent hydrolysis and normalizing to WT. Interestingly, the dGTPase activity of R145Q, Y155C, P158S, and R366C is severely impaired compared to wild type SAMHD1 (Figure 3.3B). R366H possesses significantly lower dGTPase activity than wild type, but is more active than R366C. It is possible that the substitution of a positively charged histidine residue at position 366 is able to mediate minor coordination of the negatively charged γ-phosphate group of the dNTP substrate, whereas cysteine cannot mediate this interaction.

Given the R366C/H mutants displayed unaltered cellular protein levels but possessed reduced dGTPase activity, we performed a complete analysis of the dNTPase activity of these mutants. Therefore, we conducted the TLC-based dNTPase assay with the three remaining radioactive dNTP substrates (dATP, dCTP, and dTTP) where the unlabeled substrate and activator dGTP were in excess (Figure 3.3C). Both the R366C and R366H mutants showed reduced dNTPase activity when incubated with each dNTP tested in comparison to wild type SAMHD1. Together with the unaltered cellular protein level of R366C and R366H, this significantly impaired hydrolysis activity suggests that alterations in the dNTPase activity of SAMHD1 may mechanistically involve the enzyme in the elevated dNTP pools observed in cancer cells.

3.3.4 X-ray crystal structures of R366C/H mutants.

For both the R366C and R366H mutants, we crystallized the HD domain of SAMHD1 (residues 113-626) in the presence of dGTP, which is capable of binding both allosteric sites 1 and 2 as well as the catalytic site of SAMHD1[52]. In the catalytic site of wild type protein, the R366 guanidinium group neutralizes the negative charge of the dNTP substrate γ-phosphate and interacts with D506 to stabilize the bound nucleotide (Figure 3.4A). An established catalytically inactive mutant (H206R/D207N; $SAMHD1_{HD/RN}$) was used to prevent hydrolysis but retain binding capacity of dGTP during crystallization. Crystals for R366C and R366H diffracted to a resolution of 1.9 Å and 3.6 Å, respectively.

Inspection of each R366 mutant structure shows neither mutation impairs oligomerization or induces significant deviations from its tetramer structure as compared to a previously solved dGTP-bound $SAMHD1_{HD/RN}$ tetramer ($RMSD_{R366C}$: 0.36 Å and $RMSD_{R366H}$: 0.39 Å when compared with PDB 4BZB). However, unlike wild type protein structure that displays dGTP substrate bound to the catalytic site, no nucleotide density was observed in the catalytic pocket of either mutant (Figure 3.4B, Supporting Figure 3.2), thus confirming that substitution of a cysteine or histidine side chain at residue 366 renders $SAMHD1_{HD/RN}$ deficient in stably binding dGTP at the catalytic site despite tetramerization. Uniquely, when dGTP was modelled to fit the catalytic site of R366H mutant, N ε2 of the mutant R366H side chain sits close to the γ-phosphate position in a modeled dGTP-bound structure and is therefore theoretically capable of an interaction, which could explain the higher relative R366H enzymatic activity for dGTP versus other mutants (Figure 3.2B).

3.3.5 Impact of the R366C/H mutation on SAMHD1 restriction of HIV-1.

SAMHD1 restricts HIV-1 replication in non-dividing cells by impairing reverse transcription[22, 23]. As this restriction activity correlates to the dNTPase activity of SAMHD1, we predicted that the R366C/H mutants would be unable to restrict HIV-1. To examine this, we utilized U937 cells, which lack endogenous SAMHD1[21]. U937 cells were transduced to express wild type or R366C/H SAMHD1 and their equal cellular protein levels were confirmed with an immunoblot (Figure 3.5A). SAMHD1 D311A active site mutant was used a negative control as this mutant is known to have dNTPase and HIV-1 restriction deficits[231]. We differentiated the transduced U937 cells into non-dividing macrophages and challenged with increasing amounts of HIV-1-GFP vector (Figure 3.5B)[81]. While expression of WT SAMHD1 was sufficient to restrict HIV-1-GFP transduction, the R366C/H mutants were unable to restrict transduction, similar to the D311A mutant. Next, we measured the dNTP levels of these differentiated cell lines using a reverse transcription-based single-nucleotide incorporation assay (Figure 3.5C)[5]. Consistent with our biochemical dNTPase activity characterization, cells expressing R366C and R366H had raised intracellular dNTP levels when compared to cells expressing wild type SAMHD1, which is responsible for the failed restriction against HIV-1. Importantly, this elevation of dNTP pools in cells expressing R366C/H SAMHD1 mimics the cancer cell phenotype.

3.3.6 R366C/H mutants have unaltered interactions with CtIP for dsDNA break repair and Cyclin A2.

SAMHD1 has multiple dNTPase independent functions including interacting with cell cycle proteins[29], mediating dsDNA break repair[159], restricting transcription from the HIV-1 proviral LTR [101], suppression of the innate immune response[150, 157], and nucleic acid binding[144]. Thus, we investigated whether these functions were preserved in the R366C/H mutants. First, we tested binding to cell cycle protein, Cyclin A2, by overexpressing HA-SAMHD1 or HA-SAMHD1 R366C/H in 293T cells and performing a co-immunoprecipitation (Figure 3.6A). Immunoprecipitation of both R366C and R366H SAMHD1 pulled down Cyclin A2 similarly to wild type SAMHD1, indicating binding to cell cycle proteins is maintained by these mutants. SAMHD1 was recently implicated in double-strand DNA break repair by homologous recombination through its interaction with CtIP [159]. To test binding of the R366C/H mutants to CtIP we probed for CtIP in the HA-SAMHD1 pull-downs described above (Figure 3.6A). Similar to Cyclin A2, we found that R366C and R366H maintained binding to CtIP.

Next, we investigated the ability of the R366C/H mutants to mediate double-stranded DNA damage repair by homologous recombination. For this, we utilized U20S cells containing an integrated direct-repeat GFP construct with a I-SceI cut site[159]. Upon addition of I-SceI endonuclease, a double strand DNA break is generated which, when repaired by homologous recombination, results in a functional GFP construct. We knocked-down endogenous SAMHD1 using siRNA and expressed either siRNA resistant RFP-WT or RFP-R366C/H SAMHD1. Therefore, the ability of the mutants to promote homologous recombination can be determined by monitoring GFP expression in RFP expressing cells. As shown in Figure 3.6B, both R366C and R366H were able to mediate homologous recombination similar to wild type SAMHD1, indicating that R366C/H maintain the dNTPase independent dsDNA damage repair function.

3.3.7 R366C/H mutants suppress HIV-1 LTR activation and innate immune activation.

In addition to restricting replication at the reverse-transcription step, SAMHD1 has been implicated in suppressing viral transcription from the HIV-1 LTR[101]. Next, we tested the ability of the dNTPase impaired R366C/H mutants to suppress expression from the proviral LTR by co-transfecting 293T cells with wild type or mutant SAMHD1 expression plasmids and an HIV-1 LTR-Luciferase construct (Figure 3.6C). As observed with wild type SAMHD1, the R366C and R366H mutants were able to suppress LTR driven luciferase production.

SAMHD1 suppresses the innate immune response in dividing cells independent of dNTPase activity through interactions with IRF7 and NF-κB[150, 157]. To assess for alterations in the ability of R366C/H to suppress the innate immune response, we transiently co-expressed firefly luciferase under the control of an interferon stimulated response element (ISRE-Luc), transfection control Renilla luciferase, IRF7-Flag, and SAMHD1 WT, HD/RN, R366C, or R366H in 293T cells. 24-hours post-transfection firefly luciferase activity was assessed as a measure of innate immune response stimulation and normalized to Renilla luciferase activity (Figure 3.6D). As anticipated, WT and HD/RN SAMHD1 both suppressed firefly luciferase activity in this assay. R366C and R366H also displayed suppressed firefly luciferase. Thus, the R366C/H mutations do not alter the SAMHD1 function for innate immune response suppression in dividing cells.

3.3.8 R366C/H mutants showed reduced nucleic acid binding activity.

SAMHD1 has been shown to bind nucleic acids, which seems to play a role in HIV-1 restriction [102, 144]. We investigated whether the R366C/H mutations induced changes in nucleic

acid binding using a fluorescent polarization assay. R366C and R366H showed reduced nucleic acid binding affinity in this assay (Figure 3.6E). It is possible that this is a consequence of overlap between the dNTPase catalytic site and the nucleic acid binding domain[102]. However, it is unclear at present that this altered nucleic acid binding activity has a connection to cancer cell phenotypes.

3.3.9 SAMHD1 reduction in human primary normal dividing cells further elevates intracellular dNTP levels.

Finally, we sought to evaluate the contribution of SAMHD1 alterations in driving elevated dNTP levels, a key molecular signature of cancer, in a primary cell model. To this end, we obtained activated/dividing $CD4^+$T cells positively selected from Peripheral Blood Mononuclear Cells (PBMCs) of three healthy donors and stimulated with PHA and IL-2 media for 3 days. In fact, we previously reported that human primary activated $CD4^+$ T cells already harbor high dNTP concentrations[5]. Furthermore, these primary dividing cells also express SAMHD1 as shown in Figure 3.7A. To test whether SAMHD1 level decrease can elevate dNTP concentration in activated $CD4^+$ T cells, we treated these CD4+ T cells with virus-like particles containing Vpx (VLPs Vpx+) to degrade endogenous SAMHD1 or VLPs Vpx- as a negative control. We then measured intracellular dNTP levels of these treated cells. As shown in Figure 7A, even though the proportion of SAMHD1 degraded was small, 30%, we observed a significant increase in dNTP levels in the cells treated with VLPs Vpx +, compared to the cells treated with VLPs Vpx - (Figure 3.7B). These data suggests that, in the context of a primary cell model, reduction in SAMHD1 protein level, which also reduces overall dNTP hydrolysis capacity, can induce the elevated dNTP levels commonly seen in cancer cells.

3.4 Discussion

The sole utility of intracellular dNTPs is DNA synthesis, whereas rNTPs harbor highly versatile utilities in cells, including RNA synthesis, kinase substrates and energy carriers. Intracellular dNTP concentrations are several hundred times lower than rNTP concentrations[41] and dNTP biosynthesis is tightly regulated during cell cycle in dividing cells[13, 18]. However, elevated dNTP levels is a biochemical marker of cancer cells[180], likely because the uncontrolled cell division observed in these cells requires an abundant dNTP supply. dNTP biosynthesis pathways are extensively investigated, particularly in the field of cancer biology, which led to discovery of various anti-cancer therapeutics targeting dNTP biosynthesis pathways[3]. However, the understanding of cellular dNTP degradation and hydrolysis mechanisms was relatively limited until the discovery of SAMHD1 dNTPase[20, 53]. Recent identification of mutations in SAMHD1 in various cancer cell types generated a unique opportunity to understand the role of the enzymatic dNTP hydrolysis and its regulation in the elevated intracellular dNTP pools observed in cancer cells.

A majority of the SAMHD1 cancer associated mutations tested were found to be structurally destructive, consistent with SAMHD1 mutations observed in the AGS patients[81, 135]. However, R366C/H mutations, which were identified in two different cancer cell types[184, 188, 189], clearly do not affect the overall structural integrity essential for its various biological functions, enabling us to directly link the biochemical change induced by these mutations to a potential functional role of SAMHD1 in cancer cells. Indeed, among all biological and biochemical assays related to SAMHD1 activities and functions that were investigated, the loss of dNTPase activity

is clearly the sole and prominent defect induced by R366C/H mutations. The loss of the interaction with γ -phosphate of the dNTP substrate at the catalytic site is directly supported by our observation that dGTP is absent in the catalytic site of the crystal packs of both R366C and R366H SAMHD1 tetramers even though we observed two dGTP molecules bound to the two allosteric sites in the same crystals.

Interestingly, several studies reported another role of SAMHD1 in anti-cancer therapeutics. We and others reported that SAMHD1 hydrolyzes ara-CTP[60, 61], and more interestingly, that cellular SAMHD1 protein levels are co-related with cellular araC resistance[62, 232]. Clearly, SAMHD1, which hydrolyzes both araCTP and dCTP, a competitor of araCTP, can regulate balance between the steady state cellular levels of araCTP and dCTP that is important for araC anti-cancer efficacy.

It remains unclear whether the genetic loss of SAMHD1 in AGS is co-related with cancers, mainly because of the rare incidence and early death of patients with this severe immune disorder[135]. Interestingly, SAMHD KO mice did not display an AGS phenotype[233, 234] and there is no report of cancer development in SAMHD1 KO mice, indicating that SAMHD1 functions may be species -dependent. Overall, our study reveals that loss of dNTPase activity induced by SAMHD1 cancer R366 mutations can mechanistically contribute to the elevated intracellular dNTP pools commonly observed in cancer cells.

3.5 Experimental Procedures

3.5.1 Cell culture.

293T cells were cultured in DMEM (Gibco) supplemented with 10% (v/v) fetal bovine serum (FBS) and 1% (v/v) penicillin/streptomycin. U20S cells were grown in DMEM supplemented with 7.5% FBS. U937 cells were grown in in RPMI (Corning) supplemented with 10% (v/v) FBS and 1% (v/v) penicillin/streptomycin. Primary human CD4+ T-cells were isolated from monocyte depleted peripheral blood buffy coats of 3 donors (New York Blood Center, New York, New York) by positive selection using anti-CD4 antibody conjugated magnetic beads as previously described[5]. CD4+ T-cells were activated by culturing in RPMI supplemented with 10% (v/v) FBS, 1% (v/v) penicillin/streptomycin, 5 μg/mL PHA (Sigma), and 5 ng/mL IL-2 (Miltenyi) for five days.

3.5.2 Structural Model with Location of Mutant Residues.

Visual Molecular Dynamics (VMD) version 1.9.4 was used to visualize the structure of wild type SAMHD1 bound to dGTP (PDB:4BZB[52]) to identify the location of selected mutations.

3.5.3 Mutant Cellular Expression.

Plasmids expressing SAMHD1 cancer-associated mutations were generated by QuikChange (Agilent), using either pKH3-SAMHD1-3xHA[159] or plvx-mCherry-SAMHD1-3xHA (Genscript) as a template and mutation specific primers (IDT). For the experiment using pKH3-3xHA constructs, 4 μg of pKH3-SAMHD1-3xHA plasmids were cotransfected with 4 μg GFP as a transfection control. For plvx-mCherry-3xHA plasmids, 4 μg of plvx-mCherry-SAMHD1-3xHA plasmids were transfected. Both experiments transfected 6-well plates of 293T cells using

polyethyleneimine (PEI) (Polysciences Inc.). Transfection media was changed 16 hr post transfection. 48 hr after transfection the cells were washed with PBS and detached using 0.25% trypsin (Corning). Half of each sample was fixed in 1% PFA and gated for GFP or mCherry using flow cytometry (MACSQuant VYB with MACSQuantify Software) to determine transfection efficiency (Supporting Table 3.1). The other half of the sample was lysed with cold RIPA buffer (50 mM Tris HCl pH 8, 0.1% SDS, 150 mM NaCl, 0.25% Deoxycholic acid, 1 mM EDTA, and 1% NP-40) supplemented 1:500 (v/v) with protease inhibitor cocktail (Sigma). Lysates were clarified using centrifugation (13,000 rpm for 10 min at 4 °C) and the supernatants were stored at -80 °C for immunoblot.

3.5.4 Immunoblots.

Lysates were diluted with Laemmli Buffer (BioRad), resolved by SDS-PAGE, and transferred onto a nitrocellulose membrane. These membranes were probed using the indicated primary antibodies and the corresponding secondary antibodies. The membranes were then imaged using SuperSignal West Femto Maximum Sensitivity Substrate (Thermo Scientific). The following primary antibodies were using during this study: SAMHD1 (abcam 67820), GAPDH (Cell Signaling 14C10), HA (Cell Signaling C23F4), CtIP (Santa Cruz 271339), Cyclin A2 (Abcam 181591), FLAG (Abcam 18230). The following secondary antibodies were used during this study: anti-mouse (Cytiva NA931V) and anti-rabbit (Cytiva NA934V).

3.5.5 SAMHD1 protein expression and purification.

Plasmids expressing the HD domain (residues 113-626) of SAMHD1 cancer-associated mutations were generated by QuikChange using pet14b-SAMHD1 as a template and mutation specific primers. The N-terminal His-tag SAMHD1 proteins were overexpressed in Rosetta DE3 cells (Novagen) by inducing with 0.2 mM IPTG at an optical density of 0.5-0.8 for 48 hr at 16 °C. Cells were harvested by centrifugation (3,500 rpm for 30 min at 4 °C), resuspended in lysis buffer (40 mM Tris HCl pH 7.5, 250 mM KCl, 5% glycerol, 0.1% Triton X-100, 5 mM β-mercaptoethanol and 0.1 mM PMSF), and sonicated. Cleared lysate was obtained by centrifugation (15,000 rpm for 30 min at 4 °C). The cleared lysate was loaded onto a HisTrap FF column (Cytiva) equilibrated with binding buffer (40 mM Tris-HCl pH 7.5, 10% glycerol, 500 mM NaCl, 5 mM β-mercaptoethanol, and 20 mM imidazole). The column was washed with 75 mL binding buffer followed by 30 mL of high salt wash buffer (40mM Tris-HCl pH 7.5, 10% glycerol, 2000 mM NaCl, 5 mM β-mercaptoethanol, and 20 mM imidazole). Protein was eluted with 50% binding buffer and 50% elution buffer (40 mM Tris-HCl pH 7.5, 10% glycerol, 300 mM NaCl, 5 mM β-mercaptoethanol, and 500 mM imidazole). Fractions were assessed for the presence of SAMHD1 using SDS-PAGE. Fractions containing SAMHD1 were combined and further purified on Superdex S200 (GE healthcare) with gel filtration buffer (50 mM Tris-HCl pH 7.5, 20% glycerol, 150 mM NaCl, and 5 mM β-mercaptoethanol). Fractions were assessed using SDS-PAGE and those containing SAMHD1 were combined, flash frozen, and stored at -80°C.

3.5.6 Thermal shift assay.

Thermal shift reaction mixtures (40 µL) were made using 2.5µM SAMHD1 WT or mutant proteins in SAMHD1 storage buffer (50 mM Tris-HCl pH 7.5, 20% glycerol, 150 mM NaCl, and

5mM β-mercaptoethanol), 1 μL Sypro Orange Protein Gel Stain (Sigma-Aldrich) diluted 1:20 in SAMHD1 storage buffer, and 10 μM dGTP. Reactions were performed in triplicate and wells containing no SAMHD1 or no dye served as negative controls. Reactions mixtures were added to a 96 well plate (Lightcycler 480 Multiwell Plate 96 white, Roche) and heated from 32 °C to 99 °C at the rate of 0.02 °C per second by a real-time PCR device (LightCycler 480 II, Roche). Florescence was read at 533-660 and 30 acquisitions were taken per °C to monitor protein unfolding signified by increased Sypro Orange fluorescence. Fluorescent intensity was plotted against temperature using Spyder Software (Anaconda). Melting temperature (T_m) was calculated for each well using the transition midpoint.

3.5.7 Cross-linking based tetramerization assay.

The SAMHD1 cross-linking assay was adapted from a protocol previously described[50]. Reaction mixtures (20 μL) contained 10 μM wild type or mutant SAMHD1 in cross-linking buffer (50 mM HEPES 7.4, 20% Glycerol, 150 mM KCl, 1 mM β-mercaptoethanol), 25 0mM KCl, and 25 mM $MgCl_2$) . These reactions contained no dGTP or 2 mM dGTP as specified in the text. Reactions were incubated on ice for 30 min followed by incubation at room temperature for 5 min. An equal amount of 2% formaldehyde was added and the reactions were incubated at 37 °C for 15 min. Reactions were quenched by adding glycine to a final concentration of 250 mM and incubating at room temperature for 15 min. Reactions were diluted with 4x Laemmli buffer without β-mercaptoethanol supplemented and loaded onto an SDS-PAGE gel (Mini-PROTEAN TGX Stain-Free Precast Gel, Biorad). The gel was imaged using ChemiDoc Touch Imaging System (BioRad).

3.5.8 SAMHD1 degradation assay.

Vpx-mediated degradation was performed as previously described[127]. Briefly, $1x10^6$ 293T cells were co-transfected with 2 μg of $pSIV3^+$ or $pSIV3^+$ ΔVpx (obtained from Dr. Nathaniel Landau, New York University) and 0.1 ug of pKH3-3xHA or pKH3-SAMHD1-3xHA (WT, R366C, or R366H) plasmids by PEI. Transfection media was changed 16 hr post transfection. 48 hr after transfection the cells were washed with PBS, and lysed with cold RIPA buffer supplemented 1:500 (v/v) with a protease inhibitor cocktail (Sigma). Lysates were clarified using centrifugation (13,000 rpm for 10 min at 4 °C) and the supernatants were stored at -80 °C for immunoblot.

3.5.9 Thin-layer chromatography based dNTPase assay.

TLC-based dNTPase assay was adapted from a protocol described previously[54]. 0.02 μM WT or mutant SAMHD1 protein was incubated with 1 μCi/μl [α-32P]dGTP (Easytide, PerkinElmer), 200 μM unlabeled dGTP (Invitrogen), in TLC reaction buffer (50 mM Tris-HCl pH 8, 50 mM KCl, 5 mM $MgCl_2$, and 0.1% Triton X-100) at 37°C for 60 minutes. Reactions were performed in triplicate. This incubation time was chosen because wild type displays significant dNTP hydrolysis at this time point, while still being under saturating substrate concentrations during a preliminary time course experiment. The reactions were heat inactivated by incubating at 70 °C for 5 minutes. 0.5 μL of each reaction was spotted onto a PolyGram 300 CEL TLC plate (Macherey-Nagel). The radioactive dGTP substrate and triphosphate product were separated using

the mobile phase (800 mM LiCl and 100 mM Tris-HCl pH 8). Radioactivity was detected using Amersham Typhoon IP (Cytiva) and densitrometry analysis was performed using ImageQuant TL 8.2 (Cytiva). Relative activity was determined by dividing triphosphate by the lane total and normalizing to WT. This was repeated for the other dNTP substrates with a modified reaction condition to account for the necessary dGTP activation: 0.04 μM WT or mutant SAMHD1 protein was incubated with 1 μCi/μl [α-32P]dNTP, 200 μM unlabeled dNTP, and 200 μM unlabeled dGTP in TLC reaction buffer at 37 °C for 60 minutes.

3.5.10 Crystallization and data collection.

Crystals for the HD domain of SAMHD1 (residues 113-626) R366C/H were obtained using catalytically inactive H206R/D207N constructs[52] with the microbatch under oil method. R366C or R366H (4 mg/mL; 50 mM Tris pH 8.0, 150 mM NaCl, 5 mM $MgCl_2$, 0.5 mM TCEP) was mixed with 4 mM dGTP, incubated on ice for 15 min, and added 1:1 with crystallization buffer (100 mM succinic acid-phosphate-glycine (SPG) buffer, 30% w/v PEG1500; Qiagen). R366C crystallized at pH 8.2 in ~2 weeks at room temperature. R366H crystallized at pH 9.0 within 1-2 days at room temperature. Both constructs were cryoprotected with 25% v/v glycerol and flash frozen in liquid nitrogen. Diffraction data were collected on the NECAT beamline 24-ID-E at the Advanced Photon Source (APS), Argonne National Lab. Data statistics are summarized in Supporting Table 2.

3.5.11 Structure determination and refinement.

Diffraction images were processed using HKL2000[235]. Structures were solved via molecular replacement (Phaser)[236] using PDB 4BZB as a search model. Models were refined through iterative rounds of restrained and TLS refinement (REFMAC5)[237], and model building (Coot)[238]. The R366H crystal was twinned with twinning fractions of 0.57 and 0.43 for the (H, K, L) and (H, -K, -H-L) twinning operators, respectively. Residues 278-283 were unresolved. Refinement statistics are summarized in Supporting Table 3.2. Coordinate and structure factors were deposited in the PDB under accession codes 7LTT and 7LU5 for R366C and R366H, respectively.

3.5.12 Generation of U937 cells expressing SAMHD1 mutations.

Plasmids expressing SAMHD1 cancer-associated mutations were generated using LPCX-SAMHD1-Flag as a template and mutation specific primers. LPCX-Flag was used as a negative "empty" control. Retroviral vectors were generated as previously reported[69]. Transduced U937 cells were selected in 0.4 μg /ml puromycin. Transduction was confirmed by lysing cells in RIPA buffer and performing an immunoblot.

3.5.13 HIV-1 vector transduction.

Recombinant HIV-1 expressing GFP and pseudotyped with the VSV-G glycoprotein were prepared as described[81]. For transductions, 6×10^4 cells seeded in 24-well plates were first treated with 10 ng/mL phorbol-12-myristate-3-acetate (PMA) for 16 hours to induce differentiation into macrophage-like cells. Cells were then transduced with the pseudotyped HIV-1 in the amounts

noted in the text. 48 hours post transduction the percentage of GFP-positive cells was determined by flow cytometry (Becton Dickinson).

3.5.14 Cellular dNTP measurement.

Cellular dNTP was measured by HIV-1 RT-based dNTP assay as described[5]. Briefly, $2x10^6$ cells for each cell type were washed with PBS and resuspended in ice cold 65% methanol. To lyse, cells were vortexed for 2 min and incubated at 95 °C for 3 min. Cells were centrifuged at 14,000 rpm for 3 min and the supernatant was dried using a speed vac. The dried sample was resuspended in water and diluted to be within the linear range of the assay. 5′ 32P-end-labeled 18-mer DNA primer (5′-GTCCCTCTTCGGGCGCCA-3′, Integrated DNA Technologies) was individually annealed to one of four 19-mer DNA templates (3′-CAGGGAGAAGCCCGCGGTN-5′, Integrated DNA Technologies), where N represents the nucleotide variation at the 5' end. Reactions (20μL) contained 200 fmol template/primer, 4 μL of purified RT (HIV-1 HXB2), 25 mM Tris–HCl, pH 8.0, 2 mM dithiothreitol, 100 mM KCl, 5 mM MgCl2, and 10 μM oligo (dT), and cellular dNTP extracts. Water or 0.5 mM dNTP mix was used as a negative and positive control, respectively. Reactions were incubated at 37 °C for 5 min and stopped by adding 10 μL 40 mM EDTA and 99% (vol/vol) formamide followed by incubation at 95 °C for 2 min. Reactions were resolved on a 14% urea-PAGE gel (AmericanBio, Inc.) and analyzed using PharosFX molecular imager. Image Lab software Version 5.1.2 (Biorad) was used to quantify single-nucleotide extensions products.

3.5.15 Immunoprecipitation.

293T cells in 10 cm dishes were transfected with pKH3-3xHA or pKH3-SAMHD1-3xHA (WT, R366C, or R366H) using PEI. Transfection media was changed 16hr post transfection. 48 hr after transfection the cells were lysed in immunoprecipitation lysis buffer (25 mM Tris-HCl pH, 50 nM NaCl, 5% glycerol, and 0.375% CHAPS) supplemented 1:500 (v/v) protease inhibitor cocktail (Sigma) and centrifuged to obtain cleared lysate (14,000 rpm for 5 min at 4 °C). Monoclonal Anti-HA Agarose (Sigma) was washed three times in RIPA buffer, added to the cleared lysate, and incubated overnight at 4 °C with gentle rocking. The next day the sample was centrifuged (3,000 x g for 2 min at 4 °C) to pellet the resin and bound protein. The supernatant was discarded and the resin was loaded onto HA spin column. The column was washed 3 times with RIPA buffer supplemented with protease inhibitor cocktail. The remaining bound protein was eluted with 8 M urea (Sigma) and stored at -80°C for immunoblot.

*3.5.16 DSB Reporter Assay***.**

Measurement of double strand DNA break repair by homologous recombination was conducted as reported previously[159]. Briefly, U20S cells stably expressing a DR-GFP reporter gene were transfected with 30 nM siRNA using Lipofectamine RNAiMax. The following day, transfection media was changed and cells were transfected with I-SceI and RFP or SAMHD1-RFP (WT, R366C, or R366H) plasmids. Cells were harvested 72 hours after transfection of plasmids. RFP expressing cells were gated and analyzed for homologous recombination based on GFP expression using FACS. This experiment was performed in quadruplicate (n=4).

3.5.17 LTR and ISRE Luciferase Assays.

293T cells were seeded in 12-well plates. For LTR suppression cells were transfected with 100 ng pBlue3'LTR-luc-C (NIH AIDS # 4789), 100 ng Renilla-Luciferase, and 300 ng pKH3-3xHA or pKH3-SAMHD1-3xHA (WT, R366C, or R366H) using PEI[101]. For ISRE suppression cells were transfected with 100 ng ISRE-Luc (obtained from Li Wu, Ohio State University), 100 ng Renilla-Luciferase, 200 ng IRF7-Flag (obtained from Li Wu, Ohio State University), and 300 ng pKH3-3xHA or pKH3-SAMHD1-3xHA (WT, HD/RN, R366C, or R366H) using PEI[148]. 16 hr later transfection media was changed to fresh media. 24 hr post transfection cells were lysed and assessed for luciferase activity using the Dual-Luciferase Reporter Assay System (Promega) following the manufacturer's instructions. The remaining lysate was stored at -20 °C for immunoblot. LTR and ISRE activity was calculated by dividing Firefly Luciferase activity by Renilla Luciferase activity and normalizing to the Empty Vector condition. The immunoblot was quantified using Image Lab Software (Biorad) (Supporting Figure 3). SAMHD1 signal/ GAPDH signal was normalized to the WT condition. The previous luciferase calculation was divided by the normalized Western Blot signal in order to account for variations in expression.

3.5.18 Oligonucleotide Binding by Fluorescence Polarization.

Wild type and mutant variants of HD-domain SAMHD (114-626) constructs were expressed using a bacterial expression system and purified, as previously described[77]. The binding of SAMHD1 to various oligonucleotides was monitored by fluorescence polarization. The reporter oligonucleotides containing a 6-carboxyfluoroscein (6-FAM) label at the 5' end were purchased from IDT. ssDNA57 and ssRNA40 oligonucleotides had the same sequences as in the original

study[144]. The binding assay contained 50 nM of fluorescently-labeled oligonucleotide and was prepared in the following buffer: 50 mM Tris-HCl pH 8.0, 50 mM KCl, and 1 mM EDTA. Fluorescence polarization measurements were performed in 384-well plates (Corning 3575) on a Synergy 2 microplate reader (Biotek) using 485/20 nm excitation and 530/20 nm emission bandpass filters. All experiments were performed in duplicate with 20 µL solution volume in each well.

3.5.19 Virus-like particle transduction of $CD4^+$ T-cells.

Virus like-particles (VLPs) Vpx^+ and Vpx^- were prepared as previously described[225]. Briefly, 293T cells were transfected with 40 µg of $pSIV3^+$ or $pSIV3^+$ ΔVpx (obtained from Dr. Nathaniel Landau, New York University) and 20 µg of pVSV-G using PEI. Supernatant was collected 2 and 3 days post-transfection and centrifuged to clear cellular debris (1,200 rpm for 7 minutes). Cleared supernatant was overlaid above a 25% sucrose solution (25% Sucrose, 25 mM Tris HCl pH 7.5, 150 mM NaCl, 5 mM EDTA) and concentrated by ultracentrifugation (23,000 rpm, for 2 hr at 4°C). Pellets were resuspended in Hanks' balanced salt solution (GIBCO), aliquoted, flash-frozen, and stored at −80 °C. Activated $CD4^+$ T-cells were transduced with either VLP Vpx^+ or VLP Vpx^-. Cells were harvested for Western Blot and dNTP measurements 24 hours post transduction.

3.5.20 Statistical Analyses.

All statistical analyses were conducted using two-tailed, unpaired Welch's t-tests. P-values obtained from each analysis are included in the figure. The cutoff for statistical significance in this study is a p-value <0.05. All experiments were performed in triplicate (n=3) unless otherwise noted. Values are reported as the mean of these replicates and error bars in each figure represent standard deviation.

3.6 Data Availability

The atomic coordinates and structure factors have been deposited in the Protein Data Bank. SAMHD1(113-626) H206R D207N R366C PDB ID 7LTT. SAMHD1(113-626) H206R D207N R366H PDB ID 7LU5.

3.7 Funding

This study was supported by NIH AI136581 (B.K.), NIH AI150451 (B.K.), NIH CA254403 (D.S.Y. and B.K.), NIH AI136737 (Y.X.), NIH CA178999 (D.S.Y), DOD BCRP BC180883 (D.S.Y.), NIH AI150455 (F. D-G.), and NIH AI136697 (D.N.I.). This work is based upon research conducted at the Northeastern Collaborative Access Team beamlines, which are funded by the National Institute of General Medical Sciences from the National Institutes of Health (P30 GM124165). The Eiger 16M detector on the 24-ID-E beam line is funded by a NIH-ORIP HEI grant (S10OD021527). This research used resources of the Advanced Photon Source, a U.S. Department of Energy (DOE) Office of Science User Facility operated for the DOE Office of Science by Argonne National Laboratory under Contract No. DE-AC02-06CH11357.

3.8 Author Contributions

N.E.B, J.T., C.S., A.O., F.A., P.K-V., M.P., C.H.Y. performed data acquisition. N.E.B, J.T., C.S., A.O., F.A., P.K-V., M.P., C.H.Y., D.N.I., F.D-G., D.S.Y., Y.X., and B.K performed data interpretation. D.-H. K., R. F. S., Y.X., and B. K. conceptualization of project. N.E.B, J.T., Y.X., and B.K. wrote the original draft. N.E.B, J.T., C.S., A.O., F.A., P.K.-V., M.P., C.H.Y., D.-H. K., R. F. S., D.N.I., F.D-G., D.S.Y., Y.X., and B.K reviewed and edited the manuscript. B.K. performed project administration.

3.9 Conflict of Interest Statement

The authors declare they have no conflicts of interest.

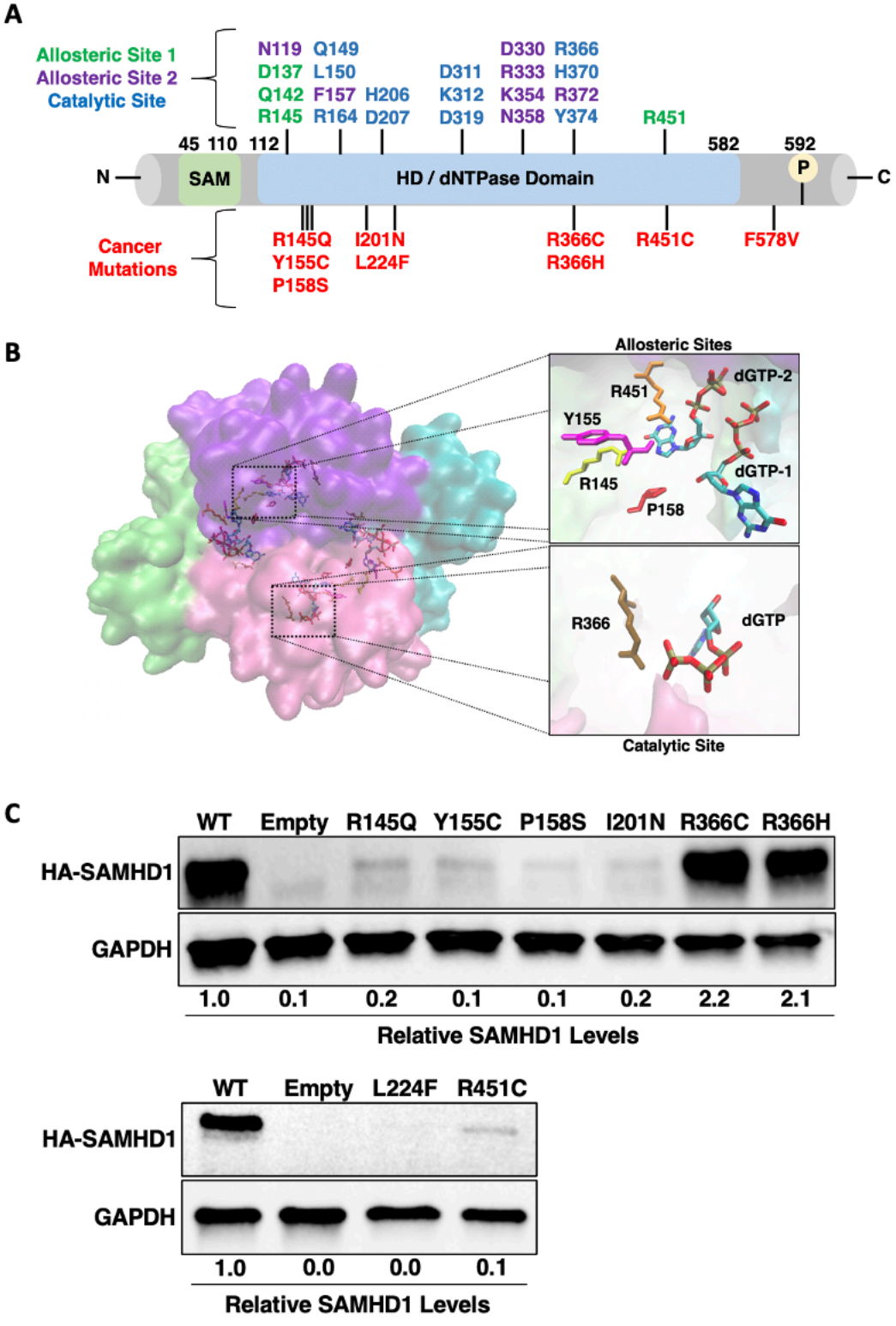
A
Allosteric Site 1
Allosteric Site 2
Catalytic Site
N119 Q149
D137 L150
Q142 F157 H206
R145 R164 D207
D311
K312
D319
D330 R366
R333 H370
K354 R372
N358 Y374
R451
45 110 112
582
592
N
SAM
HD / dNTPase Domain
P
C
Cancer Mutations
R145Q
Y155C
P158S
I201N
L224F
R366C
R366H
R451C
F578V
B
Allosteric Sites
R451
dGTP-2
Y155
dGTP-1
R145
P158
R366
dGTP
Catalytic Site
C
WT Empty R145Q Y155C P158S I201N R366C R366H
HA-SAMHD1
GAPDH
1.0 0.1 0.2 0.1 0.1 0.2 2.2 2.1
Relative SAMHD1 Levels
WT Empty L224F R451C
HA-SAMHD1
GAPDH
1.0 0.0 0.0 0.1
Relative SAMHD1 Levels

Figure 3.1: Structural locations of selected SAMHD1 cancer mutations and their impact on intracellular SAMHD1 protein levels. A) Linear map of SAMHD1 mutations selected in this study. Cancer specific mutations are in red at the bottom, and residues in catalytic sites and two allosteric sites are marked in different colors. **B)** Structural locations of SAMHD1 cancer mutations found in the allosteric or catalytic sites. Our previously solved wild type HD domain tetramer structure (4BZB), which is bound to dGTP at its two allosteric sites (dGTP-1 and dGTP-2) and catalytic site, was used for locating the selected mutations. Subunits of the tetramers are displayed in different colors. **C)** The SAMHD1 protein levels in 293T cells transfected with an equal amount of plasmids expressing HA-tagged SAMHD1 proteins. Empty: Backbone plasmids, pKH3-3xHA (left) and pLVX-IRES-mCherry (right). Transfection efficiency was determined by GFP expression from the co-transfected eGFP control plasmid (left) or from mCherry expression (right) by flow cytometry. (Supporting Table 1). The relative SAMHD1 protein levels were normalized by GAPDH protein level and the ratios between wild type and mutant SAMHD1 protein levels were calculated.

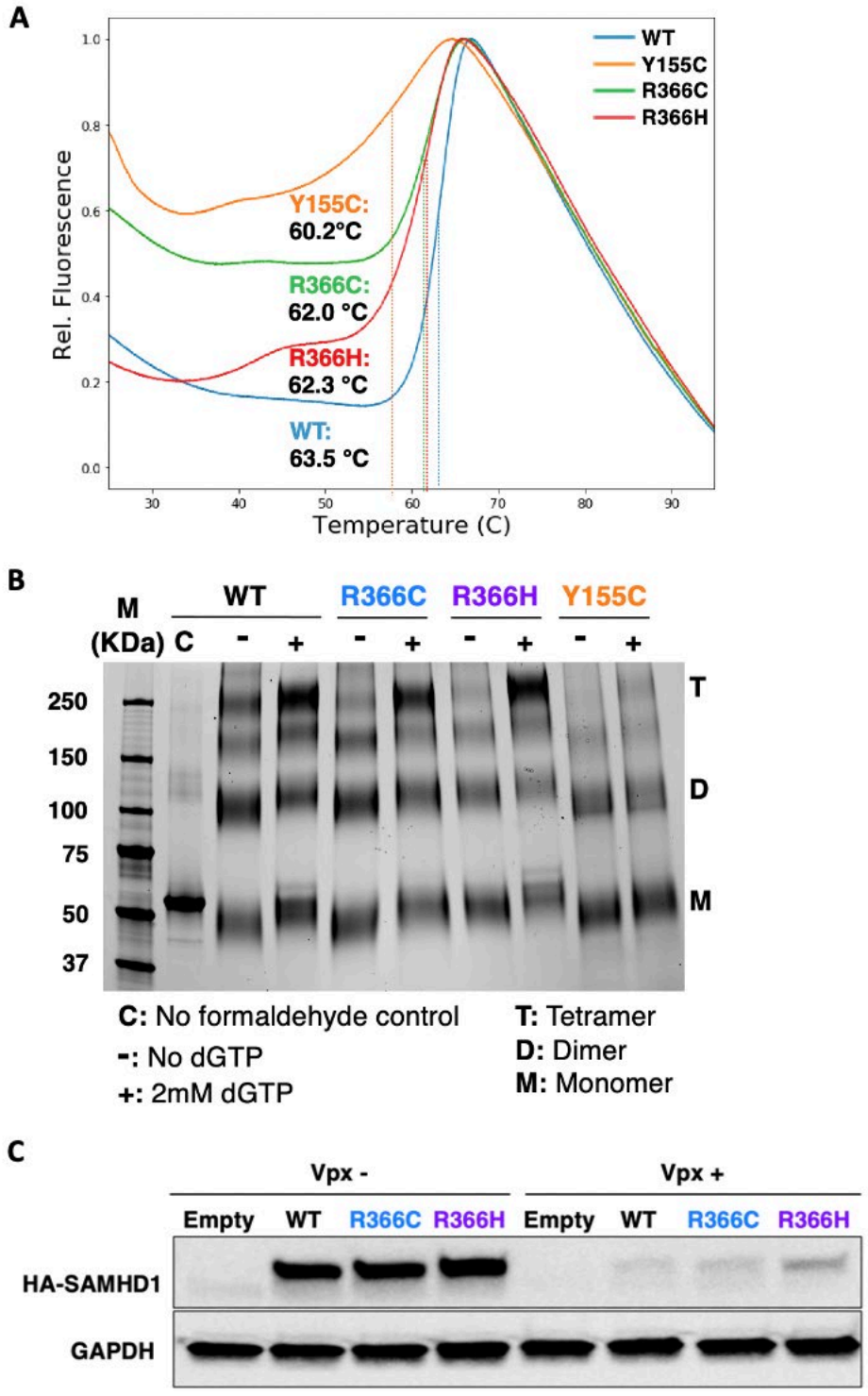

Figure 3.2: Thermostability, tetramerization, and Vpx-mediated degradation of SAMHD1 mutant proteins. A) Thermal shift assay of wild type and mutant HD proteins was conducted after

preincubation with SYPRO Orange dye. The melting temperature (T_m) of each protein was calculated as described in Methods. T_m: WT= 63.5 ± 0.1°C, Y155C= 60.2 ± 0.3°C, R366C= 62.0 ± 0.4°C, R366H= 62.3 ± 0.1°C **B)** Tetramerization of wild type and mutant HD domain proteins was analyzed by SDS-PAGE after formaldehyde-mediated crosslinking in the presence and absence of 2mM dGTP. M: Monomer, D: Dimer, T: Tetramer. M: Molecular weight markers. C: No formaldehyde control. **C)** Vpx-mediated proteasomal degradation of wild type and mutant SAMHD1 proteins in cells was monitored. 293T cells were co-transfected with SAMHD1 expressing plasmids and Vpx expressing (Vpx+) or non-expressing (Vpx-) plasmid. SAMHD1 protein levels in the transfected cells were determined by immunoblot with anti-SAMHD1 antibody.

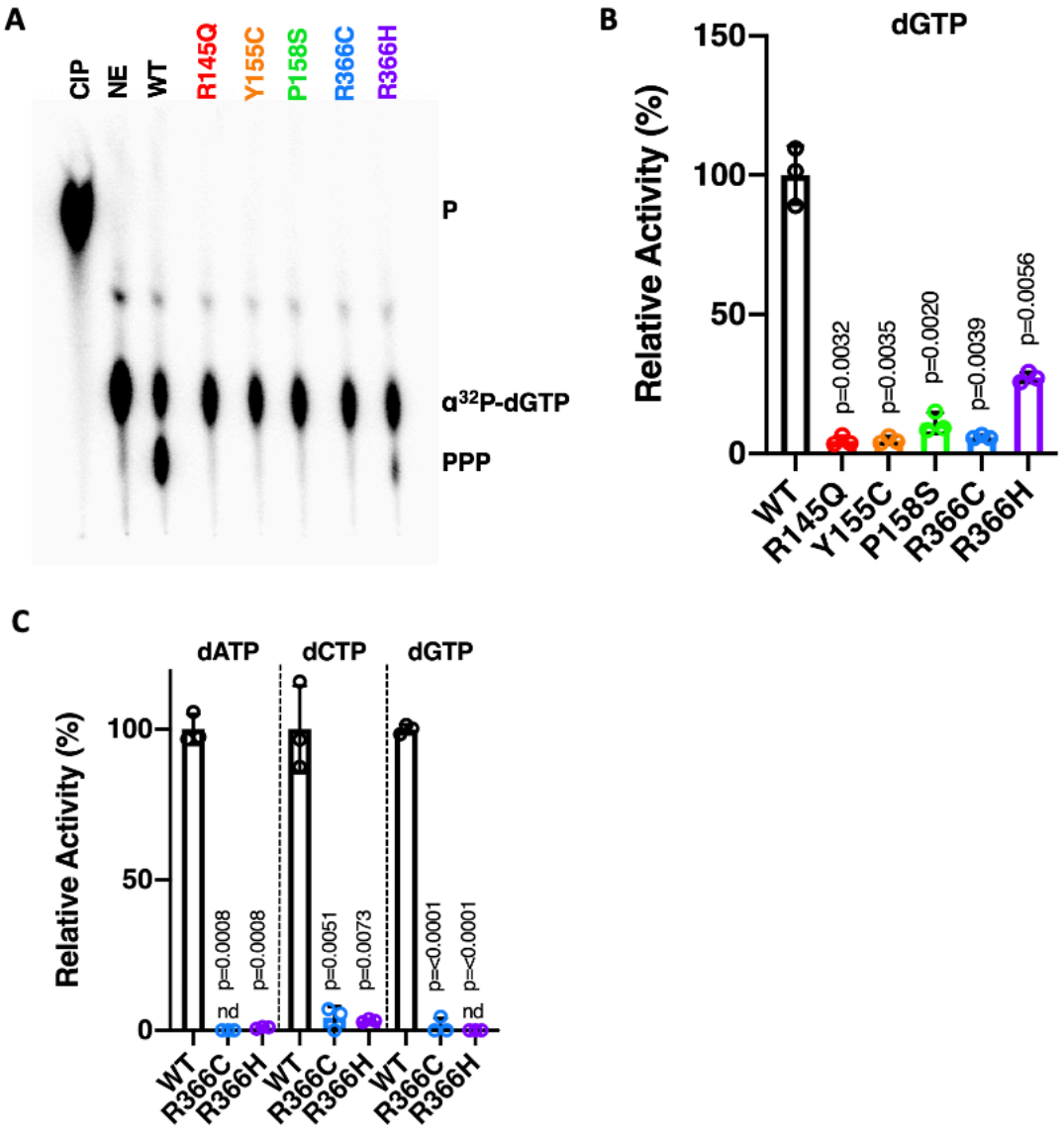

Figure 3.3: Biochemical dNTPase activity comparison of wild type and cancer mutant SAMHD1 proteins. A) TLC-based dNTPase assay was conducted using the same concentration of purified HD domain protein for each mutant. This assay monitors the production of triphosphate from α^{32}P-dNTP substrate under the condition that triphosphate product generation was linear to protein amounts at the saturating dNTP substrate concentration. The reactions were analyzed by TLC as described in Methods. CIP: calf-intestinal phosphatase control. NE: No enzyme negative control. P: Monophosphate. PPP: Triphosphate. **B)** Relative dGTPase activity of wild type and

mutant SAMHD1 proteins (HD domain) was calculated by dividing the triphosphate product by the lane total and normalizing to wild type dGTPase activity. **C)** The relative dNTPase activities of wild type, R336C and R366H proteins were determined for dATP, dCTP, and dTTP. nd: not detected. Data are the mean of three replicates and error bars reflect standard deviation from the mean. P-values were determined using two-tailed, unpaired Welch's t-test with WT, wild type.

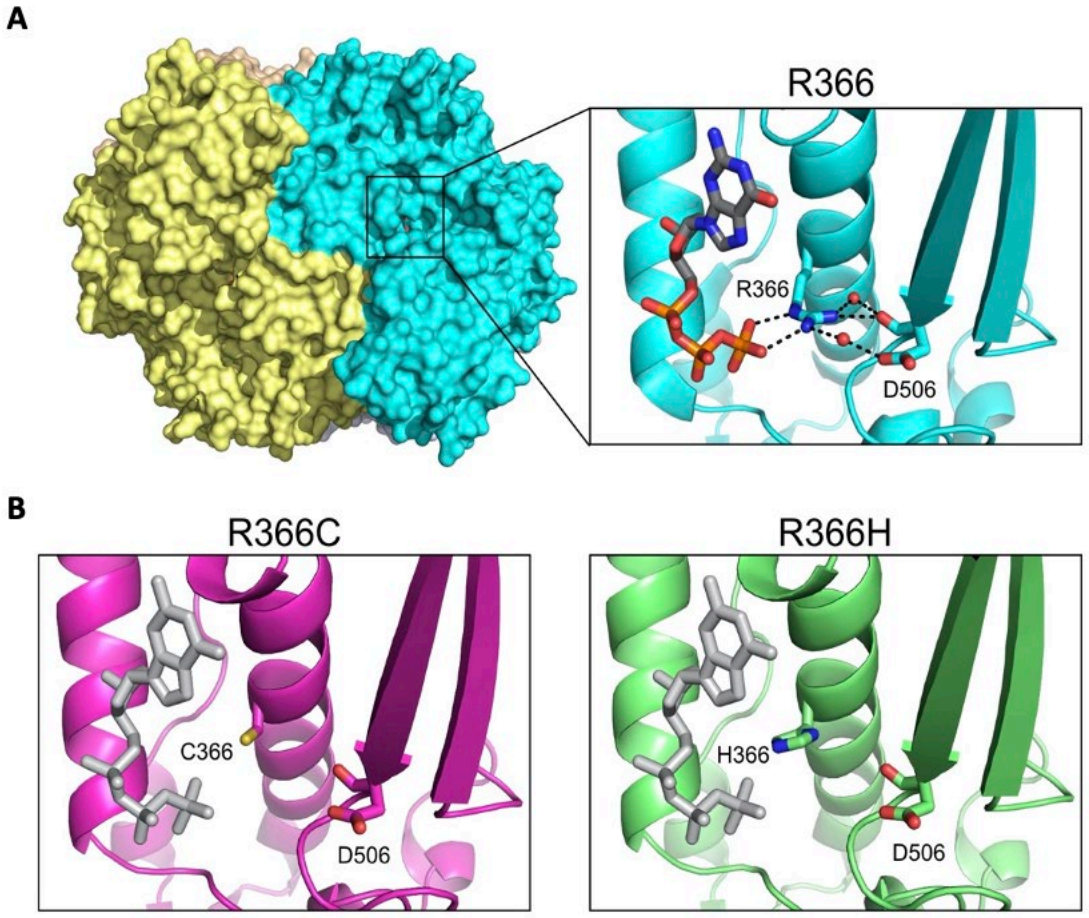

Figure 3.4. R366C/H mutations abrogate catalytic nucleotide binding. **A)** Overall structure of the SAMHD1 tetramer in surface representation (left). The right inset shows selected interactions of R336 and the catalytic nucleotide in SAMHD1$_{HD/RN}$. H-bonds and salt bridges are shown as dashed lines. **B)** R336C (left) or R366H (right) leads to the disruption of the interactions and the loss of nucleotide binding at the catalytic site. The catalytic nucleotides (gray) are modeled in based on their positions in SAMHD1$_{HD/RN}$. Portions of the structure have been hidden for clarity.

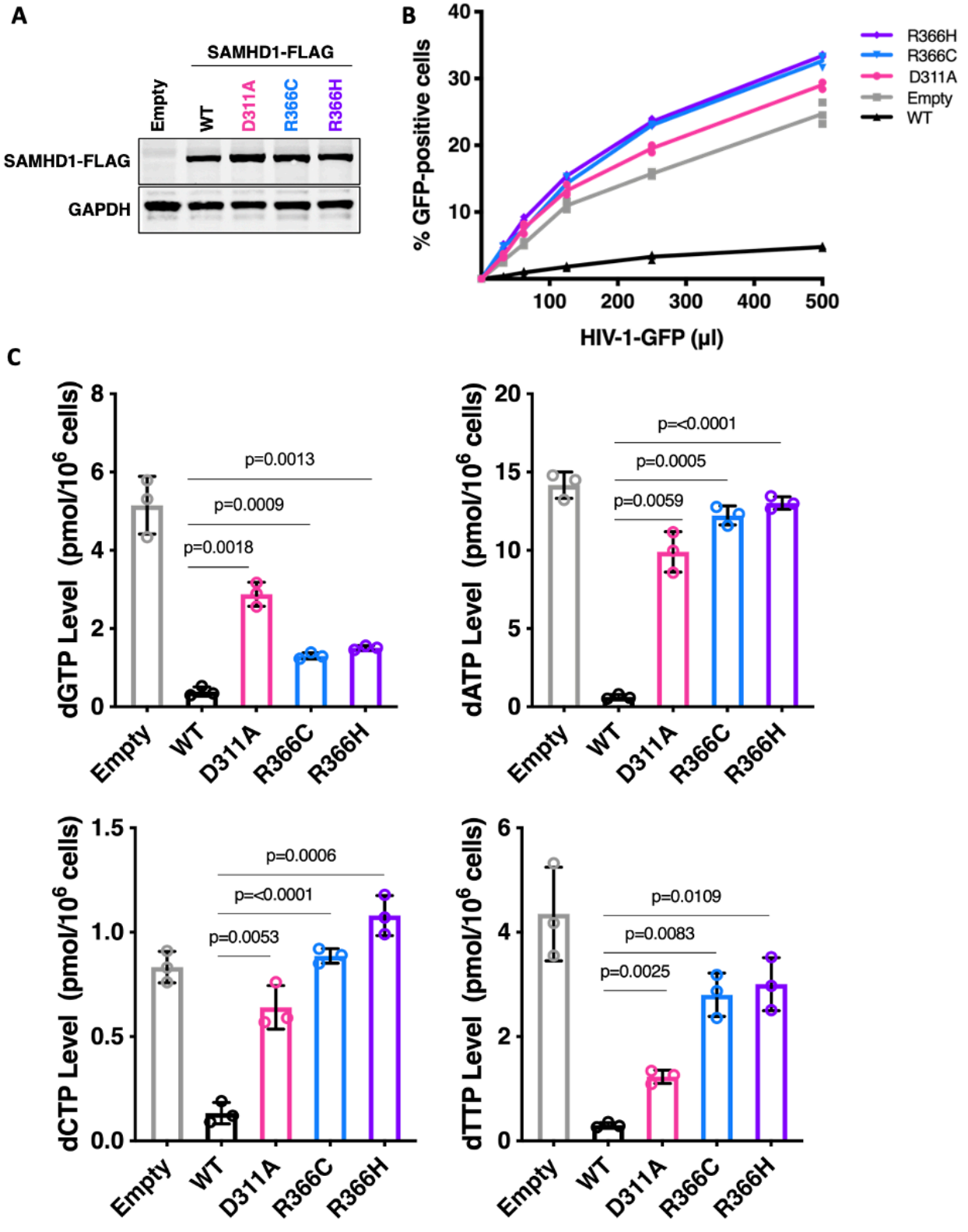
A
SAMHD1-FLAG
Empty
WT
D311A
R366C
R366H
SAMHD1-FLAG
GAPDH
B
% GFP-positive cells
HIV-1-GFP (µl)
R366H
R366C
D311A
Empty
WT
C
dGTP Level (pmol/10^6 cells)
p=0.0013
p=0.0009
p=0.0018
dATP Level (pmol/10^6 cells)
p=<0.0001
p=0.0005
p=0.0059
dCTP Level (pmol/10^6 cells)
p=0.0006
p=<0.0001
p=0.0053
dTTP Level (pmol/10^6 cells)
p=0.0109
p=0.0083
p=0.0025
Empty
WT
D311A
R366C
R366H

Figure 3.5: HIV-1 restriction capability of R366H/C SAMHD1 mutants. **A)** U937 cells were transduced with lentiviral vector expressing FLAG-tagged wild type, D311A inactive mutant, R366C, and R366H proteins. The expression level of each SAMHD1 protein was determined by western blot with anti-FLAG antibody and normalized with GAPDH. **B)** The transduced U937 cells were differentiated to nondividing macrophage stage, and transduced with eGFP expressing HIV-1 vector. Transduction efficiency using different quantities of HIV-1 vector was determined using flow cytometry. **C)** Intracellular dNTP levels in differentiated U937 cells expressing wild type and mutant SAMHD1 proteins were determined by RT-based dNTP assay. Data are the mean of three replicates and error bars reflect standard deviation from the mean. P-values were determined using two-tailed, unpaired Welch's t-test to WT knock-in cells.

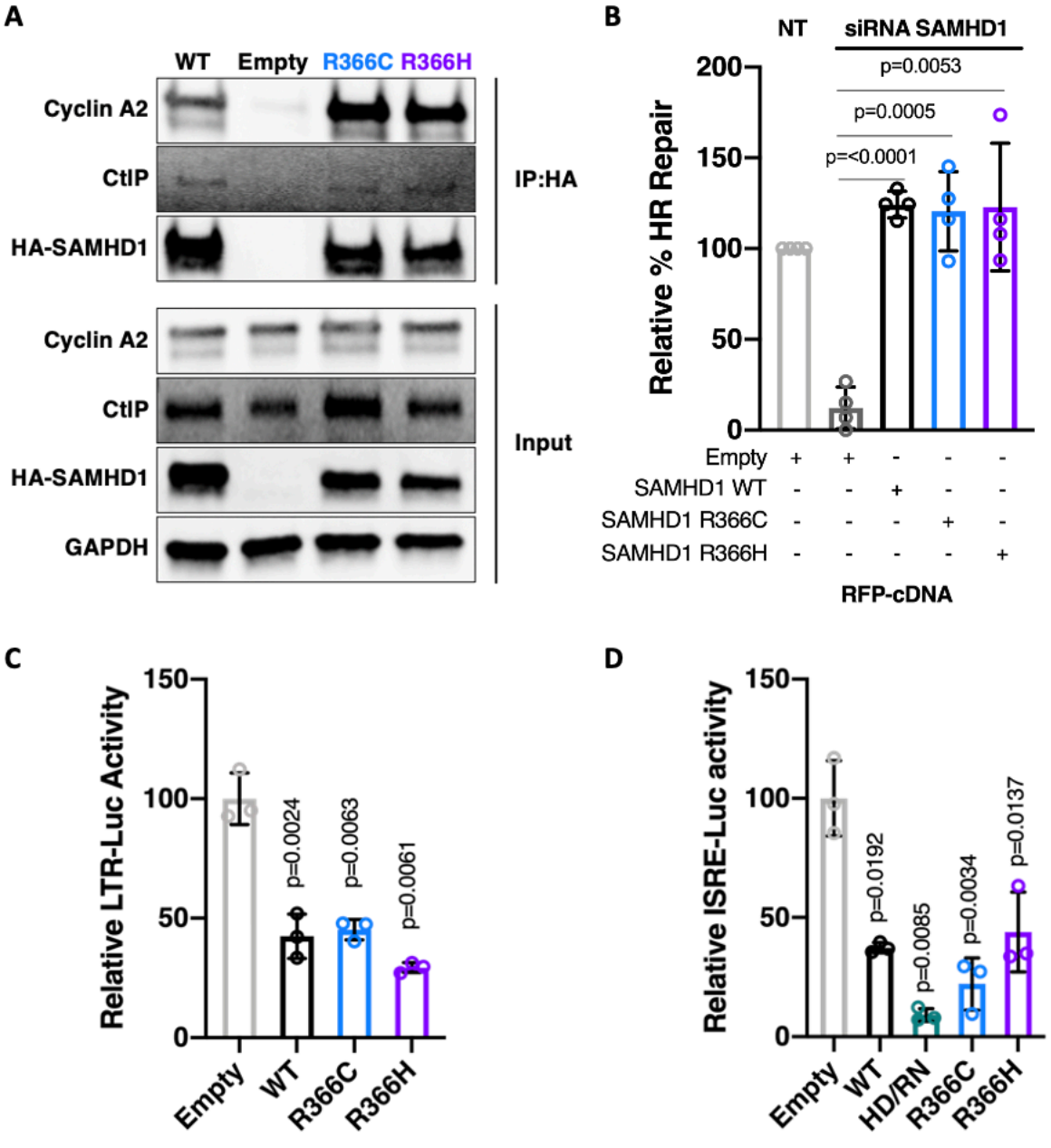
A
WT
Empty
R366C
R366H
Cyclin A2
CtIP
HA-SAMHD1
IP:HA
Cyclin A2
CtIP
HA-SAMHD1
GAPDH
Input
B
NT
siRNA SAMHD1
p=0.0053
p=0.0005
p=<0.0001
Relative % HR Repair
200
150
100
50
0
Empty + + - - -
SAMHD1 WT - - + - -
SAMHD1 R366C - - - + -
SAMHD1 R366H - - - - +
RFP-cDNA
C
Relative LTR-Luc Activity
150
100
50
0
p=0.0024
p=0.0063
p=0.0061
Empty
WT
R366C
R366H
D
Relative ISRE-Luc activity
150
100
50
0
p=0.0192
p=0.0085
p=0.0034
p=0.0137
Empty
WT
HD/RN
R366C
R366H

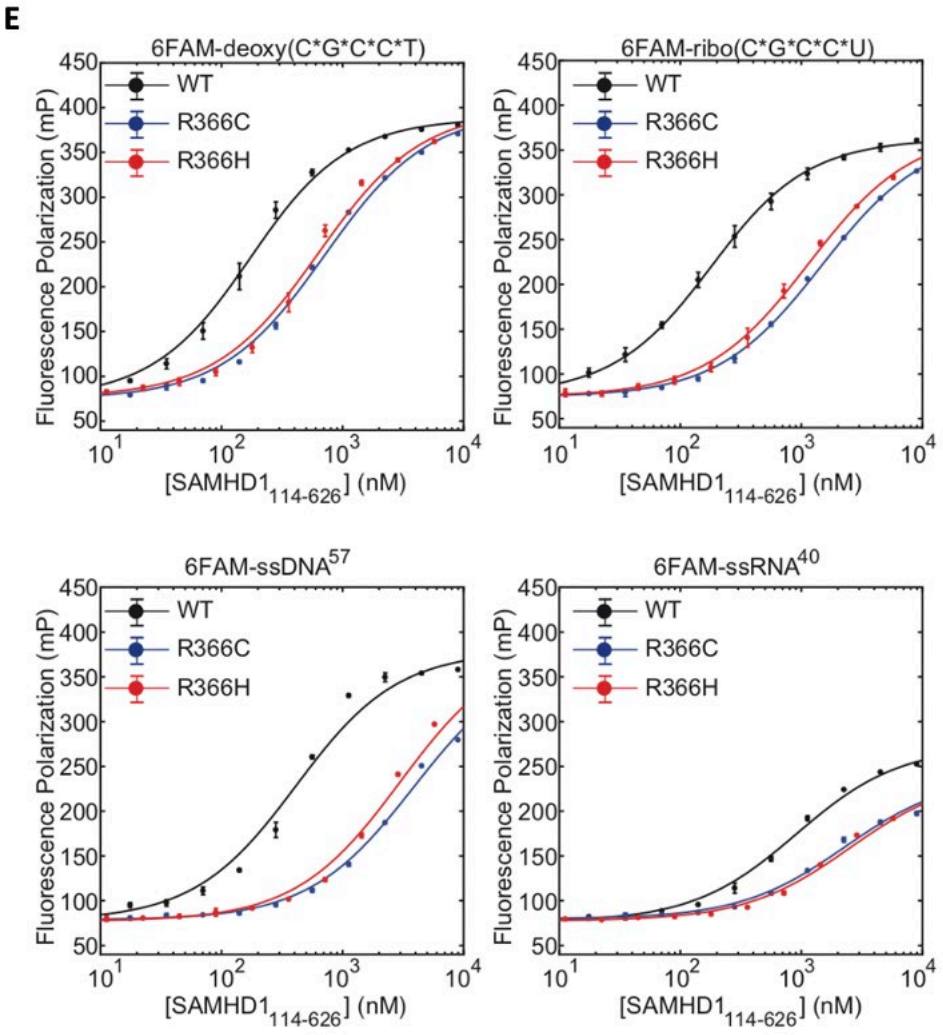

Figure 3.6: Effect of R366C and R366H SAMHD1 mutations on SAMHD1 dNTPase independent functions. A) Immunoprecipitation of Cyclin A2 and CtlP nuclease by SAMHD1. 293T cells were transfected with an equal amount of HA-tagged SAMHD1 expressing plasmids, and the expressed SAMHD1 proteins were pulled down by HA antibody beads. The lysates (Input) of the transfected cells and the pulldown fractions (IP:HA) were assessed by immunoblot using anti-HA antibody, Cyclin A2 antibody, and CtlP antibody. GAPDH was used for the loading control. Empty: Empty plasmid (pLVX-IRES-mCherry). **B)** dsDNA break repair activity of wild type and R366C/H mutants. U20S cells with integrated DR-GFP reporter construct were

transfected with I-Sce-I, SAMHD1-UTR siRNA, and RFP-SAMHD1 WT or R366C/H cDNA. Flow cytometry was used to assess for homologous recombination, as measured by GFP expression in cells expressing RFP. Empty: RFP plasmid. **C)** Suppression of LTR driven gene expression by wild type and R366C/H mutants. 293T cells were transfected with SAMHD1 expressing plasmids, HIV-1 LTR-firefly luciferase plasmid (LTR-Luc), and Renilla luciferase plasmid as a transfection control. Firefly luciferase activity was measured and normalized to Renilla luciferase activity 24 hr post-transfection. **D)** Suppression of ISRE stimulation by wild type ad R366C/H mutants. 293T cells were transfected by SAMHD1 expressing plasmids, ISRE-firefly luciferase plasmid (ISRE-Luc), IRF7 plasmid, and Renilla luciferase plasmid as a transfection control. Firefly luciferase activity was measured and normalized to Renilla luciferase activity 24hr post-transfection. **E)** Nucleic acid binding curves and binding constants of wild type and two R366 mutant SAMHD1 proteins were determined using fluorescence polarization. 6FAM-deoxy(C*G*C*C*T): WT K_d= 146.8± 8.3 nM, R366C K_d =689 ± 39 nM ,R366H K_d= 606 ± 46 nM. 6FAM-ribo(C*G*C*C*U): WT K_d= 153.8 ± 4.2 nM, R366C K_d= 1449 ± 51 nM , R366H K_d= 1125 ± 42 nM. 6FAM-ssDNA[57]: WT K_d= 387.2 ± 45.4 nM, R366C K_d= 3825 ± 340 nM, R366H K_d= 2965 ± 328 nM. 6FAM-ssRNA[40]: WT K_d= 884.8 ± 59.9 nM, R366C K_d= 2252 ± 249 nM , R366H K_d= 2476 ± 264 nM. Data are the mean of three replicates and error bars reflect standard deviation from the mean. P-values were determined using two-tailed, unpaired Welch's t-test to b. SAMHD1 siRNA +Empty, c. Empty, d. Empty.

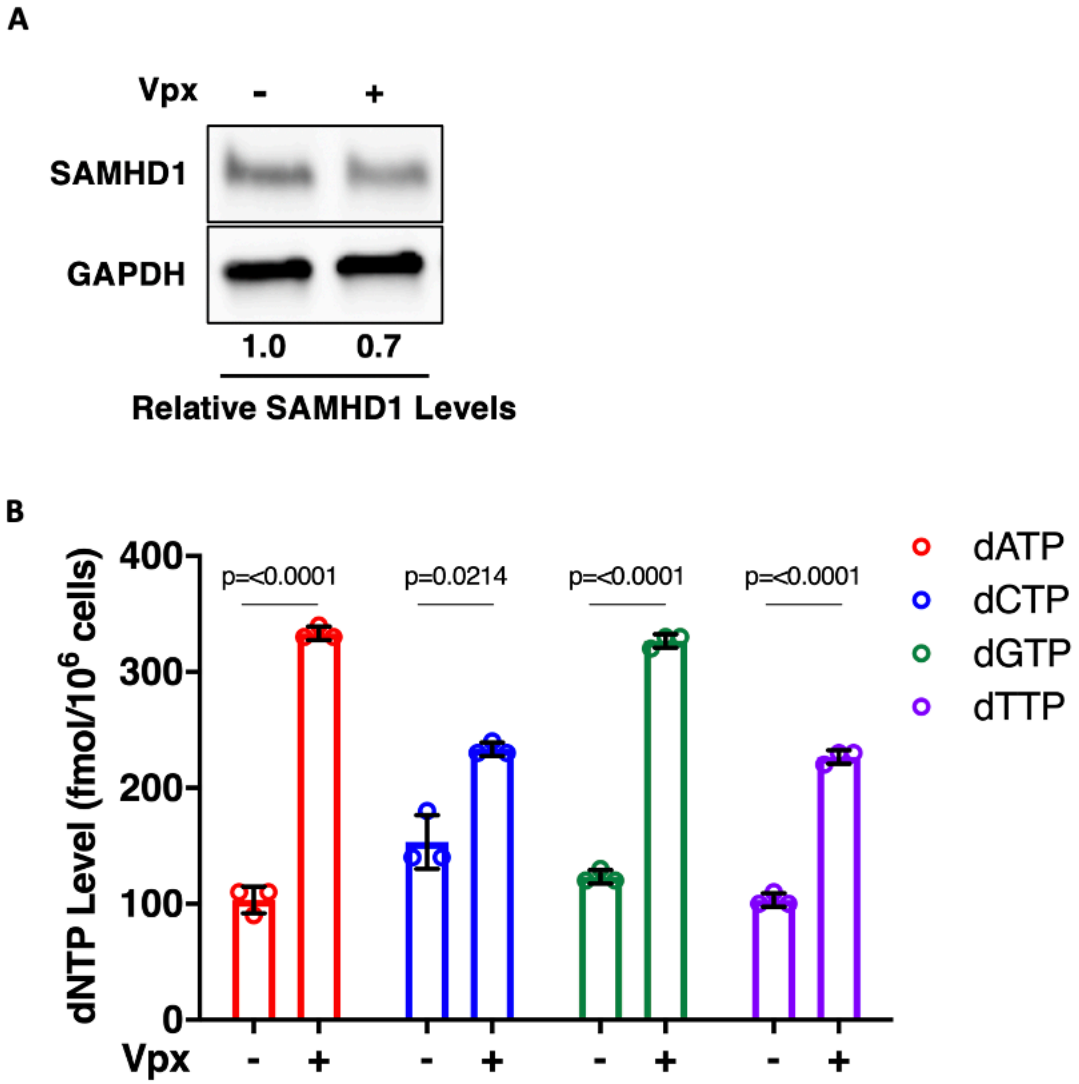

Figure 3.7: Effect of SAMHD1 degradation on intracellular dNTP levels in human primary activated/dividing CD4+ T cells. Human primary CD4+ T cells were isolated from 3 healthy donors, activated by PHA and IL-2 for 5 days, and treated with VLP Vpx (-) or VLP Vpx (+) for 24 hours. **A)** Cellular SAMHD1 protein levels were determined by immunoblot using anti-SAMHD1 antibody and anti-GAPDH antibody as a loading control. The relative SAMHD1 protein levels were normalized by GAPDH protein level and the ratios between wild type and mutant SAMHD1 protein levels were calculated. **B)** Intracellular dNTP levels were determined by RT-based dNTP assay. Data are the mean of three replicates and error bars reflect standard deviation

from the mean. P-values were determined using two-tailed, unpaired Welch's t-test to VLP Vpx-condition.

A

Condition	%GFP Positive Cells
WT	28.72%
Empty	25.24%
R145Q	29.84%
Y155C	38.16%
P158S	35.66%
I201N	42.69%
R366C	37.47%
R366H	21.81%

B

Condition	%mCherry Positive Cells
WT	69.2%
Empty	86.4%
L224F	68.9%
R451C	93.6%
F578V	72.2%

Supporting Table 3.1: Transfection efficiency of SAMHD1 cancer mutants. A) 293T cells were transfected with SAMHD1 plasmids and a GFP plasmid or **B)** an mCherry labelled SAMHD1 plasmid. Half of the sample was fixed and analyzed for GFP or mCherry using flow cytometry to determine transfection efficiency.

	R366C	R366H
Data collection		
Wavelength (Å)	**0.97918**	**0.97918**
Space group	**$P2_1$**	**$P2_1$**
Cell dimensions		
a, b, c (Å)	**80.9, 140.1, 97.2**	**83.7, 573.5, 100.5**
α, β, γ (˚)	**90.0, 114.2, 90.0**	**90.0, 114.7, 90.0**
No. molecules/asymmetric unit	**4**	**16**
Resolution (Å)	**50.0-1.9 (1.93-1.90)**	**50.0-3.60 (3.66-3.60)**
R_{merge}	**0.071 (>1)**	**0.143 (>1)**
Mean I / σI	**17.3 (1.0)**	**13.8 (1.6)**
$CC_{1/2}$	**0.999 (0.297)**	**0.996 (0.690)**
Completeness (%)	**99.1 (98.8)**	**85.6 (83.1)**
Redundancy	**3.3 (3.3)**	**5.1 (4.8)**
Unique reflections	**153,730 (7,622)**	**84,897 (4,131)**
Refinement		
No. nonhydrogen atoms	**16,683**	**64,032**
R_{work}/R_{free}	**0.173/0.207**	**0.227/0.259**
Mean B-factor ($Å^2$)	**31**	**144**
R.m.s.d.		
Bond lengths (Å)	**0.012**	**0.008**
Bond angles (˚)	**1.7**	**1.4**

Ramachandran		
Favored (%)	**98.64**	**97.84**
Allowed (%)	**1.26**	**2.11**
Outliers (%)	**0.10**	**0.05**

Supporting Table 3.2: Crystal Structure data collection and refinement statistics.

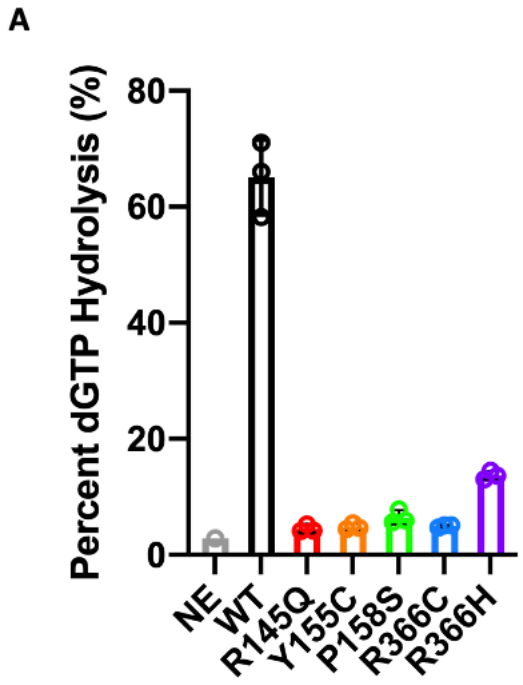

Supporting Figure 3.1: Percent dGTP hydrolysis of SAMHD1 mutants. A) Wild type and mutant SAMHD1 were incubated with α^{32}P-dGTP in the presence of excess unlabeled dGTP. Reaction substrate and product were separated using TLC (Figure 3.3A). Densitometry analysis of the TLC plate was performed and percent dGTP hydrolysis was calculated by dividing the triphosphate product by the lane total.

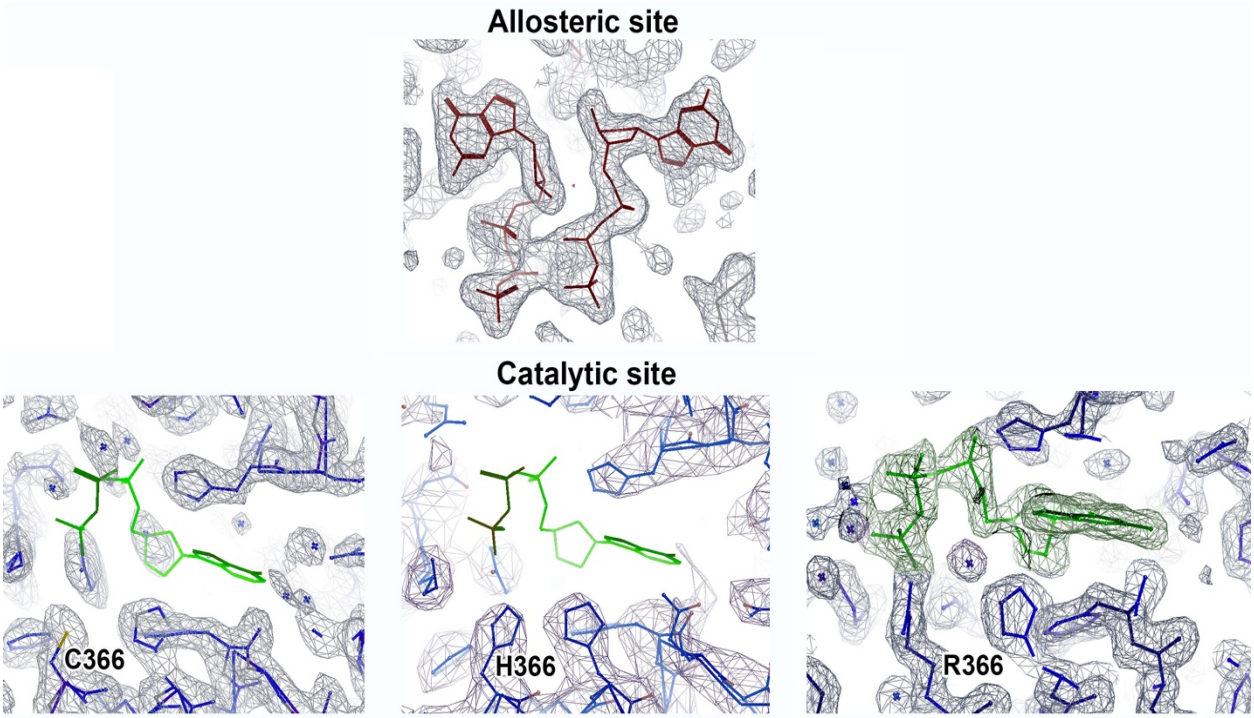

Supporting Figure 3.2: Electron density in the allosteric and catalytic sites of R366C/H. 2Fo-Fc electron density (1s level, gray mesh) of the regions around the allosteric nucleotides of the R366C structure (top) and the catalytic site of the R366C (bottom left), the R366H (bottom middle, sharpened by a B-factor of -80 $Å^2$), and the $SAMHD1_{HD/RN}$ (bottom right, PDB 4BZB) structures. There is a lack of nucleotide density in the catalytic site of the R366C/H mutant structures, where the nucleotide substrate (green) was modeled in based on its position in the $SAMHD1_{HD/RN}$ structure.

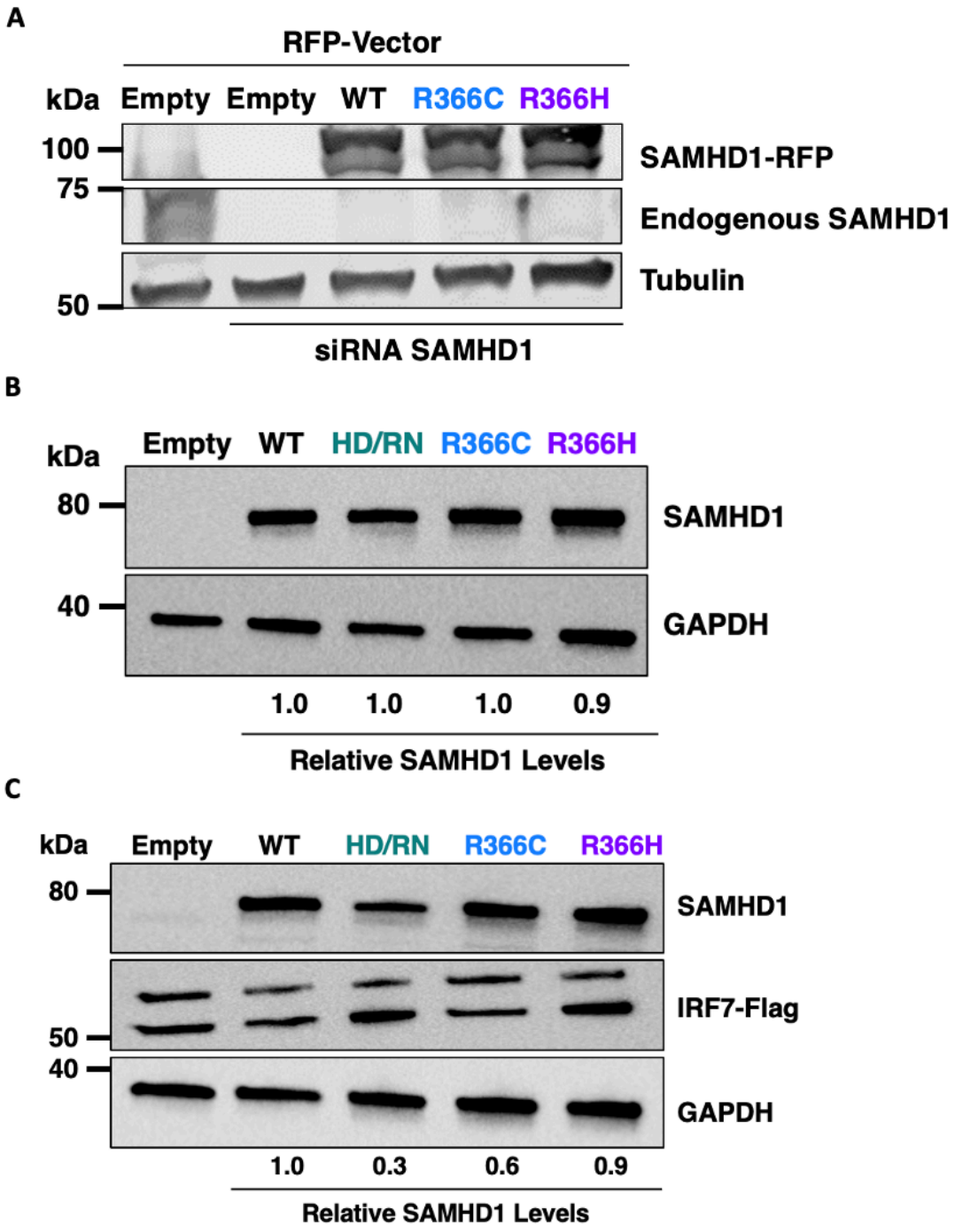

Supporting Figure 3.3: Immunoblot for SAMHD1 expression levels. A) dsDNA repair by Homologous Recombination **B)** LTR-Luciferase assay **C)** ISRE-Luciferase assay. Expression levels of SAMHD1 were used to normalize activity data in Figure 3.6.

Chapter 4

Concluding Remarks.

Nicole E. Bowen[1]

[1.] Center for ViroScience and Cure, Department of Pediatrics, School of Medicine, Emory University, Atlanta, Georgia, USA.

4.1 Abstract

The findings described in Chapter 2 and Chapter 3 of this work provide mechanistic insight into how lentiviruses and cancer cells, respectively, modulate intracellular dNTP pools during pathogenesis. In this chapter, I 1) summarize and contextualize these findings with respect to outstanding questions in their respective fields and 2) discuss future directions for addressing these remaining gaps in knowledge.

4.2 Macrophage tropism as a driver of lentiviral evolution.

4.2.1 Lentiviruses have acquired adaptations to infect macrophages over evolutionary time.

HIV-1 primarily infects and kills CD4+ T-cells, which is why HIV disease progression in the clinic is monitored using CD4+ T-cell count. dNTPs, substrates of reverse transcriptase, are ~200-fold higher in CD4+T-cells than in macrophages, resulting in faster replication kinetics and a more permissive infection in CD4+T-cells when compared to macrophages[5]. Indeed, previous work from our laboratory established that the dNTP concentrations available in macrophages is lower than the K_M of reverse transcriptase, thus providing a kinetic block to reverse transcription[42]. This begs the question: why infect macrophages? Interestingly, many non-primate lentiviruses including equine infectious anemia virus[239], ovine lentivirus[240], visna-maedi virus[241], and caprine arthritis-encephalitis virus[242] are mainly or exclusively macrophage trophic. The lack of a dUTPase gene in all primate lentiviruses and the distance between primate lentiviruses as compared to the distance between other mammalian lentiviruses, suggest that non-primate lentiviruses served as

the evolutionary ancestor of the primate lentiviruses[243]. Therefore, macrophage tropism can be viewed as a more intrinsic property of the lentivirus, with T-cell tropism emerging later in evolutionary history.

Due to the conservation of macrophages as targets of lentiviral infection, it is likely that macrophage tropism posed an important selective pressure on these viruses over evolutionary time. One example of adaptation to the low dNTP pools present during macrophage infection is the ability to directly counteract SAMHD1. While mammals have functional SAMHD1 that restricts non-primate lentiviruses, feline, equine, and bovine lentiviruses do not have the ability target SAMHD1 for proteasomal degradation[127]. This would imply that non-primate lentiviruses do not have the ability to counteract SAMHD1 and that this function evolved specifically in primate lentiviruses. Indeed, phylogenetic evidence suggests that Vpr was neofunctionalized to degrade SAMHD1 leading up to the split of the SIVagm and SIVdeb/mus/mon lineages[115]. Thereafter, a gene duplication of Vpr occurred leading to the origin of Vpx.[115] Due to the host-pathogen evolutionary arms-race, SAMHD1 was rapidly diversifying to escape Vpr recognition and some have speculated that this gene duplication event allowed for the virus to maintain other Vpr targets while maximizing the ability to target SAMHD1[115]. Notably, Chapter 2 of this work highlights that the SAMHD1 counteracting function of Vpr/Vpx could only evolve due to the presence of ongoing dNTP biosynthesis in macrophages. In addition to just degrading SAMHD1, lentiviruses must exploit the active dNTP biosynthesis in macrophages in order to raise intracellular dNTP pools and relieve restriction. Future work can confirm this through a similar study using a SAMHD1-counteracting Vpr.

While some lentiviral lineages have evolved a mechanism to directly counteract SAMHD1 and elevate dNTP pools in order to replicate in macrophages, HIV-1 has evolved a different

approach, likely due to the distinct ancestry of the virus. Globally, HIV-1 infections are dominated by group M[244], which originated from a cross-species transmission event from chimpanzees, SIVcpz, which lacks Vpx[245, 246]. SIVcpz, in turn was generated from an interspecies transmission event and recombination between SIVrcm from red-capped mangabeys and SIVmus/mon/gsn from Cercopithecus monkeys[247]. Phylogenic analyses demonstrate that SIVcpz acquired Vif and Vpr from SIVrcm, but interestingly, SIVrcm codes for Vpx between these two genes[246]. Phylogeny would suggest a deletion event of Vpx occurred in SIVcpz which also resulted in a 160bp deletion in Vif in an area of overlap[113]. Due to a related overprinting event during this recombination, Vif aquired 61 bp from the 5' end of Vpr and a completely novel 60–75 bp, thus producing a unique Vif C-terminal domain[113]. Strikingly, these novel 60-75 bases did not match known lentiviral or primate genomic sequences and are unique to SIVcpz and related strains[113]. However, these sequences harbor the "cullin box" and PPLP motif necessary for HIV-1 to degrade host APOBEC3G[248], a cytidine deaminase that restricts viral replication through hypermutation[249, 250]. This may suggest that the selective pressure exerted from the cross-species jump from old world monkeys to chimpanzees favored a virus that could counteract APOBEC3G to a virus that could counteract SAMHD1[113]. However, it is also possible that SIVcpz acquired functions to circumvent the absence of a direct SAMHD1 antagonism. In the case of HIV-1, a more efficient reverse transcriptase evolved that can more efficiently polymerize DNA than the RTs of SAMHD1 counteracting lentiviruses[42, 124]. This is a result of a faster conformational change step (k_{conf}) during polymerization[125]. This increased efficiency allows HIV-1 to bypass SAMHD1 restriction and replicate in the low dNTP pool environment of macrophages[125]. Moreover, previous work from our laboratory has shown that RTs from SIVmac239 Vpx- infections acquire mutations that result in enhanced RT kinetics when compared to RTs from SIVmac239 Vpx+ infections[126]. This

strongly suggests that the absence of Vpx in SIVcpz and HIV-1 could have directly driven HIV-1 RT to become more efficient in order to indirectly counteract the limited availability of dNTPs in macrophages.

4.2.2 Herpesviruses have evolved adaptations distinct from lentiviruses for macrophage infection.

More broadly, other macrophage-tropic viruses that utilize dNTPs during their replicative processes, like herpesviruses, have uniquely adapted to infect macrophages[251]. For example, herpesviruses encode for orthologous serine and threonine protein kinases known as conserved herpesvirus protein kinases (CHPKs)[252]. These CHPKs are known to phosphorylate a number of cellular targets in order to facilitate viral replication[253-255]. More recently, SAMHD1 was identified as a shared target of CHPKs from betaherpesviruses, such as CMV pUL97, and gammaherpesviruses, such as EBV BGLF4[256, 257]. This phosphorylation event inactivates SAMHD1 dNTPase activity in biochemical assays[256], but future studies are needed to demonstrate conclusively that this translates to elevated dNTP levels in macrophages during infection. Based on work from Chapter 2, it could be proposed that this direct counteraction of SAMHD1 is also dependent on the presence of ongoing dNTP biosynthesis in macrophages to elevate dNTPs once SAMHD1 has been inactivated. While further work would be needed to test this hypothesis, this mechanism is potentially another example of viral adaptation to macrophage infection that could only be possible due to active dNTP biosynthesis. At the same time, some herpesviruses encode their own dNTP biosynthesis machinery as an adaptation to infection in low dNTP pools[251, 258]. For example, alphaherpesviruses, such as HSV-1[259, 260], and gammherpesviruses, such as EBV[261,

[262], encode for a viral thymidine kinase (TK). Additionally, herpesviruses contain a viral RNR[263]. Although, all herpesviruses encode for the large subunit of RNR, M1[264, 265], only alphaherpesviruses and gammaherpesviruses code for the small unit of RNR, R2[8, 266], to make an enzymatically active protein. Taken together, herpesviruses have evolved distinct mechanisms from lentiviruses to ensure productive replication in the macrophage environment.

4.2.3 The inhibitory "cost" of individual adaptations to infect macrophages depends on viral background.

The types of mechanisms different viruses have evolved to adapt to infection in macrophages is likely dependent on a variety of factors. One consideration, as discussed previously for HIV-1, is viral lineage. As HIV-1 and HIV-2 came from separate paths before transmission to humans, their lineages were influenced by different cross-species transmission events. These events provided distinct sources for bottlenecks and selective pressures established by adaptations to different hosts. In short, HIV-1 likely developed a more efficient RT to replicate in macrophages because it came from a lineage without Vpx to directly counteract SAMHD1. Another consideration is the trade-offs associated with different mechanisms and how "expensive" those trade-offs would be for a particular type of virus. For example, SAMHD1 suppresses the innate immune response[148, 150] and therefore SAMHD1 depletion results in a hyper-interferon (IFN) state as seen in AGS patients[137, 143]. This would generate a hostile environment for infection and, indeed, SAMHD1 depletion inhibits the replication of viruses such as SARS-CoV-2[154]. However, lentiviruses such as HIV-1 utilize NF-κB, an element of the innate immune response, to drive proviral transcription[230, 267, 268] and HIV-1 stimulates NF-κB activity with accessory protein Tat

for this reason [269, 270]. In addition to exploiting elements of the innate immune response for transcription, every transmission event selects for viruses that have maximized IFN insensitivities[271]. Due to these aspects, a lentivirus may have been able to afford the "cost" of an adaptation that depletes SAMHD1 whereas this would not be as feasible for other viruses. For viruses like herpesviruses, simply inactivating SAMHD1 dNTPase activity with a viral kinase or coding for viral dNTP biosynthesis enzymes may have served as a way to counteract SAMHD1 without inducing the innate immune response. Although, coding additional enzymes is a luxury that typically only DNA viruses with large genomes like herpesviruses can afford[272], making this adaptation not practical for a lentivirus. HIV-1, on the other hand, evolved an RT with a lower K_M than that of SAMHD1 counteracting viruses in order to replicate in macrophage dNTP concentrations[42]. In a previous review[273], we proposed that adapting to replicate in these low dNTP concentrations was also the selective pressure that drove the error prone nature of HIV-1. In low dNTP concentrations polymerases are more likely to pause, generating mutation hot spots [175]. However, to survive and generate progeny the virus must complete reverse transcription regardless of the likely increase in mutation synthesis due to these low dNTPs. The ability to extend after nucleotide misincorporation would be a replicative advantage in this environment therefore selecting for the efficient mismatch extension capabilities and increased error rate of HIV-1 RT[274]. Given this hypothesis, evolving a more efficient polymerase at the cost of increased error rate would be inhibitory for viruses such as herpesviruses, which are able to maintain large genome sizes with increased coding capacity due to the fidelity of their replicative cycles.

4.2.4 The search for the significance of macrophage infection to lentiviruses is ongoing.

It is clear the evolution of lentiviruses has been shaped by macrophage tropism. However, if macrophages do not serve as the primary target for primate lentiviruses, are difficult to establish infection in, and require the virus to have additional adaptations, why have these viruses maintained their macrophage tropism? That primate lentiviruses have accepted certain costly trade-offs to preserve macrophage tropism is, perhaps, indicative of some importance. However, this importance remains unclear. For a time, scientists in the field believed that macrophages served an important role during HIV-1 transmission. Macrophages patrolling the lamina would be among the first cells that an infecting virus would encounter[275] and infected macrophages can transfer virus to uninfected cells through synapses[276-278]. Additionally, transmitted founder viruses are almost exclusively CCR5 (R5) coreceptor trophic, a phenotype originally associated with macrophage tropism[279]. The virus then undergoes a change in coreceptor usage to predominantly use CXCR4 (X4) later in the course of infection[280]. Later research demonstrated this was an oversimplification that led to erroneous conclusions[281]. While transmitted founder viruses are indeed R5 tropic, they poorly infect low density CD4+ cells such as macrophages[282, 283]. Whereas the primary targets of these initial founder viruses are CCR5+ cells with high density CD4 that is characteristic of memory T-cells[284, 285]. The coreceptor switch that occurs later in infection aids the virus in infecting naïve T-cells[284, 285], possibly when running low on the preferential T-cell target[281]. Macrophage tropic viruses arise from T-cell R5 tropic viruses that bind CD4 more strongly and can enter low CD4 density cells such as macrophages[281]. These variants are not typically found in the blood[286, 287] and are instead associated with compartmentalized replication in the central nervous system (CNS)[288, 289]. To more strongly bind CD4, envelope needs to adopt a slightly more open conformation that makes it more susceptible to CD4-binding site

antibodies[290]. This is turn might restrict more viruses from adopting a high CD4 affinity even though it would, in theory, allow entry into T-cells and macrophages[281].

That founder viruses are T-cell tropic and macrophage infection generally occurs in compartments may indicate that the importance of macrophage infection does not lie in early viral transmission or dissemination. A study using SIVmac239 without Vpx demonstrated that during infection in rhesus macaques Vpx is required for macrophage infection, but macaques infected with SIVmac239Δvpx still progressed to AIDS[291]. However, SIVmac239Δvpx infected monkeys had lower viral loads and a slower progression to AIDS, suggesting some significance of macrophage infection in overall disease progression[291]. Indeed, compartments like the CNS serve as viral sanctuaries that contribute to viral persistence due to their immune privilege and relative difficulty in being reached by antiretroviral therapy[292-294]. Infections in these areas can contribute to the viral reservoir as infected macrophages can persist even in antiretroviral therapy (ART) treated patients with undetectable viral loads[295, 296]. Though, macrophage contribution to the viral reservoir is controversial and one study has found that most rebound viruses after ART cessation required high levels of CD4 for entry, suggesting rebound viruses originated from T-cells rather than macrophages[297]. Nevertheless, macrophage infection in the CNS contributes to HIV-associated neurocognitive disorders (HAND)[298, 299] which even affects patients treated effectively with ART[300-302].

As it stands, the importance of maintaining macrophage tropism to primate lentiviruses remains unclear. One hypothesis is that macrophages serve as sites of mutation synthesis and therefore, infection in this cell type contributes to the overall genetic diversity during infection. Polymerases are more likely to pause in low dNTP pool environments, which can generate mutational hot spots[175]. HIV-1 RT, as discussed previously, has a high rate of mismatched primer

extension after mutation synthesis[274]. From these biochemical data it would be reasonable to expect the mutation rate of HIV-1 in macrophages to be higher than that in T-cells. Although, a study using primary monocyte-derived-macrophages (MDMs) and T-cells conversely found the mutation rate of HIV-1 to be higher in T-cells than in MDMs[303]. While the types of mutations observed in MDMs vs T-cells were similar, the authors did not comment on the location of these mutations or potential differences in mutational hotspots depending on cell type[303]. Therefore, it is possible that HIV-1 infection in macrophages produces unique mutation patterns that benefit viral diversity. This is plausible given biochemical data indicating that the limited dNTP concentration in macrophages generates unique pause sites during reverse transcription and these pause sites can serve as sites of mutation synthesis[5, 175]. While the Mak group did not observe increased mutation frequency in macrophages, they did observe more recombination events during macrophage infection than in T-cell infection[303], which is consistent with other studies[94, 304]. These recombination events provide an additional mechanism of genetic diversity whereby the virus switches between the two co-packaged viral RNA templates during reverse transcription[305, 306]. Therefore, HIV-1 infection in macrophages may uniquely contribute to the overall genetic diversity during an infection through increased recombination events. An interesting way to further probe the impact of macrophage infection on viral diversity would be to compare the overall viral genetic diversity in macaques infected with SIVmac239, which infects macrophages, to that of macaques infected with SIVmac239Δvpx, which cannot infect macrophages. The importance of viral diversity to evading the immune response and ART to maintain infection at the population level cannot be understated and could prove to be a reason primate lentivirus have adapted to maintain their macrophage tropism.

4.3 Mechanisms of cancer cell dNTP pool elevation and therapeutic implications.

4.3.1 Cancer cells utilize diverse mechanisms to elevate intracellular dNTP pools.

Cancer cells, like lentiviruses infecting macrophages, encounter the obstacle of insufficient dNTPs for genome replication. Cancer cells ubiquitously address this problem by elevating dNTP concentrations 6-11 fold[180] to support rapid genomic DNA synthesis and cell replication[307]. In fact, nucleotide metabolism can be considered a critical link in tumorigenesis, as providing sufficient amounts of dNTPs requires the upregulation of several metabolic pathways that produce nonessential amino acids, ribose, and one-carbon donors[205, 308]. Therefore, cancer cells can use a variety of mechanisms to achieve dNTP elevation[211]. Many pathways that are commonly manipulated by cancer have an influence on dNTP metabolism. For example, 70% of cancers constitutively and aberrantly express c-myc, a master transcription factor known to also regulate nucleotide biosynthesis enzymes[309, 310]. c-myc induces the expression of phosphoribosyl pyrophosphate synthetase 2 (PRPS2) and carbamoyl phosphate synthetase II (CAD), which initiate purine and pyrimidine ring biosynthesis, respectively[311-313]. Additionally, 50-65% of cancers will have mutations in p53, a tumor suppressor[314, 315]. Some mutant p53 associate with the promoters of genes coding for nucleotide biosynthesis enzymes such as deoxycytidine kinase (dCK) and thymidine kinase (TK1) to drive their transcription[316]. pRb is a tumor suppressor that is also frequently mutated in a variety of cancers[317]. Loss of function in pRb overactivates E2F-1, a major G1/S phase transition transcription factor[318]. E2F-1 the controls expression thymidylate synthase (TYMS), which catalyzes the methylation dUMP to generate dTMP to feed into the dNTP salvage pathway, and dihydrofolate reductase (DHFR), which restores the methyl group donor for the

TYMS reaction, MTHF[319, 320]. DHFR can also reduce folic acid from the environment to THF which it can subsequently restore to MTHF to generate additional cofactors for TYMS[321]. E2F-1 is also a transcription factor for RNR M2 and thymidine kinase 1 (TK1)[318, 322]. Finally, 38% of cancers will have a mutation in the PI3K/AKT/mTOR pathway[323]. This is pertinent as activation of mTORC1 stimulates *de novo* synthesis of both purines and pyrimidines[324, 325] and activation of mTORC2 enhances RNR activity[326]. Overexpression of RNR M2 is considered to be tumorigenic[327] and it has been proposed to use RNR M2 as a prognostic and diagnostic biomarker for cancer[328-331].

While cancers can influence dNTP metabolism indirectly with common mutations that upregulate broad acting pathways, some cancers take a more direct approach. Recently, SAMHD1 has become of interest to the cancer field as downregulation of the enzyme could in theory lead to an accumulation of dNTPs for hyperproliferation. Indeed, SAMHD1 expression was found to be reduced in cutaneous T-cell lymphoma (CTCL), T-cell acute lymphoblastic leukemia (T-ALL), and lung cell adenocarcinoma due to promoter methylation[90, 185, 192]. SAMHD1 mutations have also been identified in cancers including leukemias[160, 181-184], lymphomas[185-187], lung cancer[171], and colon cancer[188-190]. In one study, SAMHD1 mutations were found in 18% of patients with T-cell prolymphocytic leukemia (T-PLL) making it the second most frequently mutated gene in the study[182]. SAMHD1 cancer-associated mutations are found throughout the entire protein and often cause reduced SAMHD1 protein levels[32, 332]. In this work, most of the SAMHD1 cancer mutants tested had poor stability profiles[191]. Therefore, decreased SAMHD1 expression in patients with these mutations is likely a result of altered protein structure causing instability, which results in cell clearance. These decreased expression patterns made it difficult to pinpoint which function of SAMHD1 was contributing to a cancer phenotype. However, Chapter 3 of this work identified the

R366C/H mutant from leukemia and colon cancer as having similar expression and stability profiles to wild type SAMHD1. Importantly, this mutant could then serve as a tool to assess which functions of SAMHD1 might contribute to cancer. Strikingly, the R366C/H mutant was only impaired in dNTPase activity. Therefore, this work found that mutations in SAMHD1 can impact overall dNTPase activity and contribute to the dNTP pool elevation observed in cancer. Notably, this establishes SAMHD1 mutations as a direct mechanism that cancer cells can utilize to elevate dNTP pools.

4.3.2 Cancer therapies target dNTP metabolism.

Due to the importance of altered dNTP metabolism to cancer cells, many FDA approved cancer therapies target dNTP metabolism[205]. Methotrexate, for example, was FDA approved in 1953 and is used to target a wide array of caners type such as acute lymphoblastic leukemia, breast cancer, lung cancer, and advanced non-Hodgkin's lymphoma[205]. Methotrexate inhibits dNTP biosynthesis by targeting enzymes such as thymidylate synthase (TYMS) and dihydrofolate reductase (DHFR) to inhibit the salvage pathway[333, 334]. In fact, TYMS is a common target for this class of cancer therapies with Fluorouracil[335], Floxuridine[336], Capecitabine[337], and Pemetrexed[338] all targeting this enzyme. RNR also serves as a common therapeutic target[205]. Fludarabine[339], Cladribine[340], and Clofarabine[341] all inhibit RNR and are used in front line drug-combination treatments for various leukemias. Gemcitabine, another RNR inhibitor, is utilized in combination treatment strategies for breast[342], ovarian[343], lung[344], and pancreatic cancers[345]. In general, more success has been found with these types of inhibitors that directly target dNTP metabolism enzymes, rather than targeting the overarching disruptions like c-myc and mTOR that are causing

the elevations. In both cases, due to the multifaceted nature of the pathways they are involved in, inhibiting c-myc or mTOR leads to toxicity or incomplete inhibition[310, 346]. Although, further work increasing the specificity of these types of inhibitors may prove successful. Due to the success of drugs targeting dNTP metabolism in the clinic, more are in the research pipeline. This includes recently completed phase 1 trials of 4-hydroxysalicylanilide (HDS), an RNR inhibitor, for multiple myeloma[347] and of CT900, a TYMS inhibitor, for ovarian cancer[348].

4.3.3 Therapeutic implications of SAMHD1.

SAMHD1 can be considered a double-edged sword when considering the role of the enzyme in cancer. One on hand, intact SAMHD1 expression can interfere with the efficacy of the triphosphorylated forms of some anti-cancer nucleoside analogues due to the enzyme's ability to hydrolyze these compounds [60, 63, 195, 196]. SAMHD1 expression has been shown to regulate the response of cancer cells to cytarabine (ara-C)[62, 197], arabinosylguanine (AraG) [192], and 2′-C-cyano-2′-deoxy-1-β-D-arabino-pentofuranosyl-cytosine (CNDAC) [198], and decitabine. [199] Given these biochemical findings, it is possible that SAMHD1 can mediate resistance to nucleotide analog based therapies. In fact, one study found that while 3% of CLL patients harbored SAMHD1 mutations pre-treatment, this percentage climbed to 11% in the relapsed group[160]. Moreover, another CLL study found that pre-existing subclones with SAMHD1 were enriched after therapy in a cohort of relapsed patients[181]. SAMHD1 is also known to play a role in Ara-C response in acute myeloid leukemia (AML) patients[62, 198] and expression of SAMHD1 is highly upregulated in AML patients with Ara-C resistance[61, 62]. In a study of solid tumors, high SAMHD1 expression was associated with a poorer prognosis in breast, ovarian, and non-small cell lung cancer

patients[349]. To remedy SAMHD1 interference with cancer treatments and help prognosis, several suggestions have been made including treatment with Vpx to degrade SAMHD1 [61] and treatment with RNR inhibitors to induce dNTP pool imbalances and inhibit SAMHD1 allosteric activation [203].

On the other hand, as previously discussed, SAMHD1 mutations can contribute to the elevated dNTP level cancer cells need to support their hyperproliferation. One current shortcoming of the field is that it mainly uses SAMHD1 expression levels in analyses of the impact of SAMHD1 on treatment outcomes. This work has provided an example of a SAMHD1 mutant that expresses well but lacks dNTPase activity[191]. Therefore, to truly analyze the prognostic value of SAMHD1 future work needs to move towards more sequencing-based methods with functional follow-ups. Otherwise, cases of well expressing SAMHD1 without dNTPase activity may be missed. This is especially pertinent in the age of personalized medicine when assessing treatment options for individual patients. SAMHD1 low expressing cancers may have different treatment options compared to SAMHD1 dNTPase inactive cancers. While SAMHD1 low expressing cancers often show better treatment prognoses, additional ways to target these cells might help patient outcomes. For example, low SAMHD1 expressing tumors showed increased γ-H2AX and apoptosis, likely due to the role of SAMHD1 in DNA damage repair[159, 349]. Therefore, tumors with low level SAMHD1 expression may be more sensitive to chemotherapeutics that induce DNA damage, such as platinum-based drugs or etoposides[350]. However, both low SAMHD1 expressing cancers and SAMHD1 dNTPase inactive cancers should be more susceptible to the cytotoxic effects of nucleotide accumulation or imbalance[193, 194]. Therefore, treatment PNP inhibitors such as forodesine which allow for the accumulation of dGTP, might be able to specifically target these cancers[193, 194].

4.3.4 Refining the role of SAMHD1 in cancer continues.

Several big picture questions about the role of SAMHD1 in cancer remain unanswered. Most obviously, more studies assessing the diagnostic and prognostic value of SAMHD1 in different cancer types and treatment courses are needed before SAMHD1 can be leveraged as a true biomarker for cancer. Additionally, it remains unclear what percentage of SAMHD1 low expressing cancers are caused by direct mutation or by promoter methylation. Hopefully, these studies will also help to address another outstanding question in the field: whether the functionality of SAMHD1 as a biomarker differs in blood cancers vs solid tumors. Many of the original studies of SAMHD1 in cancer were conducted in blood cancers including cutaneous T-cell lymphoma (CTCL)[185, 186], T-cell acute lymphoblastic leukemia (T-ALL)[192], T-cell prolymphocytic leukemia[182], chronic lymphocytic leukemia (CLL)[160, 181, 351-353], acute myeloid leukemia (AML)[61, 183], acute lymphoblastic leukemia (ALL)[192, 198], Hodgkin lymphoma[201], and mantle cell lymphoma[187]. Much less data are available on SAMHD1 in solid tumors despite mutations being identified in the International Cancer Genome Consortium (ICGC) database[332]. Indeed, data have been limited to colon cancers[188-190], lung adenocarcinoma (LAC)[171], non-small lung cancer (NSLC)[354], lung adenocarcinoma[332], cutaneous melanoma[355], and breast cancer[160]. Moreover, several of the solid tumor studies have identified SAMHD1 downregulation but have not directly studied SAMHD1 as is the case in blood cancers. At present, it remains unclear whether this is because SAMHD1 truly plays a larger role in blood cancers or if this is due to a selection effect.

Due to the above studies many groups have called to designate SAMHD1 as a tumor suppressor, which is a gene that regulates normal cell proliferation and therefore is typically

repressed by cancers[356]. However, a more complicated issue is the potential of SAMHD1 as a driver of cancer. Driver genes, when mutated confer a growth advantage to cancer cells and can promote tumorigenesis[357]. Conversely, mutations that do not confer this advantage when mutated are termed passenger genes[357]. Definitionally, it seems like SAMHD1 could function as a driver of cancer, but the data to support this is limited. In one CLL patient, a mutation in SAMHD1 was detected in a founder subclone, indicating it could have served as a driver in this instance[351]. SAMHD1 is recurrently mutated in CLL, but at 2.5% the frequency of SAMHD1 mutations occurs at a much lower level than established CLL driver genes[358]. Moreover, only one report of an AGS patient with a SAMHD1 deficiency developing cancer exists[160]. Although, it is unclear if this is because AGS patients typically die at a young age perhaps before cancer would be aquired[135]. There is no cancer reported in SAMHD1 knock-out mice, however, these mice also do not display the traditional AGS phenotype, indicating some SAMHD1 functions could be species specific[233, 234]. Certainly, more data are needed before SAMHD1 can be classified as a driver and it is possible that the driver status of SAMHD1 is dependent on cancer type and progression state[332]. Interestingly, SAMHD1 has been found to exert a mutator phenotype more strongly when paired with mutations in DNA repair pathways[188]. This may suggest that SAMHD1 belongs to a newer category of genes termed “mini-drivers”. Mutations in mini-drivers only slightly increase the fitness of a cancer cell, but this effect can in combination with mutations in other mini-drivers add up to an advantage comparable to a mutation in a driver gene[359]. If SAMHD1 is indeed a “mini-driver”, advantages of a mutation would be highly context dependent. Therefore, future work would need to characterize the co-occurrence of SAMHD1 with mutations across other pathways.

4.4 Summary

Both lentiviruses and cancer cells use distinct, but intrinsically linked mechanisms to modulate dNTP pools during pathogenesis. This work established the presence of active dNTP biosynthesis in non-dividing macrophages as a major determinant of the ability of Vpx to raise intracellular dNTP levels in this cell type. While the significance of macrophage tropism to overall lentiviral infection is undetermined, lentiviruses have adapted to maintain macrophage tropism over evolutionary time. An entire lineage of lentiviruses evolved the ability to counteract SAMHD1 to preserve macrophage tropism based on the ongoing dNTP biosynthesis uncovered by this work. This work also utilized a well expressed and stable cancer associated SAMHD1 mutant to demonstrate that mutations in SAMHD1 can contribute to the increase in dNTP pools characteristic of cancer cells. The overall significance of mutations in SAMHD1 as a driver of cancer or as a prognostic/diagnostic marker are open questions with the potential for large clinical impact. Together, this dissertation highlights dNTP elevation as a mechanistic crossroad underlying lentiviral and cancer pathogenesis.

References

1. Mohsen MG, Ji D, Kool ET. Polymerase synthesis of four-base DNA from two stable dimeric nucleotides. Nucleic Acids Res. 2019;47(18):9495-501. doi: 10.1093/nar/gkz741. PubMed PMID: 31504784; PMCID: PMC6765132.
2. Berdis AJ. Mechanisms of DNA polymerases. Chem Rev. 2009;109(7):2862-79. doi: 10.1021/cr800530b. PubMed PMID: 19489544.
3. Kohnken R, Kodigepalli KM, Wu L. Regulation of deoxynucleotide metabolism in cancer: novel mechanisms and therapeutic implications. Mol Cancer. 2015;14:176. Epub 2015/09/30. doi: 10.1186/s12943-015-0446-6. PubMed PMID: 26416562; PMCID: PMC4587406.
4. Rampazzo C, Miazzi C, Franzolin E, Pontarin G, Ferraro P, Frangini M, Reichard P, Bianchi V. Regulation by degradation, a cellular defense against deoxyribonucleotide pool imbalances. Mutat Res. 2010;703(1):2-10. Epub 2010/06/22. doi: 10.1016/j.mrgentox.2010.06.002. PubMed PMID: 20561600.
5. Diamond TL, Roshal M, Jamburuthugoda VK, Reynolds HM, Merriam AR, Lee KY, Balakrishnan M, Bambara RA, Planelles V, Dewhurst S, Kim B. Macrophage tropism of HIV-1 depends on efficient cellular dNTP utilization by reverse transcriptase. J Biol Chem. 2004;279(49):51545-53. Epub 2004/09/29. doi: 10.1074/jbc.M408573200. PubMed PMID: 15452123; PMCID: PMC1351161.
6. Arnér ES, Eriksson S. Mammalian deoxyribonucleoside kinases. Pharmacol Ther. 1995;67(2):155-86. Epub 1995/01/01. doi: 10.1016/0163-7258(95)00015-9. PubMed PMID: 7494863.
7. Young JD, Yao SY, Baldwin JM, Cass CE, Baldwin SA. The human concentrative and equilibrative nucleoside transporter families, SLC28 and SLC29. Mol Aspects Med. 2013;34(2-3):529-47. Epub 2013/03/20. doi: 10.1016/j.mam.2012.05.007. PubMed PMID: 23506887.
8. Nordlund P, Reichard P. Ribonucleotide reductases. Annu Rev Biochem. 2006;75:681-706. Epub 2006/06/08. doi: 10.1146/annurev.biochem.75.103004.142443. PubMed PMID: 16756507.
9. Greene BL, Kang G, Cui C, Bennati M, Nocera DG, Drennan CL, Stubbe J. Ribonucleotide Reductases: Structure, Chemistry, and Metabolism Suggest New Therapeutic Targets. Annu Rev Biochem. 2020;89:45-75. doi: 10.1146/annurev-biochem-013118-111843. PubMed PMID: 32569524; PMCID: PMC7316142.
10. Elledge SJ, Zhou Z, Allen JB. Ribonucleotide reductase: regulation, regulation, regulation. Trends Biochem Sci. 1992;17(3):119-23. doi: 10.1016/0968-0004(92)90249-9. PubMed PMID: 1412696.
11. Brignole EJ, Tsai KL, Chittuluru J, Li H, Aye Y, Penczek PA, Stubbe J, Drennan CL, Asturias F. 3.3-Å resolution cryo-EM structure of human ribonucleotide reductase with substrate and allosteric regulators bound. Elife. 2018;7. Epub 20180220. doi: 10.7554/eLife.31502. PubMed PMID: 29460780; PMCID: PMC5819950.

12. Kashlan OB, Scott CP, Lear JD, Cooperman BS. A comprehensive model for the allosteric regulation of mammalian ribonucleotide reductase. Functional consequences of ATP- and dATP-induced oligomerization of the large subunit. Biochemistry. 2002;41(2):462-74. Epub 2002/01/10. doi: 10.1021/bi011653a. PubMed PMID: 11781084.

13. Engström Y, Eriksson S, Jildevik I, Skog S, Thelander L, Tribukait B. Cell cycle-dependent expression of mammalian ribonucleotide reductase. Differential regulation of the two subunits. J Biol Chem. 1985;260(16):9114-6. Epub 1985/08/05. PubMed PMID: 3894352.

14. Eriksson S, Gräslund A, Skog S, Thelander L, Tribukait B. Cell cycle-dependent regulation of mammalian ribonucleotide reductase. The S phase-correlated increase in subunit M2 is regulated by de novo protein synthesis. J Biol Chem. 1984;259(19):11695-700. Epub 1984/10/10. PubMed PMID: 6090444.

15. Björklund S, Skog S, Tribukait B, Thelander L. S-phase-specific expression of mammalian ribonucleotide reductase R1 and R2 subunit mRNAs. Biochemistry. 1990;29(23):5452-8. Epub 1990/06/12. doi: 10.1021/bi00475a007. PubMed PMID: 1696835.

16. Yao R, Zhang Z, An X, Bucci B, Perlstein DL, Stubbe J, Huang M. Subcellular localization of yeast ribonucleotide reductase regulated by the DNA replication and damage checkpoint pathways. Proc Natl Acad Sci U S A. 2003;100(11):6628-33. Epub 2003/05/07. doi: 10.1073/pnas.1131932100. PubMed PMID: 12732713; PMCID: PMC164498.

17. Huang M, Zhou Z, Elledge SJ. The DNA replication and damage checkpoint pathways induce transcription by inhibition of the Crt1 repressor. Cell. 1998;94(5):595-605. Epub 1998/09/19. doi: 10.1016/s0092-8674(00)81601-3. PubMed PMID: 9741624.

18. Coppock DL, Pardee AB. Control of thymidine kinase mRNA during the cell cycle. Mol Cell Biol. 1987;7(8):2925-32. Epub 1987/08/01. doi: 10.1128/mcb.7.8.2925. PubMed PMID: 3670299; PMCID: PMC367911.

19. Franzolin E, Pontarin G, Rampazzo C, Miazzi C, Ferraro P, Palumbo E, Reichard P, Bianchi V. The deoxynucleotide triphosphohydrolase SAMHD1 is a major regulator of DNA precursor pools in mammalian cells. Proc Natl Acad Sci U S A. 2013;110(35):14272-7. Epub 2013/07/17. doi: 10.1073/pnas.1312033110. PubMed PMID: 23858451; PMCID: PMC3761606.

20. Goldstone DC, Ennis-Adeniran V, Hedden JJ, Groom HC, Rice GI, Christodoulou E, Walker PA, Kelly G, Haire LF, Yap MW, de Carvalho LP, Stoye JP, Crow YJ, Taylor IA, Webb M. HIV-1 restriction factor SAMHD1 is a deoxynucleoside triphosphate triphosphohydrolase. Nature. 2011;480(7377):379-82. Epub 2011/11/08. doi: 10.1038/nature10623. PubMed PMID: 22056990.

21. Laguette N, Sobhian B, Casartelli N, Ringeard M, Chable-Bessia C, Segeral E, Yatim A, Emiliani S, Schwartz O, Benkirane M. SAMHD1 is the dendritic- and myeloid-cell-specific HIV-1 restriction factor counteracted by Vpx. Nature. 2011;474(7353):654-7. Epub 2011/05/27. doi: 10.1038/nature10117. PubMed PMID: 21613998; PMCID: PMC3595993.

22. Lahouassa H, Daddacha W, Hofmann H, Ayinde D, Logue EC, Dragin L, Bloch N, Maudet C, Bertrand M, Gramberg T, Pancino G, Priet S, Canard B, Laguette N, Benkirane M, Transy C, Landau NR, Kim B, Margottin-Goguet F. SAMHD1 restricts the replication of

human immunodeficiency virus type 1 by depleting the intracellular pool of deoxynucleoside triphosphates. Nat Immunol. 2012;13(3):223-8. Epub 2012/02/14. doi: 10.1038/ni.2236. PubMed PMID: 22327569; PMCID: PMC3771401.

23. Kim B, Nguyen LA, Daddacha W, Hollenbaugh JA. Tight interplay among SAMHD1 protein level, cellular dNTP levels, and HIV-1 proviral DNA synthesis kinetics in human primary monocyte-derived macrophages. J Biol Chem. 2012;287(26):21570-4. Epub 2012/05/17. doi: 10.1074/jbc.C112.374843. PubMed PMID: 22589553; PMCID: PMC3381122.

24. Brandariz-Nuñez A, Valle-Casuso JC, White TE, Laguette N, Benkirane M, Brojatsch J, Diaz-Griffero F. Role of SAMHD1 nuclear localization in restriction of HIV-1 and SIVmac. Retrovirology. 2012;9:49. Epub 2012/06/14. doi: 10.1186/1742-4690-9-49. PubMed PMID: 22691373; PMCID: PMC3410799.

25. Schaller T, Pollpeter D, Apolonia L, Goujon C, Malim MH. Nuclear import of SAMHD1 is mediated by a classical karyopherin α/β1 dependent pathway and confers sensitivity to VpxMAC induced ubiquitination and proteasomal degradation. Retrovirology. 2014;11:29. Epub 2014/04/10. doi: 10.1186/1742-4690-11-29. PubMed PMID: 24712655; PMCID: PMC4098787.

26. Hofmann H, Logue EC, Bloch N, Daddacha W, Polsky SB, Schultz ML, Kim B, Landau NR. The Vpx lentiviral accessory protein targets SAMHD1 for degradation in the nucleus. J Virol. 2012;86(23):12552-60. Epub 2012/09/14. doi: 10.1128/jvi.01657-12. PubMed PMID: 22973040; PMCID: PMC3497686.

27. White TE, Brandariz-Nunez A, Valle-Casuso JC, Amie S, Nguyen L, Kim B, Brojatsch J, Diaz-Griffero F. Contribution of SAM and HD domains to retroviral restriction mediated by human SAMHD1. Virology. 2013;436(1):81-90. Epub 2012/11/20. doi: 10.1016/j.virol.2012.10.029. PubMed PMID: 23158101; PMCID: PMC3767443.

28. Aravind L, Koonin EV. The HD domain defines a new superfamily of metal-dependent phosphohydrolases. Trends Biochem Sci. 1998;23(12):469-72. Epub 1998/12/30. doi: 10.1016/s0968-0004(98)01293-6. PubMed PMID: 9868367.

29. Cribier A, Descours B, Valadao AL, Laguette N, Benkirane M. Phosphorylation of SAMHD1 by cyclin A2/CDK1 regulates its restriction activity toward HIV-1. Cell Rep. 2013;3(4):1036-43. Epub 2013/04/23. doi: 10.1016/j.celrep.2013.03.017. PubMed PMID: 23602554.

30. St Gelais C, Kim SH, Ding L, Yount JS, Ivanov D, Spearman P, Wu L. A Putative Cyclin-binding Motif in Human SAMHD1 Contributes to Protein Phosphorylation, Localization, and Stability. J Biol Chem. 2016;291(51):26332-42. Epub 2016/11/07. doi: 10.1074/jbc.M116.753947. PubMed PMID: 27815502; PMCID: PMC5159495.

31. Yan J, Hao C, DeLucia M, Swanson S, Florens L, Washburn MP, Ahn J, Skowronski J. CyclinA2-Cyclin-dependent Kinase Regulates SAMHD1 Protein Phosphohydrolase Domain. J Biol Chem. 2015;290(21):13279-92. Epub 2015/04/08. doi: 10.1074/jbc.M115.646588. PubMed PMID: 25847232; PMCID: PMC4505580.

32. Schott K, Fuchs NV, Derua R, Mahboubi B, Schnellbächer E, Seifried J, Tondera C, Schmitz H, Shepard C, Brandariz-Nuñez A, Diaz-Griffero F, Reuter A, Kim B, Janssens

V, König R. Dephosphorylation of the HIV-1 restriction factor SAMHD1 is mediated by PP2A-B55α holoenzymes during mitotic exit. Nat Commun. 2018;9(1):2227. Epub 2018/06/10. doi: 10.1038/s41467-018-04671-1. PubMed PMID: 29884836; PMCID: PMC5993806.

33. Varmus H. Retroviruses. Science. 1988;240(4858):1427-35. doi: 10.1126/science.3287617. PubMed PMID: 3287617.

34. Baltimore D. RNA-dependent DNA polymerase in virions of RNA tumour viruses. Nature. 1970;226(5252):1209-11. doi: 10.1038/2261209a0. PubMed PMID: 4316300.

35. Temin HM, Mizutani S. RNA-dependent DNA polymerase in virions of Rous sarcoma virus. Nature. 1970;226(5252):1211-3. doi: 10.1038/2261211a0. PubMed PMID: 4316301.

36. Barré-Sinoussi F, Chermann JC, Rey F, Nugeyre MT, Chamaret S, Gruest J, Dauguet C, Axler-Blin C, Vézinet-Brun F, Rouzioux C, Rozenbaum W, Montagnier L. Isolation of a T-lymphotropic retrovirus from a patient at risk for acquired immune deficiency syndrome (AIDS). Science. 1983;220(4599):868-71. doi: 10.1126/science.6189183. PubMed PMID: 6189183.

37. Gallo RC, Salahuddin SZ, Popovic M, Shearer GM, Kaplan M, Haynes BF, Palker TJ, Redfield R, Oleske J, Safai B, et al. Frequent detection and isolation of cytopathic retroviruses (HTLV-III) from patients with AIDS and at risk for AIDS. Science. 1984;224(4648):500-3. doi: 10.1126/science.6200936. PubMed PMID: 6200936.

38. Campbell-Yesufu OT, Gandhi RT. Update on human immunodeficiency virus (HIV)-2 infection. Clin Infect Dis. 2011;52(6):780-7. doi: 10.1093/cid/ciq248. PubMed PMID: 21367732; PMCID: PMC3106263.

39. Klatt NR, Silvestri G, Hirsch V. Nonpathogenic simian immunodeficiency virus infections. Cold Spring Harb Perspect Med. 2012;2(1):a007153. doi: 10.1101/cshperspect.a007153. PubMed PMID: 22315718; PMCID: PMC3253032.

40. Vodicka MA. Determinants for lentiviral infection of non-dividing cells. Somat Cell Mol Genet. 2001;26(1-6):35-49. doi: 10.1023/a:1021022629126. PubMed PMID: 12465461.

41. Kennedy EM, Gavegnano C, Nguyen L, Slater R, Lucas A, Fromentin E, Schinazi RF, Kim B. Ribonucleoside triphosphates as substrate of human immunodeficiency virus type 1 reverse transcriptase in human macrophages. J Biol Chem. 2010;285(50):39380-91. Epub 2010/10/07. doi: 10.1074/jbc.M110.178582. PubMed PMID: 20924117; PMCID: PMC2998149.

42. Lenzi GM, Domaoal RA, Kim DH, Schinazi RF, Kim B. Kinetic variations between reverse transcriptases of viral protein X coding and noncoding lentiviruses. Retrovirology. 2014;11:111. Epub 2014/12/20. doi: 10.1186/s12977-014-0111-y. PubMed PMID: 25524560; PMCID: PMC4282736.

43. Collin M, Gordon S. The kinetics of human immunodeficiency virus reverse transcription are slower in primary human macrophages than in a lymphoid cell line. Virology. 1994;200(1):114-20. Epub 1994/04/01. doi: 10.1006/viro.1994.1169. PubMed PMID: 7510432.

44. Bejarano DA, Puertas MC, Börner K, Martinez-Picado J, Müller B, Kräusslich HG. Detailed Characterization of Early HIV-1 Replication Dynamics in Primary Human Macrophages. Viruses. 2018;10(11). Epub 2018/11/15. doi: 10.3390/v10110620. PubMed PMID: 30423802; PMCID: PMC6266216.

45. Kruize Z, Kootstra NA. The Role of Macrophages in HIV-1 Persistence and Pathogenesis. Front Microbiol. 2019;10:2828. Epub 2019/12/24. doi: 10.3389/fmicb.2019.02828. PubMed PMID: 31866988; PMCID: PMC6906147.

46. Veenhuis RT, Abreu CM, Shirk EN, Gama L, Clements JE. HIV replication and latency in monocytes and macrophages. Semin Immunol. 2021;51:101472. Epub 2021/03/03. doi: 10.1016/j.smim.2021.101472. PubMed PMID: 33648815.

47. Wong ME, Jaworowski A, Hearps AC. The HIV Reservoir in Monocytes and Macrophages. Front Immunol. 2019;10:1435. Epub 2019/07/13. doi: 10.3389/fimmu.2019.01435. PubMed PMID: 31297114; PMCID: PMC6607932.

48. Igarashi T, Brown CR, Endo Y, Buckler-White A, Plishka R, Bischofberger N, Hirsch V, Martin MA. Macrophage are the principal reservoir and sustain high virus loads in rhesus macaques after the depletion of CD4+ T cells by a highly pathogenic simian immunodeficiency virus/HIV type 1 chimera (SHIV): Implications for HIV-1 infections of humans. Proc Natl Acad Sci U S A. 2001;98(2):658-63. Epub 2001/01/03. doi: 10.1073/pnas.98.2.658. PubMed PMID: 11136236; PMCID: PMC14644.

49. Zhu C, Gao W, Zhao K, Qin X, Zhang Y, Peng X, Zhang L, Dong Y, Zhang W, Li P, Wei W, Gong Y, Yu XF. Structural insight into dGTP-dependent activation of tetrameric SAMHD1 deoxynucleoside triphosphate triphosphohydrolase. Nat Commun. 2013;4:2722. Epub 2013/11/13. doi: 10.1038/ncomms3722. PubMed PMID: 24217394.

50. Yan J, Kaur S, DeLucia M, Hao C, Mehrens J, Wang C, Golczak M, Palczewski K, Gronenborn AM, Ahn J, Skowronski J. Tetramerization of SAMHD1 is required for biological activity and inhibition of HIV infection. J Biol Chem. 2013;288(15):10406-17. Epub 2013/02/22. doi: 10.1074/jbc.M112.443796. PubMed PMID: 23426366; PMCID: PMC3624423.

51. Ji X, Tang C, Zhao Q, Wang W, Xiong Y. Structural basis of cellular dNTP regulation by SAMHD1. Proc Natl Acad Sci U S A. 2014;111(41):E4305-14. Epub 2014/10/01. doi: 10.1073/pnas.1412289111. PubMed PMID: 25267621; PMCID: PMC4205617.

52. Ji X, Wu Y, Yan J, Mehrens J, Yang H, DeLucia M, Hao C, Gronenborn AM, Skowronski J, Ahn J, Xiong Y. Mechanism of allosteric activation of SAMHD1 by dGTP. Nat Struct Mol Biol. 2013;20(11):1304-9. Epub 2013/10/22. doi: 10.1038/nsmb.2692. PubMed PMID: 24141705; PMCID: PMC3833828.

53. Powell RD, Holland PJ, Hollis T, Perrino FW. Aicardi-Goutieres syndrome gene and HIV-1 restriction factor SAMHD1 is a dGTP-regulated deoxynucleotide triphosphohydrolase. J Biol Chem. 2011;286(51):43596-600. Epub 2011/11/10. doi: 10.1074/jbc.C111.317628. PubMed PMID: 22069334; PMCID: PMC3243528.

54. Amie SM, Bambara RA, Kim B. GTP is the primary activator of the anti-HIV restriction factor SAMHD1. J Biol Chem. 2013;288(35):25001-6. Epub 2013/07/25. doi: 10.1074/jbc.C113.493619. PubMed PMID: 23880768; PMCID: PMC3757166.

55. Koharudin LM, Wu Y, DeLucia M, Mehrens J, Gronenborn AM, Ahn J. Structural basis of allosteric activation of sterile α motif and histidine-aspartate domain-containing protein 1 (SAMHD1) by nucleoside triphosphates. J Biol Chem. 2014;289(47):32617-27. Epub 2014/10/08. doi: 10.1074/jbc.M114.591958. PubMed PMID: 25288794; PMCID: PMC4239615.

56. Patra KK, Bhattacharya A, Bhattacharya S. Uncovering allostery and regulation in SAMHD1 through molecular dynamics simulations. Proteins. 2017;85(7):1266-75. Epub 2017/03/23. doi: 10.1002/prot.25287. PubMed PMID: 28321930.

57. Hansen EC, Seamon KJ, Cravens SL, Stivers JT. GTP activator and dNTP substrates of HIV-1 restriction factor SAMHD1 generate a long-lived activated state. Proc Natl Acad Sci U S A. 2014;111(18):E1843-51. Epub 2014/04/23. doi: 10.1073/pnas.1401706111. PubMed PMID: 24753578; PMCID: PMC4020072.

58. Wang Z, Bhattacharya A, Villacorta J, Diaz-Griffero F, Ivanov DN. Allosteric Activation of SAMHD1 Protein by Deoxynucleotide Triphosphate (dNTP)-dependent Tetramerization Requires dNTP Concentrations That Are Similar to dNTP Concentrations Observed in Cycling T Cells. J Biol Chem. 2016;291(41):21407-13. Epub 2016/08/28. doi: 10.1074/jbc.C116.751446. PubMed PMID: 27566548; PMCID: PMC5076810.

59. Arnold LH, Groom HC, Kunzelmann S, Schwefel D, Caswell SJ, Ordonez P, Mann MC, Rueschenbaum S, Goldstone DC, Pennell S, Howell SA, Stoye JP, Webb M, Taylor IA, Bishop KN. Phospho-dependent Regulation of SAMHD1 Oligomerisation Couples Catalysis and Restriction. PLoS Pathog. 2015;11(10):e1005194. Epub 2015/10/03. doi: 10.1371/journal.ppat.1005194. PubMed PMID: 26431200; PMCID: PMC4592219.

60. Hollenbaugh JA, Shelton J, Tao S, Amiralaei S, Liu P, Lu X, Goetze RW, Zhou L, Nettles JH, Schinazi RF, Kim B. Substrates and Inhibitors of SAMHD1. PLoS One. 2017;12(1):e0169052. Epub 2017/01/04. doi: 10.1371/journal.pone.0169052. PubMed PMID: 28046007; PMCID: PMC5207538.

61. Herold N, Rudd SG, Ljungblad L, Sanjiv K, Myrberg IH, Paulin CB, Heshmati Y, Hagenkort A, Kutzner J, Page BD, Calderón-Montaño JM, Loseva O, Jemth AS, Bulli L, Axelsson H, Tesi B, Valerie NC, Höglund A, Bladh J, Wiita E, Sundin M, Uhlin M, Rassidakis G, Heyman M, Tamm KP, Warpman-Berglund U, Walfridsson J, Lehmann S, Grandér D, Lundbäck T, Kogner P, Henter JI, Helleday T, Schaller T. Targeting SAMHD1 with the Vpx protein to improve cytarabine therapy for hematological malignancies. Nat Med. 2017;23(2):256-63. Epub 2017/01/10. doi: 10.1038/nm.4265. PubMed PMID: 28067901.

62. Schneider C, Oellerich T, Baldauf HM, Schwarz SM, Thomas D, Flick R, Bohnenberger H, Kaderali L, Stegmann L, Cremer A, Martin M, Lohmeyer J, Michaelis M, Hornung V, Schliemann C, Berdel WE, Hartmann W, Wardelmann E, Comoglio F, Hansmann ML, Yakunin AF, Geisslinger G, Strobel P, Ferreiros N, Serve H, Keppler OT, Cinatl J, Jr. SAMHD1 is a biomarker for cytarabine response and a therapeutic target in acute myeloid leukemia. Nat Med. 2017;23(2):250-5. Epub 2016/12/20. doi: 10.1038/nm.4255. PubMed PMID: 27991919.

63. Amie SM, Daly MB, Noble E, Schinazi RF, Bambara RA, Kim B. Anti-HIV host factor SAMHD1 regulates viral sensitivity to nucleoside reverse transcriptase inhibitors via

modulation of cellular deoxyribonucleoside triphosphate (dNTP) levels. J Biol Chem. 2013;288(28):20683-91. Epub 2013/06/08. doi: 10.1074/jbc.M113.472159. PubMed PMID: 23744077; PMCID: PMC3711331.

64. Huber AD, Michailidis E, Schultz ML, Ong YT, Bloch N, Puray-Chavez MN, Leslie MD, Ji J, Lucas AD, Kirby KA, Landau NR, Sarafianos SG. SAMHD1 has differential impact on the efficacies of HIV nucleoside reverse transcriptase inhibitors. Antimicrob Agents Chemother. 2014;58(8):4915-9. Epub 2014/05/29. doi: 10.1128/aac.02745-14. PubMed PMID: 24867973; PMCID: PMC4136039.

65. Morris ER, Caswell SJ, Kunzelmann S, Arnold LH, Purkiss AG, Kelly G, Taylor IA. Crystal structures of SAMHD1 inhibitor complexes reveal the mechanism of water-mediated dNTP hydrolysis. Nat Commun. 2020;11(1):3165. Epub 2020/06/25. doi: 10.1038/s41467-020-16983-2. PubMed PMID: 32576829; PMCID: PMC7311409.

66. Liu S, Mansour MN, Dillman KS, Perez JR, Danley DE, Aeed PA, Simons SP, Lemotte PK, Menniti FS. Structural basis for the catalytic mechanism of human phosphodiesterase 9. Proc Natl Acad Sci U S A. 2008;105(36):13309-14. Epub 2008/09/02. doi: 10.1073/pnas.0708850105. PubMed PMID: 18757755; PMCID: PMC2533186.

67. Rinaldo S, Paiardini A, Stelitano V, Brunotti P, Cervoni L, Fernicola S, Protano C, Vitali M, Cutruzzolà F, Giardina G. Structural basis of functional diversification of the HD-GYP domain revealed by the Pseudomonas aeruginosa PA4781 protein, which displays an unselective bimetallic binding site. J Bacteriol. 2015;197(8):1525-35. Epub 2015/02/19. doi: 10.1128/jb.02606-14. PubMed PMID: 25691523; PMCID: PMC4372746.

68. Huynh TN, Luo S, Pensinger D, Sauer JD, Tong L, Woodward JJ. An HD-domain phosphodiesterase mediates cooperative hydrolysis of c-di-AMP to affect bacterial growth and virulence. Proc Natl Acad Sci U S A. 2015;112(7):E747-56. Epub 2015/01/15. doi: 10.1073/pnas.1416485112. PubMed PMID: 25583510; PMCID: PMC4343097.

69. White TE, Brandariz-Nuñez A, Valle-Casuso JC, Amie S, Nguyen LA, Kim B, Tuzova M, Diaz-Griffero F. The retroviral restriction ability of SAMHD1, but not its deoxynucleotide triphosphohydrolase activity, is regulated by phosphorylation. Cell Host Microbe. 2013;13(4):441-51. Epub 2013/04/23. doi: 10.1016/j.chom.2013.03.005. PubMed PMID: 23601106; PMCID: PMC3864637.

70. Pauls E, Ruiz A, Badia R, Permanyer M, Gubern A, Riveira-Muñoz E, Torres-Torronteras J, Alvarez M, Mothe B, Brander C, Crespo M, Menéndez-Arias L, Clotet B, Keppler OT, Martí R, Posas F, Ballana E, Esté JA. Cell cycle control and HIV-1 susceptibility are linked by CDK6-dependent CDK2 phosphorylation of SAMHD1 in myeloid and lymphoid cells. J Immunol. 2014;193(4):1988-97. Epub 2014/07/13. doi: 10.4049/jimmunol.1400873. PubMed PMID: 25015816.

71. Coiras M, Bermejo M, Descours B, Mateos E, García-Pérez J, López-Huertas MR, Lederman MM, Benkirane M, Alcamí J. IL-7 Induces SAMHD1 Phosphorylation in CD4+ T Lymphocytes, Improving Early Steps of HIV-1 Life Cycle. Cell Rep. 2016;14(9):2100-7. Epub 2016/03/01. doi: 10.1016/j.celrep.2016.02.022. PubMed PMID: 26923586; PMCID: PMC5063304.

72. Mlcochova P, Sutherland KA, Watters SA, Bertoli C, de Bruin RA, Rehwinkel J, Neil SJ, Lenzi GM, Kim B, Khwaja A, Gage MC, Georgiou C, Chittka A, Yona S, Noursadeghi M,

Towers GJ, Gupta RK. A G1-like state allows HIV-1 to bypass SAMHD1 restriction in macrophages. Embo j. 2017;36(5):604-16. Epub 2017/01/27. doi: 10.15252/embj.201696025. PubMed PMID: 28122869; PMCID: PMC5331754.

73. Patra KK, Bhattacharya A, Bhattacharya S. Allosteric Signal Transduction in HIV-1 Restriction Factor SAMHD1 Proceeds via Reciprocal Handshake across Monomers. J Chem Inf Model. 2017;57(10):2523-38. Epub 2017/09/29. doi: 10.1021/acs.jcim.7b00279. PubMed PMID: 28956603.

74. Tang C, Ji X, Wu L, Xiong Y. Impaired dNTPase activity of SAMHD1 by phosphomimetic mutation of Thr-592. J Biol Chem. 2015;290(44):26352-9. Epub 2015/08/22. doi: 10.1074/jbc.M115.677435. PubMed PMID: 26294762; PMCID: PMC4646291.

75. Ruiz A, Pauls E, Badia R, Torres-Torronteras J, Riveira-Muñoz E, Clotet B, Martí R, Ballana E, Esté JA. Cyclin D3-dependent control of the dNTP pool and HIV-1 replication in human macrophages. Cell Cycle. 2015;14(11):1657-65. Epub 2015/05/01. doi: 10.1080/15384101.2015.1030558. PubMed PMID: 25927932; PMCID: PMC4614030.

76. Pauls E, Badia R, Torres-Torronteras J, Ruiz A, Permanyer M, Riveira-Muñoz E, Clotet B, Marti R, Ballana E, Esté JA. Palbociclib, a selective inhibitor of cyclin-dependent kinase4/6, blocks HIV-1 reverse transcription through the control of sterile α motif and HD domain-containing protein-1 (SAMHD1) activity. Aids. 2014;28(15):2213-22. Epub 2014/07/19. doi: 10.1097/qad.0000000000000399. PubMed PMID: 25036183.

77. Bhattacharya A, Wang Z, White T, Buffone C, Nguyen LA, Shepard CN, Kim B, Demeler B, Diaz-Griffero F, Ivanov DN. Effects of T592 phosphomimetic mutations on tetramer stability and dNTPase activity of SAMHD1 can not explain the retroviral restriction defect. Sci Rep. 2016;6:31353. Epub 2016/08/12. doi: 10.1038/srep31353. PubMed PMID: 27511536; PMCID: PMC4980677.

78. Welbourn S, Dutta SM, Semmes OJ, Strebel K. Restriction of virus infection but not catalytic dNTPase activity is regulated by phosphorylation of SAMHD1. J Virol. 2013;87(21):11516-24. Epub 2013/08/24. doi: 10.1128/jvi.01642-13. PubMed PMID: 23966382; PMCID: PMC3807338.

79. Welbourn S, Strebel K. Low dNTP levels are necessary but may not be sufficient for lentiviral restriction by SAMHD1. Virology. 2016;488:271-7. Epub 2015/12/15. doi: 10.1016/j.virol.2015.11.022. PubMed PMID: 26655245; PMCID: PMC4744553.

80. Tramentozzi E, Ferraro P, Hossain M, Stillman B, Bianchi V, Pontarin G. The dNTP triphosphohydrolase activity of SAMHD1 persists during S-phase when the enzyme is phosphorylated at T592. Cell Cycle. 2018;17(9):1102-14. Epub 2018/07/25. doi: 10.1080/15384101.2018.1480216. PubMed PMID: 30039733; PMCID: PMC6110608.

81. White TE, Brandariz-Nunez A, Martinez-Lopez A, Knowlton C, Lenzi G, Kim B, Ivanov D, Diaz-Griffero F. A SAMHD1 mutation associated with Aicardi-Goutieres syndrome uncouples the ability of SAMHD1 to restrict HIV-1 from its ability to downmodulate type I interferon in humans. Hum Mutat. 2017;38(6):658-68. Epub 2017/02/24. doi: 10.1002/humu.23201. PubMed PMID: 28229507; PMCID: PMC5738905.

82. Sharifi HJ, Paine DN, Fazzari VA, Tipple AF, Patterson E, de Noronha CMC. Sulforaphane Reduces SAMHD1 Phosphorylation To Protect Macrophages from HIV-1

Infection. J Virol. 2022;96(23):e0118722. Epub 20221115. doi: 10.1128/jvi.01187-22. PubMed PMID: 36377871; PMCID: PMC9749475.

83. Orris B, Huynh KW, Ammirati M, Han S, Bolaños B, Carmody J, Petroski MD, Bosbach B, Shields DJ, Stivers JT. Phosphorylation of SAMHD1 Thr592 increases C-terminal domain dynamics, tetramer dissociation and ssDNA binding kinetics. Nucleic Acids Res. 2022;50(13):7545-59. doi: 10.1093/nar/gkac573. PubMed PMID: 35801923; PMCID: PMC9303311.

84. Lee EJ, Seo JH, Park JH, Vo TTL, An S, Bae SJ, Le H, Lee HS, Wee HJ, Lee D, Chung YH, Kim JA, Jang MK, Ryu SH, Yu E, Jang SH, Park ZY, Kim KW. SAMHD1 acetylation enhances its deoxynucleotide triphosphohydrolase activity and promotes cancer cell proliferation. Oncotarget. 2017;8(40):68517-29. Epub 2017/10/06. doi: 10.18632/oncotarget.19704. PubMed PMID: 28978134; PMCID: PMC5620274.

85. Bonifati S, Daly MB, St Gelais C, Kim SH, Hollenbaugh JA, Shepard C, Kennedy EM, Kim DH, Schinazi RF, Kim B, Wu L. SAMHD1 controls cell cycle status, apoptosis and HIV-1 infection in monocytic THP-1 cells. Virology. 2016;495:92-100. Epub 2016/05/18. doi: 10.1016/j.virol.2016.05.002. PubMed PMID: 27183329; PMCID: PMC4912869.

86. Martinat C, Cormier A, Tobaly-Tapiero J, Palmic N, Casartelli N, Mahboubi B, Coggins SA, Buchrieser J, Persaud M, Diaz-Griffero F, Espert L, Bossis G, Lesage P, Schwartz O, Kim B, Margottin-Goguet F, Saïb A, Zamborlini A. SUMOylation of SAMHD1 at Lysine 595 is required for HIV-1 restriction in non-cycling cells. Nat Commun. 2021;12(1):4582. Epub 2021/07/30. doi: 10.1038/s41467-021-24802-5. PubMed PMID: 34321470; PMCID: PMC8319325.

87. Kerscher O. SUMO junction-what's your function? New insights through SUMO-interacting motifs. EMBO Rep. 2007;8(6):550-5. Epub 2007/06/05. doi: 10.1038/sj.embor.7400980. PubMed PMID: 17545995; PMCID: PMC2002525.

88. Zhu CF, Wei W, Peng X, Dong YH, Gong Y, Yu XF. The mechanism of substrate-controlled allosteric regulation of SAMHD1 activated by GTP. Acta Crystallogr D Biol Crystallogr. 2015;71(Pt 3):516-24. Epub 2015/03/12. doi: 10.1107/s1399004714027527. PubMed PMID: 25760601.

89. Mauney CH, Rogers LC, Harris RS, Daniel LW, Devarie-Baez NO, Wu H, Furdui CM, Poole LB, Perrino FW, Hollis T. The SAMHD1 dNTP Triphosphohydrolase Is Controlled by a Redox Switch. Antioxid Redox Signal. 2017;27(16):1317-31. Epub 2017/04/12. doi: 10.1089/ars.2016.6888. PubMed PMID: 28398823; PMCID: PMC5655415.

90. Wang Z, Bhattacharya A, White T, Buffone C, McCabe A, Nguyen LA, Shepard CN, Pardo S, Kim B, Weintraub ST, Demeler B, Diaz-Griffero F, Ivanov DN. Functionality of Redox-Active Cysteines Is Required for Restriction of Retroviral Replication by SAMHD1. Cell Rep. 2018;24(4):815-23. Epub 2018/07/26. doi: 10.1016/j.celrep.2018.06.090. PubMed PMID: 30044979; PMCID: PMC6067006.

91. Patra KK, Bhattacharya A, Bhattacharya S. Molecular dynamics investigation of a redox switch in the anti-HIV protein SAMHD1. Proteins. 2019;87(9):748-59. Epub 2019/04/25. doi: 10.1002/prot.25701. PubMed PMID: 31017331.

92. Thapa G, Bhattacharya A, Bhattacharya S. Dimeric Hold States of Anti-HIV Protein SAMHD1 are Redox Tunable. J Chem Inf Model. 2020;60(12):6377-91. Epub 2020/11/03. doi: 10.1021/acs.jcim.0c00629. PubMed PMID: 33135886.

93. Batalis S, Rogers LC, Hemphill WO, Mauney CH, Ornelles DA, Hollis T. SAMHD1 Phosphorylation at T592 Regulates Cellular Localization and S-phase Progression. Front Mol Biosci. 2021;8:724870. Epub 2021/09/14. doi: 10.3389/fmolb.2021.724870. PubMed PMID: 34513928; PMCID: PMC8426622.

94. Operario DJ, Balakrishnan M, Bambara RA, Kim B. Reduced dNTP interaction of human immunodeficiency virus type 1 reverse transcriptase promotes strand transfer. J Biol Chem. 2006;281(43):32113-21. Epub 2006/08/24. doi: 10.1074/jbc.M604665200. PubMed PMID: 16926150.

95. Skasko M, Kim B. Compensatory role of human immunodeficiency virus central polypurine tract sequence in kinetically disrupted reverse transcription. J Virol. 2008;82(15):7716-20. Epub 2008/05/23. doi: 10.1128/jvi.00120-08. PubMed PMID: 18495776; PMCID: PMC2493349.

96. Van Cor-Hosmer SK, Daddacha W, Kim B. Mechanistic interplay among the M184I HIV-1 reverse transcriptase mutant, the central polypurine tract, cellular dNTP concentrations and drug sensitivity. Virology. 2010;406(2):253-60. Epub 2010/08/13. doi: 10.1016/j.virol.2010.07.028. PubMed PMID: 20701944; PMCID: PMC3097044.

97. Kennedy EM, Amie SM, Bambara RA, Kim B. Frequent incorporation of ribonucleotides during HIV-1 reverse transcription and their attenuated repair in macrophages. J Biol Chem. 2012;287(17):14280-8. Epub 2012/03/03. doi: 10.1074/jbc.M112.348482. PubMed PMID: 22383524; PMCID: PMC3340154.

98. Goetze RW, Kim DH, Schinazi RF, Kim B. A CRISPR/Cas9 approach reveals that the polymerase activity of DNA polymerase beta is dispensable for HIV-1 infection in dividing and nondividing cells. J Biol Chem. 2017;292(34):14016-25. Epub 2017/07/08. doi: 10.1074/jbc.M117.793661. PubMed PMID: 28684413; PMCID: PMC5572920.

99. Van Cor-Hosmer SK, Kim DH, Daly MB, Daddacha W, Kim B. Restricted 5'-end gap repair of HIV-1 integration due to limited cellular dNTP concentrations in human primary macrophages. J Biol Chem. 2013;288(46):33253-62. Epub 2013/10/08. doi: 10.1074/jbc.M113.486787. PubMed PMID: 24097986; PMCID: PMC3829171.

100. Mahboubi B, Gavegnano C, Kim DH, Schinazi RF, Kim B. Host SAMHD1 protein restricts endogenous reverse transcription of HIV-1 in nondividing macrophages. Retrovirology. 2018;15(1):69. Epub 2018/10/15. doi: 10.1186/s12977-018-0452-z. PubMed PMID: 30316304; PMCID: PMC6186296.

101. Antonucci JM, Kim SH, St Gelais C, Bonifati S, Li TW, Buzovetsky O, Knecht KM, Duchon AA, Xiong Y, Musier-Forsyth K, Wu L. SAMHD1 Impairs HIV-1 Gene Expression and Negatively Modulates Reactivation of Viral Latency in CD4(+) T Cells. J Virol. 2018;92(15). Epub 2018/05/26. doi: 10.1128/jvi.00292-18. PubMed PMID: 29793958; PMCID: PMC6052313.

102. Yu CH, Bhattacharya A, Persaud M, Taylor AB, Wang Z, Bulnes-Ramos A, Xu J, Selyutina A, Martinez-Lopez A, Cano K, Demeler B, Kim B, Hardies SC, Diaz-Griffero

F, Ivanov DN. Nucleic acid binding by SAMHD1 contributes to the antiretroviral activity and is enhanced by the GpsN modification. Nat Commun. 2021;12(1):731. Epub 2021/02/04. doi: 10.1038/s41467-021-21023-8. PubMed PMID: 33531504; PMCID: PMC7854603.

103. Hrecka K, Hao C, Gierszewska M, Swanson SK, Kesik-Brodacka M, Srivastava S, Florens L, Washburn MP, Skowronski J. Vpx relieves inhibition of HIV-1 infection of macrophages mediated by the SAMHD1 protein. Nature. 2011;474(7353):658-61. Epub 2011/07/02. doi: 10.1038/nature10195. PubMed PMID: 21720370; PMCID: PMC3179858.

104. Guyader M, Emerman M, Montagnier L, Peden K. VPX mutants of HIV-2 are infectious in established cell lines but display a severe defect in peripheral blood lymphocytes. Embo j. 1989;8(4):1169-75. Epub 1989/04/01. PubMed PMID: 2743977; PMCID: PMC400930.

105. Yu XF, Yu QC, Essex M, Lee TH. The vpx gene of simian immunodeficiency virus facilitates efficient viral replication in fresh lymphocytes and macrophage. J Virol. 1991;65(9):5088-91. Epub 1991/09/01. PubMed PMID: 1714525; PMCID: PMC248975.

106. Schwefel D, Groom HC, Boucherit VC, Christodoulou E, Walker PA, Stoye JP, Bishop KN, Taylor IA. Structural basis of lentiviral subversion of a cellular protein degradation pathway. Nature. 2014;505(7482):234-8. Epub 2013/12/18. doi: 10.1038/nature12815. PubMed PMID: 24336198; PMCID: PMC3886899.

107. Hrecka K, Gierszewska M, Srivastava S, Kozaczkiewicz L, Swanson SK, Florens L, Washburn MP, Skowronski J. Lentiviral Vpr usurps Cul4-DDB1[VprBP] E3 ubiquitin ligase to modulate cell cycle. Proc Natl Acad Sci U S A. 2007;104(28):11778-83. Epub 2007/07/05. doi: 10.1073/pnas.0702102104. PubMed PMID: 17609381; PMCID: PMC1906728.

108. Ahn J, Hao C, Yan J, DeLucia M, Mehrens J, Wang C, Gronenborn AM, Skowronski J. HIV/simian immunodeficiency virus (SIV) accessory virulence factor Vpx loads the host cell restriction factor SAMHD1 onto the E3 ubiquitin ligase complex CRL4DCAF1. J Biol Chem. 2012;287(15):12550-8. Epub 2012/03/01. doi: 10.1074/jbc.M112.340711. PubMed PMID: 22362772; PMCID: PMC3321004.

109. Srivastava S, Swanson SK, Manel N, Florens L, Washburn MP, Skowronski J. Lentiviral Vpx accessory factor targets VprBP/DCAF1 substrate adaptor for cullin 4 E3 ubiquitin ligase to enable macrophage infection. PLoS Pathog. 2008;4(5):e1000059. Epub 2008/05/10. doi: 10.1371/journal.ppat.1000059. PubMed PMID: 18464893; PMCID: PMC2330158.

110. Guo H, Zhang N, Shen S, Yu XF, Wei W. Determinants of lentiviral Vpx-CRL4 E3 ligase-mediated SAMHD1 degradation in the substrate adaptor protein DCAF1. Biochem Biophys Res Commun. 2019;513(4):933-9. Epub 2019/04/21. doi: 10.1016/j.bbrc.2019.04.085. PubMed PMID: 31003777.

111. Oo A, Kim DH, Schinazi RF, Kim B. Viral protein X reduces the incorporation of mutagenic noncanonical rNTPs during lentivirus reverse transcription in macrophages. J Biol Chem. 2020;295(2):657-66. Epub 2019/12/07. doi: 10.1074/jbc.RA119.011466. PubMed PMID: 31806704; PMCID: PMC6956541.

112. Sharp PM, Bailes E, Stevenson M, Emerman M, Hahn BH. Gene acquisition in HIV and SIV. Nature. 1996;383(6601):586-7. Epub 1996/10/17. doi: 10.1038/383586a0. PubMed PMID: 8857532.

113. Etienne L, Hahn BH, Sharp PM, Matsen FA, Emerman M. Gene loss and adaptation to hominids underlie the ancient origin of HIV-1. Cell Host Microbe. 2013;14(1):85-92. Epub 2013/07/23. doi: 10.1016/j.chom.2013.06.002. PubMed PMID: 23870316; PMCID: PMC3733229.

114. Tristem M, Marshall C, Karpas A, Hill F. Evolution of the primate lentiviruses: evidence from vpx and vpr. Embo j. 1992;11(9):3405-12. Epub 1992/09/01. doi: 10.1002/j.1460-2075.1992.tb05419.x. PubMed PMID: 1324171; PMCID: PMC556875.

115. Lim ES, Fregoso OI, McCoy CO, Matsen FA, Malik HS, Emerman M. The ability of primate lentiviruses to degrade the monocyte restriction factor SAMHD1 preceded the birth of the viral accessory protein Vpx. Cell Host Microbe. 2012;11(2):194-204. Epub 2012/01/31. doi: 10.1016/j.chom.2012.01.004. PubMed PMID: 22284954; PMCID: PMC3288607.

116. Belzile JP, Duisit G, Rougeau N, Mercier J, Finzi A, Cohen EA. HIV-1 Vpr-mediated G2 arrest involves the DDB1-CUL4AVPRBP E3 ubiquitin ligase. PLoS Pathog. 2007;3(7):e85. Epub 2007/07/17. doi: 10.1371/journal.ppat.0030085. PubMed PMID: 17630831; PMCID: PMC1914068.

117. Emerman M, Malik HS. Paleovirology--modern consequences of ancient viruses. PLoS Biol. 2010;8(2):e1000301. Epub 2010/02/18. doi: 10.1371/journal.pbio.1000301. PubMed PMID: 20161719; PMCID: PMC2817711.

118. Kirchhoff F. Immune evasion and counteraction of restriction factors by HIV-1 and other primate lentiviruses. Cell Host Microbe. 2010;8(1):55-67. Epub 2010/07/20. doi: 10.1016/j.chom.2010.06.004. PubMed PMID: 20638642.

119. Daugherty MD, Malik HS. Rules of engagement: molecular insights from host-virus arms races. Annu Rev Genet. 2012;46:677-700. Epub 2012/11/14. doi: 10.1146/annurev-genet-110711-155522. PubMed PMID: 23145935.

120. McNatt MW, Zang T, Hatziioannou T, Bartlett M, Fofana IB, Johnson WE, Neil SJ, Bieniasz PD. Species-specific activity of HIV-1 Vpu and positive selection of tetherin transmembrane domain variants. PLoS Pathog. 2009;5(2):e1000300. Epub 2009/02/14. doi: 10.1371/journal.ppat.1000300. PubMed PMID: 19214216; PMCID: PMC2633611.

121. Sawyer SL, Wu LI, Emerman M, Malik HS. Positive selection of primate TRIM5alpha identifies a critical species-specific retroviral restriction domain. Proc Natl Acad Sci U S A. 2005;102(8):2832-7. Epub 2005/02/04. doi: 10.1073/pnas.0409853102. PubMed PMID: 15689398; PMCID: PMC549489.

122. Laguette N, Rahm N, Sobhian B, Chable-Bessia C, Münch J, Snoeck J, Sauter D, Switzer WM, Heneine W, Kirchhoff F, Delsuc F, Telenti A, Benkirane M. Evolutionary and functional analyses of the interaction between the myeloid restriction factor SAMHD1 and the lentiviral Vpx protein. Cell Host Microbe. 2012;11(2):205-17. Epub 2012/02/07. doi: 10.1016/j.chom.2012.01.007. PubMed PMID: 22305291; PMCID: PMC3595996.

123. Fregoso OI, Ahn J, Wang C, Mehrens J, Skowronski J, Emerman M. Evolutionary toggling of Vpx/Vpr specificity results in divergent recognition of the restriction factor SAMHD1. PLoS Pathog. 2013;9(7):e1003496. Epub 2013/07/23. doi: 10.1371/journal.ppat.1003496. PubMed PMID: 23874202; PMCID: PMC3715410.

124. Lenzi GM, Domaoal RA, Kim DH, Schinazi RF, Kim B. Mechanistic and Kinetic Differences between Reverse Transcriptases of Vpx Coding and Non-coding Lentiviruses. J Biol Chem. 2015;290(50):30078-86. Epub 2015/10/21. doi: 10.1074/jbc.M115.691576. PubMed PMID: 26483545; PMCID: PMC4705996.

125. Coggins SA, Holler JM, Kimata JT, Kim DH, Schinazi RF, Kim B. Efficient pre-catalytic conformational change of reverse transcriptases from SAMHD1 non-counteracting primate lentiviruses during dNTP incorporation. Virology. 2019;537:36-44. Epub 2019/08/24. doi: 10.1016/j.virol.2019.08.010. PubMed PMID: 31442614; PMCID: PMC6901729.

126. Coggins SA, Kim DH, Schinazi RF, Desrosiers RC, Kim B. Enhanced enzyme kinetics of reverse transcriptase variants cloned from animals infected with SIVmac239 lacking Viral Protein X. J Biol Chem. 2020. Epub 2020/10/04. doi: 10.1074/jbc.RA120.015273. PubMed PMID: 33008888.

127. Mereby SA, Maehigashi T, Holler JM, Kim DH, Schinazi RF, Kim B. Interplay of ancestral non-primate lentiviruses with the virus-restricting SAMHD1 proteins of their hosts. J Biol Chem. 2018;293(42):16402-12. Epub 2018/09/06. doi: 10.1074/jbc.RA118.004567. PubMed PMID: 30181218; PMCID: PMC6200947.

128. Gramberg T, Kahle T, Bloch N, Wittmann S, Müllers E, Daddacha W, Hofmann H, Kim B, Lindemann D, Landau NR. Restriction of diverse retroviruses by SAMHD1. Retrovirology. 2013;10:26. Epub 2013/03/19. doi: 10.1186/1742-4690-10-26. PubMed PMID: 23497255; PMCID: PMC3605129.

129. Sze A, Belgnaoui SM, Olagnier D, Lin R, Hiscott J, van Grevenynghe J. Host restriction factor SAMHD1 limits human T cell leukemia virus type 1 infection of monocytes via STING-mediated apoptosis. Cell Host Microbe. 2013;14(4):422-34. Epub 2013/10/22. doi: 10.1016/j.chom.2013.09.009. PubMed PMID: 24139400.

130. Kaushik R, Zhu X, Stranska R, Wu Y, Stevenson M. A cellular restriction dictates the permissivity of nondividing monocytes/macrophages to lentivirus and gammaretrovirus infection. Cell Host Microbe. 2009;6(1):68-80. Epub 2009/07/21. doi: 10.1016/j.chom.2009.05.022. PubMed PMID: 19616766; PMCID: PMC2777639.

131. Goujon C, Rivière L, Jarrosson-Wuilleme L, Bernaud J, Rigal D, Darlix JL, Cimarelli A. SIVSM/HIV-2 Vpx proteins promote retroviral escape from a proteasome-dependent restriction pathway present in human dendritic cells. Retrovirology. 2007;4:2. Epub 2007/01/11. doi: 10.1186/1742-4690-4-2. PubMed PMID: 17212817; PMCID: PMC1779362.

132. Moebes A, Enssle J, Bieniasz PD, Heinkelein M, Lindemann D, Bock M, McClure MO, Rethwilm A. Human foamy virus reverse transcription that occurs late in the viral replication cycle. J Virol. 1997;71(10):7305-11. Epub 1997/10/06. doi: 10.1128/jvi.71.10.7305-7311.1997. PubMed PMID: 9311807; PMCID: PMC192074.

133. Delelis O, Saïb A, Sonigo P. Biphasic DNA synthesis in spumaviruses. J Virol. 2003;77(14):8141-6. Epub 2003/06/28. doi: 10.1128/jvi.77.14.8141-8146.2003. PubMed PMID: 12829852; PMCID: PMC161954.

134. Yu SF, Baldwin DN, Gwynn SR, Yendapalli S, Linial ML. Human foamy virus replication: a pathway distinct from that of retroviruses and hepadnaviruses. Science. 1996;271(5255):1579-82. Epub 1996/03/15. doi: 10.1126/science.271.5255.1579. PubMed PMID: 8599113.

135. Crow YJ, Chase DS, Lowenstein Schmidt J, Szynkiewicz M, Forte GM, Gornall HL, Oojageer A, Anderson B, Pizzino A, Helman G, Abdel-Hamid MS, Abdel-Salam GM, Ackroyd S, Aeby A, Agosta G, Albin C, Allon-Shalev S, Arellano M, Ariaudo G, Aswani V, Babul-Hirji R, Baildam EM, Bahi-Buisson N, Bailey KM, Barnerias C, Barth M, Battini R, Beresford MW, Bernard G, Bianchi M, Billette de Villemeur T, Blair EM, Bloom M, Burlina AB, Carpanelli ML, Carvalho DR, Castro-Gago M, Cavallini A, Cereda C, Chandler KE, Chitayat DA, Collins AE, Sierra Corcoles C, Cordeiro NJ, Crichiutti G, Dabydeen L, Dale RC, D'Arrigo S, De Goede CG, De Laet C, De Waele LM, Denzler I, Desguerre I, Devriendt K, Di Rocco M, Fahey MC, Fazzi E, Ferrie CD, Figueiredo A, Gener B, Goizet C, Gowrinathan NR, Gowrishankar K, Hanrahan D, Isidor B, Kara B, Khan N, King MD, Kirk EP, Kumar R, Lagae L, Landrieu P, Lauffer H, Laugel V, La Piana R, Lim MJ, Lin JP, Linnankivi T, Mackay MT, Marom DR, Marques Lourenco C, McKee SA, Moroni I, Morton JE, Moutard ML, Murray K, Nabbout R, Nampoothiri S, Nunez-Enamorado N, Oades PJ, Olivieri I, Ostergaard JR, Perez-Duenas B, Prendiville JS, Ramesh V, Rasmussen M, Regal L, Ricci F, Rio M, Rodriguez D, Roubertie A, Salvatici E, Segers KA, Sinha GP, Soler D, Spiegel R, Stodberg TI, Straussberg R, Swoboda KJ, Suri M, Tacke U, Tan TY, te Water Naude J, Wee Teik K, Thomas MM, Till M, Tonduti D, Valente EM, Van Coster RN, van der Knaap MS, Vassallo G, Vijzelaar R, Vogt J, Wallace GB, Wassmer E, Webb HJ, Whitehouse WP, Whitney RN, Zaki MS, Zuberi SM, Livingston JH, Rozenberg F, Lebon P, Vanderver A, Orcesi S, Rice GI. Characterization of human disease phenotypes associated with mutations in TREX1, RNASEH2A, RNASEH2B, RNASEH2C, SAMHD1, ADAR, and IFIH1. Am J Med Genet A. 2015;167a(2):296-312. Epub 2015/01/22. doi: 10.1002/ajmg.a.36887. PubMed PMID: 25604658; PMCID: PMC4382202.

136. Aicardi J, Goutieres F. A progressive familial encephalopathy in infancy with calcifications of the basal ganglia and chronic cerebrospinal fluid lymphocytosis. Ann Neurol. 1984;15(1):49-54. Epub 1984/01/01. doi: 10.1002/ana.410150109. PubMed PMID: 6712192.

137. Rice GI, Bond J, Asipu A, Brunette RL, Manfield IW, Carr IM, Fuller JC, Jackson RM, Lamb T, Briggs TA, Ali M, Gornall H, Couthard LR, Aeby A, Attard-Montalto SP, Bertini E, Bodemer C, Brockmann K, Brueton LA, Corry PC, Desguerre I, Fazzi E, Cazorla AG, Gener B, Hamel BC, Heiberg A, Hunter M, van der Knaap MS, Kumar R, Lagae L, Landrieu PG, Lourenco CM, Marom D, McDermott MF, van der Merwe W, Orcesi S, Prendiville JS, Rasmussen M, Shalev SA, Soler DM, Shinawi M, Spiegel R, Tan TY, Vanderver A, Wakeling EL, Wassmer E, Whittaker E, Lebon P, Stetson DB, Bonthron DT, Crow YJ. Mutations involved in Aicardi-Goutières syndrome implicate SAMHD1 as regulator of the innate immune response. Nat Genet. 2009;41(7):829-32. Epub 2009/06/16. doi: 10.1038/ng.373. PubMed PMID: 19525956; PMCID: PMC4154505.

138. Crow YJ, Hayward BE, Parmar R, Robins P, Leitch A, Ali M, Black DN, van Bokhoven H, Brunner HG, Hamel BC, Corry PC, Cowan FM, Frints SG, Klepper J, Livingston JH, Lynch SA, Massey RF, Meritet JF, Michaud JL, Ponsot G, Voit T, Lebon P, Bonthron DT, Jackson AP, Barnes DE, Lindahl T. Mutations in the gene encoding the 3'-5' DNA exonuclease TREX1 cause Aicardi-Goutières syndrome at the AGS1 locus. Nat Genet. 2006;38(8):917-20. Epub 2006/07/18. doi: 10.1038/ng1845. PubMed PMID: 16845398.

139. Fye JM, Orebaugh CD, Coffin SR, Hollis T, Perrino FW. Dominant mutation of the TREX1 exonuclease gene in lupus and Aicardi-Goutieres syndrome. J Biol Chem. 2011;286(37):32373-82. Epub 2011/08/03. doi: 10.1074/jbc.M111.276287. PubMed PMID: 21808053; PMCID: PMC3173215.

140. Orebaugh CD, Fye JM, Harvey S, Hollis T, Perrino FW. The TREX1 exonuclease R114H mutation in Aicardi-Goutières syndrome and lupus reveals dimeric structure requirements for DNA degradation activity. J Biol Chem. 2011;286(46):40246-54. Epub 2011/09/23. doi: 10.1074/jbc.M111.297903. PubMed PMID: 21937424; PMCID: PMC3220555.

141. Crow YJ, Leitch A, Hayward BE, Garner A, Parmar R, Griffith E, Ali M, Semple C, Aicardi J, Babul-Hirji R, Baumann C, Baxter P, Bertini E, Chandler KE, Chitayat D, Cau D, Déry C, Fazzi E, Goizet C, King MD, Klepper J, Lacombe D, Lanzi G, Lyall H, Martínez-Frías ML, Mathieu M, McKeown C, Monier A, Oade Y, Quarrell OW, Rittey CD, Rogers RC, Sanchis A, Stephenson JB, Tacke U, Till M, Tolmie JL, Tomlin P, Voit T, Weschke B, Woods CG, Lebon P, Bonthron DT, Ponting CP, Jackson AP. Mutations in genes encoding ribonuclease H2 subunits cause Aicardi-Goutières syndrome and mimic congenital viral brain infection. Nat Genet. 2006;38(8):910-6. Epub 2006/07/18. doi: 10.1038/ng1842. PubMed PMID: 16845400.

142. Rice GI, Kasher PR, Forte GM, Mannion NM, Greenwood SM, Szynkiewicz M, Dickerson JE, Bhaskar SS, Zampini M, Briggs TA, Jenkinson EM, Bacino CA, Battini R, Bertini E, Brogan PA, Brueton LA, Carpanelli M, De Laet C, de Lonlay P, del Toro M, Desguerre I, Fazzi E, Garcia-Cazorla A, Heiberg A, Kawaguchi M, Kumar R, Lin JP, Lourenco CM, Male AM, Marques W, Jr., Mignot C, Olivieri I, Orcesi S, Prabhakar P, Rasmussen M, Robinson RA, Rozenberg F, Schmidt JL, Steindl K, Tan TY, van der Merwe WG, Vanderver A, Vassallo G, Wakeling EL, Wassmer E, Whittaker E, Livingston JH, Lebon P, Suzuki T, McLaughlin PJ, Keegan LP, O'Connell MA, Lovell SC, Crow YJ. Mutations in ADAR1 cause Aicardi-Goutières syndrome associated with a type I interferon signature. Nat Genet. 2012;44(11):1243-8. Epub 2012/09/25. doi: 10.1038/ng.2414. PubMed PMID: 23001123; PMCID: PMC4154508.

143. Martinez-Lopez A, Martin-Fernandez M, Buta S, Kim B, Bogunovic D, Diaz-Griffero F. SAMHD1 deficient human monocytes autonomously trigger type I interferon. Mol Immunol. 2018;101:450-60. Epub 2018/08/14. doi: 10.1016/j.molimm.2018.08.005. PubMed PMID: 30099227; PMCID: PMC6258080.

144. Seamon KJ, Sun Z, Shlyakhtenko LS, Lyubchenko YL, Stivers JT. SAMHD1 is a single-stranded nucleic acid binding protein with no active site-associated nuclease activity. Nucleic Acids Res. 2015;43(13):6486-99. Epub 2015/06/24. doi: 10.1093/nar/gkv633. PubMed PMID: 26101257; PMCID: PMC4513882.

145. Seamon KJ, Bumpus NN, Stivers JT. Single-Stranded Nucleic Acids Bind to the Tetramer Interface of SAMHD1 and Prevent Formation of the Catalytic Homotetramer. Biochemistry. 2016;55(44):6087-99. Epub 2016/10/25. doi: 10.1021/acs.biochem.6b00986. PubMed PMID: 27775344; PMCID: PMC5531264.

146. Maelfait J, Bridgeman A, Benlahrech A, Cursi C, Rehwinkel J. Restriction by SAMHD1 Limits cGAS/STING-Dependent Innate and Adaptive Immune Responses to HIV-1. Cell Rep. 2016;16(6):1492-501. Epub 2016/08/02. doi: 10.1016/j.celrep.2016.07.002. PubMed PMID: 27477283; PMCID: PMC4978700.

147. Goncalves A, Karayel E, Rice GI, Bennett KL, Crow YJ, Superti-Furga G, Bürckstümmer T. SAMHD1 is a nucleic-acid binding protein that is mislocalized due to aicardi-goutières syndrome-associated mutations. Hum Mutat. 2012;33(7):1116-22. Epub 2012/03/31. doi: 10.1002/humu.22087. PubMed PMID: 22461318.

148. Chen S, Bonifati S, Qin Z, St Gelais C, Kodigepalli KM, Barrett BS, Kim SH, Antonucci JM, Ladner KJ, Buzovetsky O, Knecht KM, Xiong Y, Yount JS, Guttridge DC, Santiago ML, Wu L. SAMHD1 suppresses innate immune responses to viral infections and inflammatory stimuli by inhibiting the NF-kappaB and interferon pathways. Proc Natl Acad Sci U S A. 2018;115(16):E3798-e807. Epub 2018/04/04. doi: 10.1073/pnas.1801213115. PubMed PMID: 29610295; PMCID: PMC5910870.

149. Chen S, Bonifati S, Qin Z, St Gelais C, Wu L. SAMHD1 Suppression of Antiviral Immune Responses. Trends Microbiol. 2019;27(3):254-67. Epub 2018/10/20. doi: 10.1016/j.tim.2018.09.009. PubMed PMID: 30336972; PMCID: PMC6377309.

150. Qin Z, Bonifati S, St Gelais C, Li TW, Kim SH, Antonucci JM, Mahboubi B, Yount JS, Xiong Y, Kim B, Wu L. The dNTPase activity of SAMHD1 is important for its suppression of innate immune responses in differentiated monocytic cells. J Biol Chem. 2020;295(6):1575-86. Epub 2020/01/09. doi: 10.1074/jbc.RA119.010360. PubMed PMID: 31914403; PMCID: PMC7008377.

151. Espada CE, St Gelais C, Bonifati S, Maksimova VV, Cahill MP, Kim SH, Wu L. TRAF6 and TAK1 Contribute to SAMHD1-Mediated Negative Regulation of NF-κB Signaling. J Virol. 2021;95(3). Epub 2020/11/13. doi: 10.1128/jvi.01970-20. PubMed PMID: 33177202; PMCID: PMC7925110.

152. Yin X, Langer S, Zhang Z, Herbert KM, Yoh S, König R, Chanda SK. Sensor Sensibility-HIV-1 and the Innate Immune Response. Cells. 2020;9(1). Epub 2020/01/24. doi: 10.3390/cells9010254. PubMed PMID: 31968566; PMCID: PMC7016969.

153. Zhang C, de Silva S, Wang JH, Wu L. Co-evolution of primate SAMHD1 and lentivirus Vpx leads to the loss of the vpx gene in HIV-1 ancestor. PLoS One. 2012;7(5):e37477. Epub 2012/05/11. doi: 10.1371/journal.pone.0037477. PubMed PMID: 22574228; PMCID: PMC3345027.

154. Oo A, Zandi K, Shepard C, Bassit LC, Musall K, Goh SL, Cho YJ, Kim DH, Schinazi RF, Kim B. Elimination of Aicardi-Goutières syndrome protein SAMHD1 activates cellular innate immunity and suppresses SARS-CoV-2 replication. J Biol Chem. 2022;298(3):101635. Epub 2022/01/28. doi: 10.1016/j.jbc.2022.101635. PubMed PMID: 35085552; PMCID: PMC8786443.

155. Mohamed A, Bakir T, Al-Hawel H, Al-Sharif I, Bakheet R, Kouser L, Murugaiah V, Al-Mozaini M. HIV-2 Vpx neutralizes host restriction factor SAMHD1 to promote viral pathogenesis. Sci Rep. 2021;11(1):20984. Epub 2021/10/27. doi: 10.1038/s41598-021-00415-2. PubMed PMID: 34697376; PMCID: PMC8545964.

156. Fink DL, Cai J, Whelan MVX, Monit C, Maluquer de Motes C, Towers GJ, Sumner RP. HIV-2/SIV Vpx antagonises NF-κB activation by targeting p65. Retrovirology. 2022;19(1):2. Epub 2022/01/26. doi: 10.1186/s12977-021-00586-w. PubMed PMID: 35073912; PMCID: PMC8785589.

157. Chen Z, Zhu M, Pan X, Zhu Y, Yan H, Jiang T, Shen Y, Dong X, Zheng N, Lu J, Ying S, Shen Y. Inhibition of Hepatitis B virus replication by SAMHD1. Biochem Biophys Res Commun. 2014;450(4):1462-8. Epub 2014/07/16. doi: 10.1016/j.bbrc.2014.07.023. PubMed PMID: 25019997.

158. Cingöz O, Arnow ND, Puig Torrents M, Bannert N. Vpx enhances innate immune responses independently of SAMHD1 during HIV-1 infection. Retrovirology. 2021;18(1):4. Epub 2021/02/11. doi: 10.1186/s12977-021-00548-2. PubMed PMID: 33563288; PMCID: PMC7871410.

159. Daddacha W, Koyen AE, Bastien AJ, Head PE, Dhere VR, Nabeta GN, Connolly EC, Werner E, Madden MZ, Daly MB, Minten EV, Whelan DR, Schlafstein AJ, Zhang H, Anand R, Doronio C, Withers AE, Shepard C, Sundaram RK, Deng X, Dynan WS, Wang Y, Bindra RS, Cejka P, Rothenberg E, Doetsch PW, Kim B, Yu DS. SAMHD1 Promotes DNA End Resection to Facilitate DNA Repair by Homologous Recombination. Cell Rep. 2017;20(8):1921-35. Epub 2017/08/24. doi: 10.1016/j.celrep.2017.08.008. PubMed PMID: 28834754; PMCID: PMC5576576.

160. Clifford R, Louis T, Robbe P, Ackroyd S, Burns A, Timbs AT, Wright Colopy G, Dreau H, Sigaux F, Judde JG, Rotger M, Telenti A, Lin YL, Pasero P, Maelfait J, Titsias M, Cohen DR, Henderson SJ, Ross MT, Bentley D, Hillmen P, Pettitt A, Rehwinkel J, Knight SJ, Taylor JC, Crow YJ, Benkirane M, Schuh A. SAMHD1 is mutated recurrently in chronic lymphocytic leukemia and is involved in response to DNA damage. Blood. 2014;123(7):1021-31. Epub 2013/12/18. doi: 10.1182/blood-2013-04-490847. PubMed PMID: 24335234; PMCID: PMC3924925.

161. Kapoor-Vazirani P, Rath SK, Liu X, Shu Z, Bowen NE, Chen Y, Haji-Seyed-Javadi R, Daddacha W, Minten EV, Danelia D, Farchi D, Duong DM, Seyfried NT, Deng X, Ortlund EA, Kim B, Yu DS. SAMHD1 deacetylation by SIRT1 promotes DNA end resection by facilitating DNA binding at double-strand breaks. Nat Commun. 2022;13(1):6707. Epub 20221107. doi: 10.1038/s41467-022-34578-x. PubMed PMID: 36344525; PMCID: PMC9640623.

162. Coquel F, Silva MJ, Techer H, Zadorozhny K, Sharma S, Nieminuszczy J, Mettling C, Dardillac E, Barthe A, Schmitz AL, Promonet A, Cribier A, Sarrazin A, Niedzwiedz W, Lopez B, Costanzo V, Krejci L, Chabes A, Benkirane M, Lin YL, Pasero P. SAMHD1 acts at stalled replication forks to prevent interferon induction. Nature. 2018;557(7703):57-61. Epub 2018/04/20. doi: 10.1038/s41586-018-0050-1. PubMed PMID: 29670289.

163. Akimova E, Gassner FJ, Schubert M, Rebhandl S, Arzt C, Rauscher S, Tober V, Zaborsky N, Greil R, Geisberger R. SAMHD1 restrains aberrant nucleotide insertions at repair

junctions generated by DNA end joining. Nucleic Acids Res. 2021;49(5):2598-608. Epub 2021/02/17. doi: 10.1093/nar/gkab051. PubMed PMID: 33591315; PMCID: PMC7969033.

164. Husain A, Xu J, Fujii H, Nakata M, Kobayashi M, Wang JY, Rehwinkel J, Honjo T, Begum NA. SAMHD1-mediated dNTP degradation is required for efficient DNA repair during antibody class switch recombination. Embo j. 2020;39(15):e102931. Epub 2020/06/09. doi: 10.15252/embj.2019102931. PubMed PMID: 32511795; PMCID: PMC7396875.

165. Park K, Ryoo J, Jeong H, Kim M, Lee S, Hwang SY, Ahn J, Kim D, Moon HC, Baek D, Kim K, Park HY, Ahn K. Aicardi-Goutières syndrome-associated gene SAMHD1 preserves genome integrity by preventing R-loop formation at transcription-replication conflict regions. PLoS Genet. 2021;17(4):e1009523. Epub 2021/04/16. doi: 10.1371/journal.pgen.1009523. PubMed PMID: 33857133; PMCID: PMC8078737.

166. Franzolin E, Coletta S, Ferraro P, Pontarin G, D'Aronco G, Stevanoni M, Palumbo E, Cagnin S, Bertoldi L, Feltrin E, Valle G, Russo A, Bianchi V, Rampazzo C. SAMHD1-deficient fibroblasts from Aicardi-Goutieres Syndrome patients can escape senescence and accumulate mutations. Faseb j. 2020;34(1):631-47. Epub 2020/01/10. doi: 10.1096/fj.201902508R. PubMed PMID: 31914608.

167. Kretschmer S, Wolf C, Konig N, Staroske W, Guck J, Hausler M, Luksch H, Nguyen LA, Kim B, Alexopoulou D, Dahl A, Rapp A, Cardoso MC, Shevchenko A, Lee-Kirsch MA. SAMHD1 prevents autoimmunity by maintaining genome stability. Ann Rheum Dis. 2015;74(3):e17. Epub 2014/01/22. doi: 10.1136/annrheumdis-2013-204845. PubMed PMID: 24445253; PMCID: PMC4345975.

168. Kodigepalli KM, Bonifati S, Tirumuru N, Wu L. SAMHD1 modulates in vitro proliferation of acute myeloid leukemia-derived THP-1 cells through the PI3K-Akt-p27 axis. Cell Cycle. 2018;17(9):1124-37. Epub 2018/06/19. doi: 10.1080/15384101.2018.1480218. PubMed PMID: 29911928; PMCID: PMC6110597.

169. Kodigepalli KM, Li M, Liu SL, Wu L. Exogenous expression of SAMHD1 inhibits proliferation and induces apoptosis in cutaneous T-cell lymphoma-derived HuT78 cells. Cell Cycle. 2017;16(2):179-88. Epub 2016/12/09. doi: 10.1080/15384101.2016.1261226. PubMed PMID: 27929746; PMCID: PMC5283819.

170. Dragin L, Munir-Matloob S, Froehlich J, Morel M, Sourisce A, Lahouassa H, Bailly K, Mangeney M, Ramirez BC, Margottin-Goguet F. Evidence that HIV-1 restriction factor SAMHD1 facilitates differentiation of myeloid THP-1 cells. Virol J. 2015;12:201. Epub 20151125. doi: 10.1186/s12985-015-0425-y. PubMed PMID: 26606981; PMCID: PMC4660839.

171. Wang JL, Lu FZ, Shen XY, Wu Y, Zhao LT. SAMHD1 is down regulated in lung cancer by methylation and inhibits tumor cell proliferation. Biochem Biophys Res Commun. 2014;455(3-4):229-33. Epub 20141106. doi: 10.1016/j.bbrc.2014.10.153. PubMed PMID: 25449277.

172. Meuth M, L'Heureux-Huard N, Trudel M. Characterization of a mutator gene in Chinese hamster ovary cells. Proc Natl Acad Sci U S A. 1979;76(12):6505-9. Epub 1979/12/01. doi: 10.1073/pnas.76.12.6505. PubMed PMID: 293738; PMCID: PMC411894.

173. Weinberg G, Ullman B, Martin DW, Jr. Mutator phenotypes in mammalian cell mutants with distinct biochemical defects and abnormal deoxyribonucleoside triphosphate pools. Proc Natl Acad Sci U S A. 1981;78(4):2447-51. Epub 1981/04/01. doi: 10.1073/pnas.78.4.2447. PubMed PMID: 7017732; PMCID: PMC319363.

174. Kunkel TA. DNA replication fidelity. J Biol Chem. 1992;267(26):18251-4. Epub 1992/09/15. PubMed PMID: 1526964.

175. Kumar D, Abdulovic AL, Viberg J, Nilsson AK, Kunkel TA, Chabes A. Mechanisms of mutagenesis in vivo due to imbalanced dNTP pools. Nucleic Acids Res. 2011;39(4):1360-71. Epub 2010/10/22. doi: 10.1093/nar/gkq829. PubMed PMID: 20961955; PMCID: PMC3045583.

176. Caras IW, Martin DW, Jr. Molecular cloning of the cDNA for a mutant mouse ribonucleotide reductase M1 that produces a dominant mutator phenotype in mammalian cells. Mol Cell Biol. 1988;8(7):2698-704. Epub 1988/07/01. doi: 10.1128/mcb.8.7.2698-2704.1988. PubMed PMID: 3043191; PMCID: PMC363480.

177. Ullman B, Clift SM, Gudas LJ, Levinson BB, Wormsted MA, Martin DW, Jr. Alterations in deoxyribonucleotide metabolism in cultured cells with ribonucleotide reductase activities refractory to feedback inhibition by 2'-deoxyadenosine triphosphate. J Biol Chem. 1980;255(17):8308-14. Epub 1980/09/10. PubMed PMID: 6997294.

178. Fersht AR. Fidelity of replication of phage phi X174 DNA by DNA polymerase III holoenzyme: spontaneous mutation by misincorporation. Proc Natl Acad Sci U S A. 1979;76(10):4946-50. Epub 1979/10/01. doi: 10.1073/pnas.76.10.4946. PubMed PMID: 159450; PMCID: PMC413055.

179. Mendelman LV, Petruska J, Goodman MF. Base mispair extension kinetics. Comparison of DNA polymerase alpha and reverse transcriptase. J Biol Chem. 1990;265(4):2338-46. Epub 1990/02/05. PubMed PMID: 1688852.

180. Traut TW. Physiological concentrations of purines and pyrimidines. Mol Cell Biochem. 1994;140(1):1-22. Epub 1994/11/09. doi: 10.1007/bf00928361. PubMed PMID: 7877593.

181. Amin NA, Seymour E, Saiya-Cork K, Parkin B, Shedden K, Malek SN. A Quantitative Analysis of Subclonal and Clonal Gene Mutations before and after Therapy in Chronic Lymphocytic Leukemia. Clin Cancer Res. 2016;22(17):4525-35. Epub 2016/04/10. doi: 10.1158/1078-0432.Ccr-15-3103. PubMed PMID: 27060156; PMCID: PMC5010528.

182. Johansson P, Klein-Hitpass L, Choidas A, Habenberger P, Mahboubi B, Kim B, Bergmann A, Scholtysik R, Brauser M, Lollies A, Siebert R, Zenz T, Duhrsen U, Kuppers R, Durig J. SAMHD1 is recurrently mutated in T-cell prolymphocytic leukemia. Blood Cancer J. 2018;8(1):11. Epub 2018/01/21. doi: 10.1038/s41408-017-0036-5. PubMed PMID: 29352181; PMCID: PMC5802577.

183. Jiang H, Li C, Liu Z, Shengjing H. Expression and Relationship of SAMHD1 with Other Apoptotic and Autophagic Genes in Acute Myeloid Leukemia Patients. Acta Haematol. 2020;143(1):51-9. Epub 2019/08/23. doi: 10.1159/000500822. PubMed PMID: 31434075.

184. Guièze R, Robbe P, Clifford R, de Guibert S, Pereira B, Timbs A, Dilhuydy MS, Cabes M, Ysebaert L, Burns A, Nguyen-Khac F, Davi F, Véronèse L, Combes P, Le Garff-Tavernier M, Leblond V, Merle-Béral H, Alsolami R, Hamblin A, Mason J, Pettitt A, Hillmen P,

Taylor J, Knight SJ, Tournilhac O, Schuh A. Presence of multiple recurrent mutations confers poor trial outcome of relapsed/refractory CLL. Blood. 2015;126(18):2110-7. Epub 2015/09/01. doi: 10.1182/blood-2015-05-647578. PubMed PMID: 26316624.

185. de Silva S, Wang F, Hake TS, Porcu P, Wong HK, Wu L. Downregulation of SAMHD1 expression correlates with promoter DNA methylation in Sézary syndrome patients. J Invest Dermatol. 2014;134(2):562-5. Epub 2013/07/26. doi: 10.1038/jid.2013.311. PubMed PMID: 23884314; PMCID: PMC3844041.

186. Merati M, Buethe DJ, Cooper KD, Honda KS, Wang H, Gerstenblith MR. Aggressive CD8(+) epidermotropic cutaneous T-cell lymphoma associated with homozygous mutation in SAMHD1. JAAD Case Rep. 2015;1(4):227-9. Epub 2016/04/07. doi: 10.1016/j.jdcr.2015.05.003. PubMed PMID: 27051737; PMCID: PMC4808729.

187. Roider T, Wang X, Hüttl K, Müller-Tidow C, Klapper W, Rosenwald A, Stewart JP, de Castro DG, Dreger P, Hermine O, Kluin-Nelemans HC, Grabe N, Dreyling M, Pott C, Ott G, Hoster E, Dietrich S. The impact of SAMHD1 expression and mutation status in mantle cell lymphoma: An analysis of the MCL Younger and Elderly trial. Int J Cancer. 2021;148(1):150-60. Epub 20200815. doi: 10.1002/ijc.33202. PubMed PMID: 32638373.

188. Rentoft M, Lindell K, Tran P, Chabes AL, Buckland RJ, Watt DL, Marjavaara L, Nilsson AK, Melin B, Trygg J, Johansson E, Chabes A. Heterozygous colon cancer-associated mutations of SAMHD1 have functional significance. Proc Natl Acad Sci U S A. 2016;113(17):4723-8. Epub 2016/04/14. doi: 10.1073/pnas.1519128113. PubMed PMID: 27071091; PMCID: PMC4855590.

189. Giannakis M, Mu XJ, Shukla SA, Qian ZR, Cohen O, Nishihara R, Bahl S, Cao Y, Amin-Mansour A, Yamauchi M, Sukawa Y, Stewart C, Rosenberg M, Mima K, Inamura K, Nosho K, Nowak JA, Lawrence MS, Giovannucci EL, Chan AT, Ng K, Meyerhardt JA, Van Allen EM, Getz G, Gabriel SB, Lander ES, Wu CJ, Fuchs CS, Ogino S, Garraway LA. Genomic Correlates of Immune-Cell Infiltrates in Colorectal Carcinoma. Cell Rep. 2016;15(4):857-65. Epub 2016/05/07. doi: 10.1016/j.celrep.2016.03.075. PubMed PMID: 27149842; PMCID: PMC4850357.

190. Giannakis M, Hodis E, Jasmine Mu X, Yamauchi M, Rosenbluh J, Cibulskis K, Saksena G, Lawrence MS, Qian ZR, Nishihara R, Van Allen EM, Hahn WC, Gabriel SB, Lander ES, Getz G, Ogino S, Fuchs CS, Garraway LA. RNF43 is frequently mutated in colorectal and endometrial cancers. Nat Genet. 2014;46(12):1264-6. Epub 2014/10/27. doi: 10.1038/ng.3127. PubMed PMID: 25344691; PMCID: PMC4283570.

191. Bowen NE, Temple J, Shepard C, Oo A, Arizaga F, Kapoor-Vazirani P, Persaud M, Yu CH, Kim DH, Schinazi RF, Ivanov DN, Diaz-Griffero F, Yu DS, Xiong Y, Kim B. Structural and functional characterization explains loss of dNTPase activity of the cancer-specific R366C/H mutant SAMHD1 proteins. J Biol Chem. 2021;297(4):101170. Epub 2021/09/08. doi: 10.1016/j.jbc.2021.101170. PubMed PMID: 34492268; PMCID: PMC8497992.

192. Rothenburger T, McLaughlin KM, Herold T, Schneider C, Oellerich T, Rothweiler F, Feber A, Fenton TR, Wass MN, Keppler OT, Michaelis M, Cinatl J, Jr. SAMHD1 is a key regulator of the lineage-specific response of acute lymphoblastic leukaemias to nelarabine. Commun Biol. 2020;3(1):324. Epub 2020/06/26. doi: 10.1038/s42003-020-1052-8.

PubMed PMID: 32581304; PMCID: PMC7314829 T.O., C.S., O.T.K. and J.C. are listed as inventors. All other authors declare no competing interests.

193. Davenne T, Rehwinkel J. PNP inhibitors selectively kill cancer cells lacking SAMHD1. Mol Cell Oncol. 2020;7(6):1804308. Epub 2020/11/26. doi: 10.1080/23723556.2020.1804308. PubMed PMID: 33235905; PMCID: PMC7671039.

194. Davenne T, Klintman J, Sharma S, Rigby RE, Blest HTW, Cursi C, Bridgeman A, Dadonaite B, De Keersmaecker K, Hillmen P, Chabes A, Schuh A, Rehwinkel J. SAMHD1 Limits the Efficacy of Forodesine in Leukemia by Protecting Cells against the Cytotoxicity of dGTP. Cell Rep. 2020;31(6):107640. Epub 2020/05/14. doi: 10.1016/j.celrep.2020.107640. PubMed PMID: 32402273; PMCID: PMC7225753.

195. Herold N, Rudd SG, Sanjiv K, Kutzner J, Myrberg IH, Paulin CBJ, Olsen TK, Helleday T, Henter JI, Schaller T. With me or against me: Tumor suppressor and drug resistance activities of SAMHD1. Exp Hematol. 2017;52:32-9. Epub 2017/05/16. doi: 10.1016/j.exphem.2017.05.001. PubMed PMID: 28502830.

196. Knecht KM, Buzovetsky O, Schneider C, Thomas D, Srikanth V, Kaderali L, Tofoleanu F, Reiss K, Ferreiros N, Geisslinger G, Batista VS, Ji X, Cinatl J, Jr., Keppler OT, Xiong Y. The structural basis for cancer drug interactions with the catalytic and allosteric sites of SAMHD1. Proc Natl Acad Sci U S A. 2018;115(43):E10022-e31. Epub 2018/10/12. doi: 10.1073/pnas.1805593115. PubMed PMID: 30305425; PMCID: PMC6205433.

197. Herold N, Rudd SG, Sanjiv K, Kutzner J, Bladh J, Paulin CBJ, Helleday T, Henter JI, Schaller T. SAMHD1 protects cancer cells from various nucleoside-based antimetabolites. Cell Cycle. 2017;16(11):1029-38. Epub 2017/04/25. doi: 10.1080/15384101.2017.1314407. PubMed PMID: 28436707; PMCID: PMC5499833.

198. Rothenburger T, Thomas D, Schreiber Y, Wratil PR, Pflantz T, Knecht K, Digianantonio K, Temple J, Schneider C, Baldauf HM, McLaughlin KM, Rothweiler F, Bilen B, Farmand S, Bojkova D, Costa R, Ferreirós N, Geisslinger G, Oellerich T, Xiong Y, Keppler OT, Wass MN, Michaelis M, Cinatl J, Jr. Differences between intrinsic and acquired nucleoside analogue resistance in acute myeloid leukaemia cells. J Exp Clin Cancer Res. 2021;40(1):317. Epub 2021/10/14. doi: 10.1186/s13046-021-02093-4. PubMed PMID: 34641952; PMCID: PMC8507139.

199. Oellerich T, Schneider C, Thomas D, Knecht KM, Buzovetsky O, Kaderali L, Schliemann C, Bohnenberger H, Angenendt L, Hartmann W, Wardelmann E, Rothenburger T, Mohr S, Scheich S, Comoglio F, Wilke A, Ströbel P, Serve H, Michaelis M, Ferreirós N, Geisslinger G, Xiong Y, Keppler OT, Cinatl J, Jr. Selective inactivation of hypomethylating agents by SAMHD1 provides a rationale for therapeutic stratification in AML. Nat Commun. 2019;10(1):3475. Epub 2019/08/04. doi: 10.1038/s41467-019-11413-4. PubMed PMID: 31375673; PMCID: PMC6677770 T.O., C. Schneider, G.G., H.S., O.T.K. and J.C. are listed as inventors. All other authors declare no competing interests.

200. Marrero RJ, Cao X, Wu H, Elsayed AH, Klco JM, Ribeiro RC, Rubnitz JE, Ma X, Meshinchi S, Aplenc R, Kolb EA, Ries RE, Alonzo T, Pounds SB, Lamba JK. SAMHD1 Single Nucleotide Polymorphisms Impact Outcome in Children with Newly Diagnosed

Acute Myeloid Leukemia. Blood Adv. 2023. Epub 20230123. doi: 10.1182/bloodadvances.2022009088. PubMed PMID: 36689724.

201. Xagoraris I, Vassilakopoulos TP, Drakos E, Angelopoulou MK, Panitsas F, Herold N, Medeiros LJ, Giakoumis X, Pangalis GA, Rassidakis GZ. Expression of the novel tumour suppressor sterile alpha motif and HD domain-containing protein 1 is an independent adverse prognostic factor in classical Hodgkin lymphoma. Br J Haematol. 2021;193(3):488-96. Epub 2021/02/03. doi: 10.1111/bjh.17352. PubMed PMID: 33528031.

202. Merrien M, Wasik AM, Ljung E, Morsy MHA, de Matos Rodrigues J, Carlsten M, Rassidakis GZ, Christensson B, Kolstad A, Jerkeman M, Ek S, Herold N, Wahlin BE, Sander B. Clinical and biological impact of SAMHD1 expression in mantle cell lymphoma. Virchows Arch. 2022;480(3):655-66. Epub 20211104. doi: 10.1007/s00428-021-03228-w. PubMed PMID: 34738194; PMCID: PMC8989861.

203. Rudd SG, Tsesmetzis N, Sanjiv K, Paulin CB, Sandhow L, Kutzner J, Hed Myrberg I, Bunten SS, Axelsson H, Zhang SM, Rasti A, Mäkelä P, Coggins SA, Tao S, Suman S, Branca RM, Mermelekas G, Wiita E, Lee S, Walfridsson J, Schinazi RF, Kim B, Lehtiö J, Rassidakis GZ, Pokrovskaja Tamm K, Warpman-Berglund U, Heyman M, Grandér D, Lehmann S, Lundbäck T, Qian H, Henter JI, Schaller T, Helleday T, Herold N. Ribonucleotide reductase inhibitors suppress SAMHD1 ara-CTPase activity enhancing cytarabine efficacy. EMBO Mol Med. 2020;12(3):e10419. Epub 2020/01/18. doi: 10.15252/emmm.201910419. PubMed PMID: 31950591; PMCID: PMC7059017.

204. Zhang F, Sun J, Tang X, Liang Y, Jiao Q, Yu B, Dai Z, Yuan X, Li J, Yan J, Zhang Z, Fan S, Wang M, Hu H, Zhang C, Lv XB. Stabilization of SAMHD1 by NONO is crucial for Ara-C resistance in AML. Cell Death Dis. 2022;13(7):590. Epub 20220708. doi: 10.1038/s41419-022-05023-0. PubMed PMID: 35803902; PMCID: PMC9270467.

205. Wu HL, Gong Y, Ji P, Xie YF, Jiang YZ, Liu GY. Targeting nucleotide metabolism: a promising approach to enhance cancer immunotherapy. J Hematol Oncol. 2022;15(1):45. Epub 20220427. doi: 10.1186/s13045-022-01263-x. PubMed PMID: 35477416; PMCID: PMC9044757.

206. Bjursell G, Skoog L. Control of nucleotide pools in mammalian cells. Antibiot Chemother (1971). 1980;28:78-85. doi: 10.1159/000386063. PubMed PMID: 6251748.

207. Cohen A, Barankiewicz J, Lederman HM, Gelfand EW. Purine and pyrimidine metabolism in human T lymphocytes. Regulation of deoxyribonucleotide metabolism. J Biol Chem. 1983;258(20):12334-40. PubMed PMID: 6605343.

208. Reichard P. Interactions between deoxyribonucleotide and DNA synthesis. Annu Rev Biochem. 1988;57:349-74. Epub 1988/01/01. doi: 10.1146/annurev.bi.57.070188.002025. PubMed PMID: 3052277.

209. Lacombe ML, Wallet V, Troll H, Véron M. Functional cloning of a nucleoside diphosphate kinase from Dictyostelium discoideum. J Biol Chem. 1990;265(17):10012-8. PubMed PMID: 2161830.

210. Bello LJ. Regulation of thymidine kinase synthesis in human cells. Exp Cell Res. 1974;89(2):263-74. Epub 1974/12/01. doi: 10.1016/0014-4827(74)90790-3. PubMed PMID: 4457349.

211. Pavlova NN, Thompson CB. The Emerging Hallmarks of Cancer Metabolism. Cell Metab. 2016;23(1):27-47. doi: 10.1016/j.cmet.2015.12.006. PubMed PMID: 26771115; PMCID: PMC4715268.

212. Yamashita M, Emerman M. Retroviral infection of non-dividing cells: old and new perspectives. Virology. 2006;344(1):88-93. doi: 10.1016/j.virol.2005.09.012. PubMed PMID: 16364740.

213. Hollenbaugh JA, Tao S, Lenzi GM, Ryu S, Kim DH, Diaz-Griffero F, Schinazi RF, Kim B. dNTP pool modulation dynamics by SAMHD1 protein in monocyte-derived macrophages. Retrovirology. 2014;11:63. Epub 20140827. doi: 10.1186/s12977-014-0063-2. PubMed PMID: 25158827; PMCID: PMC4161909.

214. Aye Y, Li M, Long MJ, Weiss RS. Ribonucleotide reductase and cancer: biological mechanisms and targeted therapies. Oncogene. 2015;34(16):2011-21. Epub 2014/06/10. doi: 10.1038/onc.2014.155. PubMed PMID: 24909171.

215. Baldauf HM, Pan X, Erikson E, Schmidt S, Daddacha W, Burggraf M, Schenkova K, Ambiel I, Wabnitz G, Gramberg T, Panitz S, Flory E, Landau NR, Sertel S, Rutsch F, Lasitschka F, Kim B, König R, Fackler OT, Keppler OT. SAMHD1 restricts HIV-1 infection in resting CD4(+) T cells. Nat Med. 2012;18(11):1682-7. doi: 10.1038/nm.2964. PubMed PMID: 22972397; PMCID: PMC3828732.

216. Sun D, Buttitta L. States of G(0) and the proliferation-quiescence decision in cells, tissues and during development. Int J Dev Biol. 2017;61(6-7):357-66. doi: 10.1387/ijdb.160343LB. PubMed PMID: 28695955.

217. DeGregori J, Kowalik T, Nevins JR. Cellular targets for activation by the E2F1 transcription factor include DNA synthesis- and G1/S-regulatory genes. Mol Cell Biol. 1995;15(8):4215-24. doi: 10.1128/mcb.15.8.4215. PubMed PMID: 7623816; PMCID: PMC230660.

218. Tsai LH, Lees E, Faha B, Harlow E, Riabowol K. The cdk2 kinase is required for the G1-to-S transition in mammalian cells. Oncogene. 1993;8(6):1593-602. PubMed PMID: 8502482.

219. Limas JC, Cook JG. Preparation for DNA replication: the key to a successful S phase. FEBS Lett. 2019;593(20):2853-67. Epub 20191015. doi: 10.1002/1873-3468.13619. PubMed PMID: 31556113; PMCID: PMC6817399.

220. Balachander S, Gombolay AL, Yang T, Xu P, Newnam G, Keskin H, El-Sayed WMM, Bryksin AV, Tao S, Bowen NE, Schinazi RF, Kim B, Koh KD, Vannberg FO, Storici F. Ribonucleotide incorporation in yeast genomic DNA shows preference for cytosine and guanosine preceded by deoxyadenosine. Nat Commun. 2020;11(1):2447. Epub 2020/05/18. doi: 10.1038/s41467-020-16152-5. PubMed PMID: 32415081; PMCID: PMC7229183.

221. Sonza S, Maerz A, Uren S, Violo A, Hunter S, Boyle W, Crowe S. Susceptibility of human monocytes to HIV type 1 infection in vitro is not dependent on their level of CD4

expression. AIDS Res Hum Retroviruses. 1995;11(7):769-76. doi: 10.1089/aid.1995.11.769. PubMed PMID: 7546902.

222. Lee B, Sharron M, Montaner LJ, Weissman D, Doms RW. Quantification of CD4, CCR5, and CXCR4 levels on lymphocyte subsets, dendritic cells, and differentially conditioned monocyte-derived macrophages. Proceedings of the National Academy of Sciences. 1999;96(9):5215-20. doi: doi:10.1073/pnas.96.9.5215.

223. Neil S, Martin F, Ikeda Y, Collins M. Postentry restriction to human immunodeficiency virus-based vector transduction in human monocytes. J Virol. 2001;75(12):5448-56. doi: 10.1128/jvi.75.12.5448-5456.2001. PubMed PMID: 11356951; PMCID: PMC114256.

224. Descours B, Cribier A, Chable-Bessia C, Ayinde D, Rice G, Crow Y, Yatim A, Schwartz O, Laguette N, Benkirane M. SAMHD1 restricts HIV-1 reverse transcription in quiescent CD4(+) T-cells. Retrovirology. 2012;9:87. Epub 2012/10/25. doi: 10.1186/1742-4690-9-87. PubMed PMID: 23092122; PMCID: PMC3494655.

225. Hollenbaugh JA, Gee P, Baker J, Daly MB, Amie SM, Tate J, Kasai N, Kanemura Y, Kim DH, Ward BM, Koyanagi Y, Kim B. Host factor SAMHD1 restricts DNA viruses in non-dividing myeloid cells. PLoS Pathog. 2013;9(6):e1003481. Epub 2013/07/05. doi: 10.1371/journal.ppat.1003481. PubMed PMID: 23825958; PMCID: PMC3694861.

226. Ashar FN, Moes A, Moore AZ, Grove ML, Chaves PHM, Coresh J, Newman AB, Matteini AM, Bandeen-Roche K, Boerwinkle E, Walston JD, Arking DE. Association of mitochondrial DNA levels with frailty and all-cause mortality. J Mol Med (Berl). 2015;93(2):177-86. Epub 20141204. doi: 10.1007/s00109-014-1233-3. PubMed PMID: 25471480; PMCID: PMC4319988.

227. James CD, Prabhakar AT, Otoa R, Evans MR, Wang X, Bristol ML, Zhang K, Li R, Morgan IM. SAMHD1 Regulates Human Papillomavirus 16-Induced Cell Proliferation and Viral Replication during Differentiation of Keratinocytes. mSphere. 2019;4(4). Epub 2019/08/09. doi: 10.1128/mSphere.00448-19. PubMed PMID: 31391281; PMCID: PMC6686230.

228. Zhao K, Du J, Han X, Goodier JL, Li P, Zhou X, Wei W, Evans SL, Li L, Zhang W, Cheung LE, Wang G, Kazazian HH, Jr., Yu XF. Modulation of LINE-1 and Alu/SVA retrotransposition by Aicardi-Goutières syndrome-related SAMHD1. Cell Rep. 2013;4(6):1108-15. Epub 2013/09/17. doi: 10.1016/j.celrep.2013.08.019. PubMed PMID: 24035396; PMCID: PMC3988314.

229. White TE, Brandariz-Nuñez A, Han K, Sawyer SL, Kim B, Diaz-Griffero F. Modulation of LINE-1 Retrotransposition by a Human SAMHD1 Polymorphism. Virol Rep. 2016;6:53-60. Epub 2016/08/03. doi: 10.1016/j.virep.2016.06.001. PubMed PMID: 27482511; PMCID: PMC4959807.

230. Nabel G, Baltimore D. An inducible transcription factor activates expression of human immunodeficiency virus in T cells. Nature. 1987;326(6114):711-3. Epub 1987/04/16. doi: 10.1038/326711a0. PubMed PMID: 3031512.

231. Ryoo J, Choi J, Oh C, Kim S, Seo M, Kim SY, Seo D, Kim J, White TE, Brandariz-Nuñez A, Diaz-Griffero F, Yun CH, Hollenbaugh JA, Kim B, Baek D, Ahn K. The ribonuclease

activity of SAMHD1 is required for HIV-1 restriction. Nat Med. 2014;20(8):936-41. Epub 2014/07/21. doi: 10.1038/nm.3626. PubMed PMID: 25038827; PMCID: PMC4318684.

232. Rassidakis GZ, Herold N, Myrberg IH, Tsesmetzis N, Rudd SG, Henter JI, Schaller T, Ng SB, Chng WJ, Yan B, Ng CH, Ravandi F, Andreeff M, Kantarjian HM, Medeiros LJ, Xagoraris I, Khoury JD. Low-level expression of SAMHD1 in acute myeloid leukemia (AML) blasts correlates with improved outcome upon consolidation chemotherapy with high-dose cytarabine-based regimens. Blood Cancer J. 2018;8(11):98. Epub 2018/10/21. doi: 10.1038/s41408-018-0134-z. PubMed PMID: 30341277; PMCID: PMC6195559.

233. Behrendt R, Schumann T, Gerbaulet A, Nguyen LA, Schubert N, Alexopoulou D, Berka U, Lienenklaus S, Peschke K, Gibbert K, Wittmann S, Lindemann D, Weiss S, Dahl A, Naumann R, Dittmer U, Kim B, Mueller W, Gramberg T, Roers A. Mouse SAMHD1 has antiretroviral activity and suppresses a spontaneous cell-intrinsic antiviral response. Cell Rep. 2013;4(4):689-96. Epub 2013/08/27. doi: 10.1016/j.celrep.2013.07.037. PubMed PMID: 23972988; PMCID: PMC4807655.

234. Rehwinkel J, Maelfait J, Bridgeman A, Rigby R, Hayward B, Liberatore RA, Bieniasz PD, Towers GJ, Moita LF, Crow YJ, Bonthron DT, Reis e Sousa C. SAMHD1-dependent retroviral control and escape in mice. Embo j. 2013;32(18):2454-62. Epub 2013/07/23. doi: 10.1038/emboj.2013.163. PubMed PMID: 23872947; PMCID: PMC3770946.

235. Otwinowski Z, Minor W. [20] Processing of X-ray diffraction data collected in oscillation mode. Methods Enzymol. 1997;276:307-26. Epub 1997/01/01. doi: 10.1016/s0076-6879(97)76066-x. PubMed PMID: 27799103.

236. McCoy AJ, Grosse-Kunstleve RW, Adams PD, Winn MD, Storoni LC, Read RJ. Phaser crystallographic software. J Appl Crystallogr. 2007;40(Pt 4):658-74. Epub 2007/08/01. doi: 10.1107/s0021889807021206. PubMed PMID: 19461840; PMCID: PMC2483472.

237. Murshudov GN, Skubák P, Lebedev AA, Pannu NS, Steiner RA, Nicholls RA, Winn MD, Long F, Vagin AA. REFMAC5 for the refinement of macromolecular crystal structures. Acta Crystallogr D Biol Crystallogr. 2011;67(Pt 4):355-67. Epub 2011/04/05. doi: 10.1107/s0907444911001314. PubMed PMID: 21460454; PMCID: PMC3069751.

238. Emsley P, Lohkamp B, Scott WG, Cowtan K. Features and development of Coot. Acta Crystallogr D Biol Crystallogr. 2010;66(Pt 4):486-501. Epub 2010/04/13. doi: 10.1107/s0907444910007493. PubMed PMID: 20383002; PMCID: PMC2852313.

239. Sellon DC, Perry ST, Coggins L, Fuller FJ. Wild-type equine infectious anemia virus replicates in vivo predominantly in tissue macrophages, not in peripheral blood monocytes. J Virol. 1992;66(10):5906-13. doi: 10.1128/jvi.66.10.5906-5913.1992. PubMed PMID: 1382143; PMCID: PMC241467.

240. Brodie SJ, Pearson LD, Zink MC, Bickle HM, Anderson BC, Marcom KA, DeMartini JC. Ovine lentivirus expression and disease. Virus replication, but not entry, is restricted to macrophages of specific tissues. Am J Pathol. 1995;146(1):250-63. PubMed PMID: 7531949; PMCID: PMC1870777.

241. Gendelman HE, Narayan O, Molineaux S, Clements JE, Ghotbi Z. Slow, persistent replication of lentiviruses: role of tissue macrophages and macrophage precursors in bone

marrow. Proc Natl Acad Sci U S A. 1985;82(20):7086-90. doi: 10.1073/pnas.82.20.7086. PubMed PMID: 2996004; PMCID: PMC391315.

242. Zink MC, Yager JA, Myers JD. Pathogenesis of caprine arthritis encephalitis virus. Cellular localization of viral transcripts in tissues of infected goats. Am J Pathol. 1990;136(4):843-54. PubMed PMID: 2327471; PMCID: PMC1877653.

243. Foley. BT. An overview of the molecular phylogeny of lentiviruses. In HIV Sequence Compendium 2000. Kuiken C.L. FB, Hahn B., Korber B., Marx P.A., McCutchan F., Mellors J.W., Mullins J.I., Sodroski J., and Wolinsky S., editor: Theoretical Biology and Biophysics Group, Los Alamos National Laboratory, Los Alamos, New Mexico, LA-UR 01–3860 2000.

244. Taylor BS, Sobieszczyk ME, McCutchan FE, Hammer SM. The challenge of HIV-1 subtype diversity. N Engl J Med. 2008;358(15):1590-602. Epub 2008/04/12. doi: 10.1056/NEJMra0706737. PubMed PMID: 18403767; PMCID: PMC2614444.

245. Keele BF, Van Heuverswyn F, Li Y, Bailes E, Takehisa J, Santiago ML, Bibollet-Ruche F, Chen Y, Wain LV, Liegeois F, Loul S, Ngole EM, Bienvenue Y, Delaporte E, Brookfield JF, Sharp PM, Shaw GM, Peeters M, Hahn BH. Chimpanzee reservoirs of pandemic and nonpandemic HIV-1. Science. 2006;313(5786):523-6. Epub 20060525. doi: 10.1126/science.1126531. PubMed PMID: 16728595; PMCID: PMC2442710.

246. Sharp PM, Hahn BH. Origins of HIV and the AIDS pandemic. Cold Spring Harb Perspect Med. 2011;1(1):a006841. doi: 10.1101/cshperspect.a006841. PubMed PMID: 22229120; PMCID: PMC3234451.

247. Bailes E, Gao F, Bibollet-Ruche F, Courgnaud V, Peeters M, Marx PA, Hahn BH, Sharp PM. Hybrid origin of SIV in chimpanzees. Science. 2003;300(5626):1713. doi: 10.1126/science.1080657. PubMed PMID: 12805540.

248. Donahue JP, Vetter ML, Mukhtar NA, D'Aquila RT. The HIV-1 Vif PPLP motif is necessary for human APOBEC3G binding and degradation. Virology. 2008;377(1):49-53. Epub 20080521. doi: 10.1016/j.virol.2008.04.017. PubMed PMID: 18499212; PMCID: PMC2474554.

249. Mangeat B, Turelli P, Caron G, Friedli M, Perrin L, Trono D. Broad antiretroviral defence by human APOBEC3G through lethal editing of nascent reverse transcripts. Nature. 2003;424(6944):99-103. Epub 20030528. doi: 10.1038/nature01709. PubMed PMID: 12808466.

250. Lecossier D, Bouchonnet F, Clavel F, Hance AJ. Hypermutation of HIV-1 DNA in the absence of the Vif protein. Science. 2003;300(5622):1112. doi: 10.1126/science.1083338. PubMed PMID: 12750511.

251. Nikitina E, Larionova I, Choinzonov E, Kzhyshkowska J. Monocytes and Macrophages as Viral Targets and Reservoirs. Int J Mol Sci. 2018;19(9). Epub 20180918. doi: 10.3390/ijms19092821. PubMed PMID: 30231586; PMCID: PMC6163364.

252. Gershburg E, Pagano JS. Conserved herpesvirus protein kinases. Biochim Biophys Acta. 2008;1784(1):203-12. Epub 20070816. doi: 10.1016/j.bbapap.2007.08.009. PubMed PMID: 17881303; PMCID: PMC2265104.

253. Li R, Zhu J, Xie Z, Liao G, Liu J, Chen MR, Hu S, Woodard C, Lin J, Taverna SD, Desai P, Ambinder RF, Hayward GS, Qian J, Zhu H, Hayward SD. Conserved herpesvirus kinases target the DNA damage response pathway and TIP60 histone acetyltransferase to promote virus replication. Cell Host Microbe. 2011;10(4):390-400. doi: 10.1016/j.chom.2011.08.013. PubMed PMID: 22018239; PMCID: PMC3253558.

254. Li R, Liao G, Nirujogi RS, Pinto SM, Shaw PG, Huang TC, Wan J, Qian J, Gowda H, Wu X, Lv DW, Zhang K, Manda SS, Pandey A, Hayward SD. Phosphoproteomic Profiling Reveals Epstein-Barr Virus Protein Kinase Integration of DNA Damage Response and Mitotic Signaling. PLoS Pathog. 2015;11(12):e1005346. Epub 20151229. doi: 10.1371/journal.ppat.1005346. PubMed PMID: 26714015; PMCID: PMC4699913.

255. Calderwood MA, Venkatesan K, Xing L, Chase MR, Vazquez A, Holthaus AM, Ewence AE, Li N, Hirozane-Kishikawa T, Hill DE, Vidal M, Kieff E, Johannsen E. Epstein-Barr virus and virus human protein interaction maps. Proc Natl Acad Sci U S A. 2007;104(18):7606-11. Epub 20070419. doi: 10.1073/pnas.0702332104. PubMed PMID: 17446270; PMCID: PMC1863443.

256. Zhang K, Lv DW, Li R. Conserved Herpesvirus Protein Kinases Target SAMHD1 to Facilitate Virus Replication. Cell Rep. 2019;28(2):449-59.e5. Epub 2019/07/11. doi: 10.1016/j.celrep.2019.04.020. PubMed PMID: 31291580; PMCID: PMC6668718.

257. Businger R, Deutschmann J, Gruska I, Milbradt J, Wiebusch L, Gramberg T, Schindler M. Human cytomegalovirus overcomes SAMHD1 restriction in macrophages via pUL97. Nat Microbiol. 2019;4(12):2260-72. Epub 20190923. doi: 10.1038/s41564-019-0557-8. PubMed PMID: 31548682.

258. Irwin CR, Hitt MM, Evans DH. Targeting Nucleotide Biosynthesis: A Strategy for Improving the Oncolytic Potential of DNA Viruses. Front Oncol. 2017;7:229. Epub 20170926. doi: 10.3389/fonc.2017.00229. PubMed PMID: 29018771; PMCID: PMC5622948.

259. Xie Y, Wu L, Wang M, Cheng A, Yang Q, Wu Y, Jia R, Zhu D, Zhao X, Chen S, Liu M, Zhang S, Wang Y, Xu Z, Chen Z, Zhu L, Luo Q, Liu Y, Yu Y, Zhang L, Chen X. Alpha-Herpesvirus Thymidine Kinase Genes Mediate Viral Virulence and Are Potential Therapeutic Targets. Front Microbiol. 2019;10:941. Epub 20190508. doi: 10.3389/fmicb.2019.00941. PubMed PMID: 31134006; PMCID: PMC6517553.

260. McKnight SL. The nucleotide sequence and transcript map of the herpes simplex virus thymidine kinase gene. Nucleic Acids Res. 1980;8(24):5949-64. doi: 10.1093/nar/8.24.5949. PubMed PMID: 6258156; PMCID: PMC328064.

261. de Turenne-Tessier M, Ooka T, de The G, Daillie J. Characterization of an Epstein-Barr virus-induced thymidine kinase. J Virol. 1986;57(3):1105-12. doi: 10.1128/jvi.57.3.1105-1112.1986. PubMed PMID: 3005613; PMCID: PMC252844.

262. Littler E, Zeuthen J, McBride AA, Trøst Sørensen E, Powell KL, Walsh-Arrand JE, Arrand JR. Identification of an Epstein-Barr virus-coded thymidine kinase. Embo j. 1986;5(8):1959-66. doi: 10.1002/j.1460-2075.1986.tb04450.x. PubMed PMID: 3019675; PMCID: PMC1167064.

263. Lembo D, Brune W. Tinkering with a viral ribonucleotide reductase. Trends Biochem Sci. 2009;34(1):25-32. Epub 20081105. doi: 10.1016/j.tibs.2008.09.008. PubMed PMID: 18990579.

264. Cheng AZ, Moraes SN, Shaban NM, Fanunza E, Bierle CJ, Southern PJ, Bresnahan WA, Rice SA, Harris RS. APOBECs and Herpesviruses. Viruses. 2021;13(3). Epub 20210228. doi: 10.3390/v13030390. PubMed PMID: 33671095; PMCID: PMC7998176.

265. Shaban NM, Yan R, Shi K, Moraes SN, Cheng AZ, Carpenter MA, McLellan JS, Yu Z, Harris RS. Cryo-EM structure of the EBV ribonucleotide reductase BORF2 and mechanism of APOBEC3B inhibition. Sci Adv. 2022;8(17):eabm2827. Epub 20220427. doi: 10.1126/sciadv.abm2827. PubMed PMID: 35476445; PMCID: PMC9045721.

266. Mocarski ES. Chapter 4: Comparative analysis of herpesvirus-common proteins. In Human Herpesviruses: Biology, Therapy, and Immunoprophylaxis. Ann Arvin GC-F, Edward Mocarski, Patrick S. Moore, Bernard Roizman, Richard Whitley, and Koichi Yamanishi, editor. Cambridge: Cambridge University Press; 2007.

267. West MJ, Lowe AD, Karn J. Activation of human immunodeficiency virus transcription in T cells revisited: NF-kappaB p65 stimulates transcriptional elongation. J Virol. 2001;75(18):8524-37. doi: 10.1128/jvi.75.18.8524-8537.2001. PubMed PMID: 11507198; PMCID: PMC115098.

268. Williams SA, Kwon H, Chen LF, Greene WC. Sustained induction of NF-kappa B is required for efficient expression of latent human immunodeficiency virus type 1. J Virol. 2007;81(11):6043-56. Epub 20070321. doi: 10.1128/jvi.02074-06. PubMed PMID: 17376917; PMCID: PMC1900291.

269. Conant K, Ma M, Nath A, Major EO. Extracellular human immunodeficiency virus type 1 Tat protein is associated with an increase in both NF-kappa B binding and protein kinase C activity in primary human astrocytes. J Virol. 1996;70(3):1384-9. doi: 10.1128/jvi.70.3.1384-1389.1996. PubMed PMID: 8627654; PMCID: PMC189957.

270. Demarchi F, d'Adda di Fagagna F, Falaschi A, Giacca M. Activation of transcription factor NF-kappaB by the Tat protein of human immunodeficiency virus type 1. J Virol. 1996;70(7):4427-37. doi: 10.1128/jvi.70.7.4427-4437.1996. PubMed PMID: 8676466; PMCID: PMC190376.

271. Fenton-May AE, Dibben O, Emmerich T, Ding H, Pfafferott K, Aasa-Chapman MM, Pellegrino P, Williams I, Cohen MS, Gao F, Shaw GM, Hahn BH, Ochsenbauer C, Kappes JC, Borrow P. Relative resistance of HIV-1 founder viruses to control by interferon-alpha. Retrovirology. 2013;10:146. Epub 20131203. doi: 10.1186/1742-4690-10-146. PubMed PMID: 24299076; PMCID: PMC3907080.

272. Davison A. Chapter 2: Comparative analysis of the genomes. In Human Herpesviruses: Biology, Therapy, and Immunoprophylaxis. Ann Arvin GC-F, Edward Mocarski , Patrick S. Moore , Bernard Roizman, Richard Whitley, and Koichi Yamanishi editor. Cambridge: Cambridge University Press; 2007.

273. Bowen NE, Oo A, Kim B. Mechanistic Interplay between HIV-1 Reverse Transcriptase Enzyme Kinetics and Host SAMHD1 Protein: Viral Myeloid-Cell Tropism and Genomic

Mutagenesis. Viruses. 2022;14(8). Epub 20220726. doi: 10.3390/v14081622. PubMed PMID: 35893688; PMCID: PMC9331428.

274. Skasko M, Weiss KK, Reynolds HM, Jamburuthugoda V, Lee K, Kim B. Mechanistic differences in RNA-dependent DNA polymerization and fidelity between murine leukemia virus and HIV-1 reverse transcriptases. J Biol Chem. 2005;280(13):12190-200. Epub 20050110. doi: 10.1074/jbc.M412859200. PubMed PMID: 15644314; PMCID: PMC1752212.

275. Shen R, Richter HE, Smith PD. Early HIV-1 target cells in human vaginal and ectocervical mucosa. Am J Reprod Immunol. 2011;65(3):261-7. Epub 20101201. doi: 10.1111/j.1600-0897.2010.00939.x. PubMed PMID: 21118402; PMCID: PMC3077123.

276. Waki K, Freed EO. Macrophages and Cell-Cell Spread of HIV-1. Viruses. 2010;2(8):1603-20. doi: 10.3390/v2081603. PubMed PMID: 21552427; PMCID: PMC3088113.

277. Gousset K, Ablan SD, Coren LV, Ono A, Soheilian F, Nagashima K, Ott DE, Freed EO. Real-time visualization of HIV-1 GAG trafficking in infected macrophages. PLoS Pathog. 2008;4(3):e1000015. Epub 20080307. doi: 10.1371/journal.ppat.1000015. PubMed PMID: 18369466; PMCID: PMC2267008.

278. Groot F, Welsch S, Sattentau QJ. Efficient HIV-1 transmission from macrophages to T cells across transient virological synapses. Blood. 2008;111(9):4660-3. Epub 20080222. doi: 10.1182/blood-2007-12-130070. PubMed PMID: 18296630.

279. van't Wout AB, Kootstra NA, Mulder-Kampinga GA, Albrecht-van Lent N, Scherpbier HJ, Veenstra J, Boer K, Coutinho RA, Miedema F, Schuitemaker H. Macrophage-tropic variants initiate human immunodeficiency virus type 1 infection after sexual, parenteral, and vertical transmission. J Clin Invest. 1994;94(5):2060-7. doi: 10.1172/jci117560. PubMed PMID: 7962552; PMCID: PMC294642.

280. Connor RI, Sheridan KE, Ceradini D, Choe S, Landau NR. Change in coreceptor use correlates with disease progression in HIV-1--infected individuals. J Exp Med. 1997;185(4):621-8. doi: 10.1084/jem.185.4.621. PubMed PMID: 9034141; PMCID: PMC2196142.

281. Joseph SB, Swanstrom R. The evolution of HIV-1 entry phenotypes as a guide to changing target cells. J Leukoc Biol. 2018;103(3):421-31. Epub 20180201. doi: 10.1002/jlb.2ri0517-200r. PubMed PMID: 29389021.

282. Joseph SB, Swanstrom R, Kashuba AD, Cohen MS. Bottlenecks in HIV-1 transmission: insights from the study of founder viruses. Nat Rev Microbiol. 2015;13(7):414-25. Epub 20150608. doi: 10.1038/nrmicro3471. PubMed PMID: 26052661; PMCID: PMC4793885.

283. Joseph SB, Arrildt KT, Swanstrom AE, Schnell G, Lee B, Hoxie JA, Swanstrom R. Quantification of entry phenotypes of macrophage-tropic HIV-1 across a wide range of CD4 densities. J Virol. 2014;88(4):1858-69. Epub 20131204. doi: 10.1128/jvi.02477-13. PubMed PMID: 24307580; PMCID: PMC3911544.

284. Brumme ZL, Goodrich J, Mayer HB, Brumme CJ, Henrick BM, Wynhoven B, Asselin JJ, Cheung PK, Hogg RS, Montaner JS, Harrigan PR. Molecular and clinical epidemiology of CXCR4-using HIV-1 in a large population of antiretroviral-naive individuals. J Infect Dis. 2005;192(3):466-74. Epub 20050623. doi: 10.1086/431519. PubMed PMID: 15995960.

285. Bleul CC, Wu L, Hoxie JA, Springer TA, Mackay CR. The HIV coreceptors CXCR4 and CCR5 are differentially expressed and regulated on human T lymphocytes. Proc Natl Acad Sci U S A. 1997;94(5):1925-30. doi: 10.1073/pnas.94.5.1925. PubMed PMID: 9050881; PMCID: PMC20019.

286. Parrish NF, Wilen CB, Banks LB, Iyer SS, Pfaff JM, Salazar-Gonzalez JF, Salazar MG, Decker JM, Parrish EH, Berg A, Hopper J, Hora B, Kumar A, Mahlokozera T, Yuan S, Coleman C, Vermeulen M, Ding H, Ochsenbauer C, Tilton JC, Permar SR, Kappes JC, Betts MR, Busch MP, Gao F, Montefiori D, Haynes BF, Shaw GM, Hahn BH, Doms RW. Transmitted/founder and chronic subtype C HIV-1 use CD4 and CCR5 receptors with equal efficiency and are not inhibited by blocking the integrin α4β7. PLoS Pathog. 2012;8(5):e1002686. Epub 20120531. doi: 10.1371/journal.ppat.1002686. PubMed PMID: 22693444; PMCID: PMC3364951.

287. Ping LH, Joseph SB, Anderson JA, Abrahams MR, Salazar-Gonzalez JF, Kincer LP, Treurnicht FK, Arney L, Ojeda S, Zhang M, Keys J, Potter EL, Chu H, Moore P, Salazar MG, Iyer S, Jabara C, Kirchherr J, Mapanje C, Ngandu N, Seoighe C, Hoffman I, Gao F, Tang Y, Labranche C, Lee B, Saville A, Vermeulen M, Fiscus S, Morris L, Karim SA, Haynes BF, Shaw GM, Korber BT, Hahn BH, Cohen MS, Montefiori D, Williamson C, Swanstrom R. Comparison of viral Env proteins from acute and chronic infections with subtype C human immunodeficiency virus type 1 identifies differences in glycosylation and CCR5 utilization and suggests a new strategy for immunogen design. J Virol. 2013;87(13):7218-33. Epub 20130424. doi: 10.1128/jvi.03577-12. PubMed PMID: 23616655; PMCID: PMC3700278.

288. Schnell G, Joseph S, Spudich S, Price RW, Swanstrom R. HIV-1 replication in the central nervous system occurs in two distinct cell types. PLoS Pathog. 2011;7(10):e1002286. Epub 20111006. doi: 10.1371/journal.ppat.1002286. PubMed PMID: 22007152; PMCID: PMC3188520.

289. Sturdevant CB, Joseph SB, Schnell G, Price RW, Swanstrom R, Spudich S. Compartmentalized replication of R5 T cell-tropic HIV-1 in the central nervous system early in the course of infection. PLoS Pathog. 2015;11(3):e1004720. Epub 20150326. doi: 10.1371/journal.ppat.1004720. PubMed PMID: 25811757; PMCID: PMC4374811.

290. Arrildt KT, LaBranche CC, Joseph SB, Dukhovlinova EN, Graham WD, Ping LH, Schnell G, Sturdevant CB, Kincer LP, Mallewa M, Heyderman RS, Rie AV, Cohen MS, Spudich S, Price RW, Montefiori DC, Swanstrom R. Phenotypic Correlates of HIV-1 Macrophage Tropism. J Virol. 2015;89(22):11294-311. Epub 20150902. doi: 10.1128/jvi.00946-15. PubMed PMID: 26339058; PMCID: PMC4645658.

291. Westmoreland SV, Converse AP, Hrecka K, Hurley M, Knight H, Piatak M, Lifson J, Mansfield KG, Skowronski J, Desrosiers RC. SIV vpx is essential for macrophage infection but not for development of AIDS. PLoS One. 2014;9(1):e84463. Epub 20140121. doi: 10.1371/journal.pone.0084463. PubMed PMID: 24465411; PMCID: PMC3897363.

292. Gras G, Kaul M. Molecular mechanisms of neuroinvasion by monocytes-macrophages in HIV-1 infection. Retrovirology. 2010;7:30. Epub 20100407. doi: 10.1186/1742-4690-7-30. PubMed PMID: 20374632; PMCID: PMC2864195.

293. Best BM, Letendre SL, Koopmans P, Rossi SS, Clifford DB, Collier AC, Gelman BB, Marra CM, McArthur JC, McCutchan JA, Morgello S, Simpson DM, Capparelli EV, Ellis RJ, Grant I. Low cerebrospinal fluid concentrations of the nucleotide HIV reverse transcriptase inhibitor, tenofovir. J Acquir Immune Defic Syndr. 2012;59(4):376-81. doi: 10.1097/QAI.0b013e318247ec54. PubMed PMID: 22217676; PMCID: PMC3299895.

294. Koppensteiner H, Brack-Werner R, Schindler M. Macrophages and their relevance in Human Immunodeficiency Virus Type I infection. Retrovirology. 2012;9:82. Epub 20121004. doi: 10.1186/1742-4690-9-82. PubMed PMID: 23035819; PMCID: PMC3484033.

295. Nath A, Clements JE. Eradication of HIV from the brain: reasons for pause. Aids. 2011;25(5):577-80. doi: 10.1097/QAD.0b013e3283437d2f. PubMed PMID: 21160414; PMCID: PMC3681810.

296. Alexaki A, Liu Y, Wigdahl B. Cellular reservoirs of HIV-1 and their role in viral persistence. Curr HIV Res. 2008;6(5):388-400. doi: 10.2174/157016208785861195. PubMed PMID: 18855649; PMCID: PMC2683678.

297. Bednar MM, Hauser BM, Zhou S, Jacobson JM, Eron JJ, Jr., Frank I, Swanstrom R. Diversity and Tropism of HIV-1 Rebound Virus Populations in Plasma Level After Treatment Discontinuation. J Infect Dis. 2016;214(3):403-7. Epub 20160430. doi: 10.1093/infdis/jiw172. PubMed PMID: 27132284; PMCID: PMC4936648.

298. Williams DW, Eugenin EA, Calderon TM, Berman JW. Monocyte maturation, HIV susceptibility, and transmigration across the blood brain barrier are critical in HIV neuropathogenesis. J Leukoc Biol. 2012;91(3):401-15. Epub 20120106. doi: 10.1189/jlb.0811394. PubMed PMID: 22227964; PMCID: PMC3289493.

299. Williams KC, Hickey WF. Central nervous system damage, monocytes and macrophages, and neurological disorders in AIDS. Annu Rev Neurosci. 2002;25:537-62. Epub 2002/06/08. doi: 10.1146/annurev.neuro.25.112701.142822. PubMed PMID: 12052920.

300. Antinori A, Arendt G, Becker JT, Brew BJ, Byrd DA, Cherner M, Clifford DB, Cinque P, Epstein LG, Goodkin K, Gisslen M, Grant I, Heaton RK, Joseph J, Marder K, Marra CM, McArthur JC, Nunn M, Price RW, Pulliam L, Robertson KR, Sacktor N, Valcour V, Wojna VE. Updated research nosology for HIV-associated neurocognitive disorders. Neurology. 2007;69(18):1789-99. Epub 20071003. doi: 10.1212/01.WNL.0000287431.88658.8b. PubMed PMID: 17914061; PMCID: PMC4472366.

301. Boissé L, Gill MJ, Power C. HIV infection of the central nervous system: clinical features and neuropathogenesis. Neurol Clin. 2008;26(3):799-819, x. doi: 10.1016/j.ncl.2008.04.002. PubMed PMID: 18657727.

302. McArthur JC, Steiner J, Sacktor N, Nath A. Human immunodeficiency virus-associated neurocognitive disorders: Mind the gap. Ann Neurol. 2010;67(6):699-714. doi: 10.1002/ana.22053. PubMed PMID: 20517932.

303. Cromer D, Schlub TE, Smyth RP, Grimm AJ, Chopra A, Mallal S, Davenport MP, Mak J. HIV-1 Mutation and Recombination Rates Are Different in Macrophages and T-cells. Viruses. 2016;8(4):118. Epub 20160422. doi: 10.3390/v8040118. PubMed PMID: 27110814; PMCID: PMC4848610.

304. Nguyen LA, Kim DH, Daly MB, Allan KC, Kim B. Host SAMHD1 protein promotes HIV-1 recombination in macrophages. J Biol Chem. 2014;289(5):2489-96. Epub 20131218. doi: 10.1074/jbc.C113.522326. PubMed PMID: 24352659; PMCID: PMC3908385.

305. Hu WS, Temin HM. Genetic consequences of packaging two RNA genomes in one retroviral particle: pseudodiploidy and high rate of genetic recombination. Proc Natl Acad Sci U S A. 1990;87(4):1556-60. doi: 10.1073/pnas.87.4.1556. PubMed PMID: 2304918; PMCID: PMC53514.

306. Hu WS, Temin HM. Retroviral recombination and reverse transcription. Science. 1990;250(4985):1227-33. doi: 10.1126/science.1700865. PubMed PMID: 1700865.

307. Aird KM, Zhang R. Nucleotide metabolism, oncogene-induced senescence and cancer. Cancer Lett. 2015;356(2 Pt A):204-10. Epub 20140129. doi: 10.1016/j.canlet.2014.01.017. PubMed PMID: 24486217; PMCID: PMC4115046.

308. Vander Heiden MG, DeBerardinis RJ. Understanding the Intersections between Metabolism and Cancer Biology. Cell. 2017;168(4):657-69. doi: 10.1016/j.cell.2016.12.039. PubMed PMID: 28187287; PMCID: PMC5329766.

309. Buj R, Aird KM. Deoxyribonucleotide Triphosphate Metabolism in Cancer and Metabolic Disease. Front Endocrinol (Lausanne). 2018;9:177. Epub 20180418. doi: 10.3389/fendo.2018.00177. PubMed PMID: 29720963; PMCID: PMC5915462.

310. Madden SK, de Araujo AD, Gerhardt M, Fairlie DP, Mason JM. Taking the Myc out of cancer: toward therapeutic strategies to directly inhibit c-Myc. Mol Cancer. 2021;20(1):3. Epub 20210104. doi: 10.1186/s12943-020-01291-6. PubMed PMID: 33397405; PMCID: PMC7780693.

311. Cunningham JT, Moreno MV, Lodi A, Ronen SM, Ruggero D. Protein and nucleotide biosynthesis are coupled by a single rate-limiting enzyme, PRPS2, to drive cancer. Cell. 2014;157(5):1088-103. doi: 10.1016/j.cell.2014.03.052. PubMed PMID: 24855946; PMCID: PMC4140650.

312. Mannava S, Grachtchouk V, Wheeler LJ, Im M, Zhuang D, Slavina EG, Mathews CK, Shewach DS, Nikiforov MA. Direct role of nucleotide metabolism in C-MYC-dependent proliferation of melanoma cells. Cell Cycle. 2008;7(15):2392-400. Epub 20080603. doi: 10.4161/cc.6390. PubMed PMID: 18677108; PMCID: PMC3744895.

313. Eberhardy SR, Farnham PJ. c-Myc mediates activation of the cad promoter via a post-RNA polymerase II recruitment mechanism. J Biol Chem. 2001;276(51):48562-71. Epub 20011022. doi: 10.1074/jbc.M109014200. PubMed PMID: 11673469.

314. Baugh EH, Ke H, Levine AJ, Bonneau RA, Chan CS. Why are there hotspot mutations in the TP53 gene in human cancers? Cell Death Differ. 2018;25(1):154-60. Epub 20171103. doi: 10.1038/cdd.2017.180. PubMed PMID: 29099487; PMCID: PMC5729536.

315. Ozaki T, Nakagawara A. Role of p53 in Cell Death and Human Cancers. Cancers (Basel). 2011;3(1):994-1013. Epub 20110303. doi: 10.3390/cancers3010994. PubMed PMID: 24212651; PMCID: PMC3756401.

316. Kollareddy M, Dimitrova E, Vallabhaneni KC, Chan A, Le T, Chauhan KM, Carrero ZI, Ramakrishnan G, Watabe K, Haupt Y, Haupt S, Pochampally R, Boss GR, Romero DG,

Radu CG, Martinez LA. Regulation of nucleotide metabolism by mutant p53 contributes to its gain-of-function activities. Nat Commun. 2015;6:7389. Epub 20150612. doi: 10.1038/ncomms8389. PubMed PMID: 26067754; PMCID: PMC4467467.

317. Sherr CJ, McCormick F. The RB and p53 pathways in cancer. Cancer Cell. 2002;2(2):103-12. doi: 10.1016/s1535-6108(02)00102-2. PubMed PMID: 12204530.

318. Fang Z, Lin M, Li C, Liu H, Gong C. A comprehensive review of the roles of E2F1 in colon cancer. Am J Cancer Res. 2020;10(3):757-68. Epub 20200301. PubMed PMID: 32266089; PMCID: PMC7136928.

319. Rahman L, Voeller D, Rahman M, Lipkowitz S, Allegra C, Barrett JC, Kaye FJ, Zajac-Kaye M. Thymidylate synthase as an oncogene: a novel role for an essential DNA synthesis enzyme. Cancer Cell. 2004;5(4):341-51. doi: 10.1016/s1535-6108(04)00080-7. PubMed PMID: 15093541.

320. Good L, Dimri GP, Campisi J, Chen KY. Regulation of dihydrofolate reductase gene expression and E2F components in human diploid fibroblasts during growth and senescence. J Cell Physiol. 1996;168(3):580-8. doi: 10.1002/(sici)1097-4652(199609)168:3<580::Aid-jcp10>3.0.Co;2-3. PubMed PMID: 8816912.

321. Bailey SW, Ayling JE. The extremely slow and variable activity of dihydrofolate reductase in human liver and its implications for high folic acid intake. Proc Natl Acad Sci U S A. 2009;106(36):15424-9. Epub 20090824. doi: 10.1073/pnas.0902072106. PubMed PMID: 19706381; PMCID: PMC2730961.

322. Bitter EE, Townsend MH, Erickson R, Allen C, O'Neill KL. Thymidine kinase 1 through the ages: a comprehensive review. Cell Biosci. 2020;10(1):138. Epub 20201127. doi: 10.1186/s13578-020-00493-1. PubMed PMID: 33292474; PMCID: PMC7694900.

323. Millis SZ, Ikeda S, Reddy S, Gatalica Z, Kurzrock R. Landscape of Phosphatidylinositol-3-Kinase Pathway Alterations Across 19 784 Diverse Solid Tumors. JAMA Oncol. 2016;2(12):1565-73. doi: 10.1001/jamaoncol.2016.0891. PubMed PMID: 27388585.

324. Ben-Sahra I, Howell JJ, Asara JM, Manning BD. Stimulation of de novo pyrimidine synthesis by growth signaling through mTOR and S6K1. Science. 2013;339(6125):1323-8. Epub 20130221. doi: 10.1126/science.1228792. PubMed PMID: 23429703; PMCID: PMC3753690.

325. Ben-Sahra I, Hoxhaj G, Ricoult SJH, Asara JM, Manning BD. mTORC1 induces purine synthesis through control of the mitochondrial tetrahydrofolate cycle. Science. 2016;351(6274):728-33. doi: 10.1126/science.aad0489. PubMed PMID: 26912861; PMCID: PMC4786372.

326. Tian L, Chen C, Guo Y, Zhang F, Mi J, Feng Q, Lin S, Xi N, Tian J, Yu L, Chen Y, Cao M, Lai C, Fan J, Zhang Y, Chen G. mTORC2 regulates ribonucleotide reductase to promote DNA replication and gemcitabine resistance in non-small cell lung cancer. Neoplasia. 2021;23(7):643-52. Epub 20210611. doi: 10.1016/j.neo.2021.05.007. PubMed PMID: 34126361; PMCID: PMC8215139.

327. Xu X, Page JL, Surtees JA, Liu H, Lagedrost S, Lu Y, Bronson R, Alani E, Nikitin AY, Weiss RS. Broad overexpression of ribonucleotide reductase genes in mice specifically

induces lung neoplasms. Cancer Res. 2008;68(8):2652-60. doi: 10.1158/0008-5472.Can-07-5873. PubMed PMID: 18413732; PMCID: PMC2459241.

328. Fan H, Villegas C, Wright JA. Ribonucleotide reductase R2 component is a novel malignancy determinant that cooperates with activated oncogenes to determine transformation and malignant potential. Proc Natl Acad Sci U S A. 1996;93(24):14036-40. doi: 10.1073/pnas.93.24.14036. PubMed PMID: 8943056; PMCID: PMC19490.

329. Dressman HK, Hans C, Bild A, Olson JA, Rosen E, Marcom PK, Liotcheva VB, Jones EL, Vujaskovic Z, Marks J, Dewhirst MW, West M, Nevins JR, Blackwell K. Gene expression profiles of multiple breast cancer phenotypes and response to neoadjuvant chemotherapy. Clin Cancer Res. 2006;12(3 Pt 1):819-26. doi: 10.1158/1078-0432.Ccr-05-1447. PubMed PMID: 16467094.

330. Fujita H, Ohuchida K, Mizumoto K, Itaba S, Ito T, Nakata K, Yu J, Kayashima T, Souzaki R, Tajiri T, Manabe T, Ohtsuka T, Tanaka M. Gene expression levels as predictive markers of outcome in pancreatic cancer after gemcitabine-based adjuvant chemotherapy. Neoplasia. 2010;12(10):807-17. doi: 10.1593/neo.10458. PubMed PMID: 20927319; PMCID: PMC2950330.

331. Liu X, Zhou B, Xue L, Yen F, Chu P, Un F, Yen Y. Ribonucleotide reductase subunits M2 and p53R2 are potential biomarkers for metastasis of colon cancer. Clin Colorectal Cancer. 2007;6(5):374-81. doi: 10.3816/CCC.2007.n.007. PubMed PMID: 17311703.

332. Schott K, Majer C, Bulashevska A, Childs L, Schmidt MHH, Rajalingam K, Munder M, König R. SAMHD1 in cancer: curse or cure? J Mol Med (Berl). 2022;100(3):351-72. Epub 20210904. doi: 10.1007/s00109-021-02131-w. PubMed PMID: 34480199; PMCID: PMC8843919.

333. Karran P, Attard N. Thiopurines in current medical practice: molecular mechanisms and contributions to therapy-related cancer. Nat Rev Cancer. 2008;8(1):24-36. doi: 10.1038/nrc2292. PubMed PMID: 18097462.

334. Sullivan RD, Miller E, Sikes MP. Antimetabolite-metabolite combination cancer chemotherapy. Effects of intraarterial methotrexate-intramuscular Citrovorum factor therapy in human cancer. Cancer. 1959;12:1248-62. doi: 10.1002/1097-0142(195911/12)12:6<1248::aid-cncr2820120619>3.0.co;2-2. PubMed PMID: 13835650.

335. Rich TA, Shepard RC, Mosley ST. Four decades of continuing innovation with fluorouracil: current and future approaches to fluorouracil chemoradiation therapy. J Clin Oncol. 2004;22(11):2214-32. doi: 10.1200/jco.2004.08.009. PubMed PMID: 15169811.

336. Ben-Josef E, Normolle D, Ensminger WD, Walker S, Tatro D, Ten Haken RK, Knol J, Dawson LA, Pan C, Lawrence TS. Phase II trial of high-dose conformal radiation therapy with concurrent hepatic artery floxuridine for unresectable intrahepatic malignancies. J Clin Oncol. 2005;23(34):8739-47. doi: 10.1200/jco.2005.01.5354. PubMed PMID: 16314634.

337. Walko CM, Lindley C. Capecitabine: a review. Clin Ther. 2005;27(1):23-44. doi: 10.1016/j.clinthera.2005.01.005. PubMed PMID: 15763604.

338. Rollins KD, Lindley C. Pemetrexed: a multitargeted antifolate. Clin Ther. 2005;27(9):1343-82. doi: 10.1016/j.clinthera.2005.09.010. PubMed PMID: 16291410.

339. Herling CD, Coombes KR, Benner A, Bloehdorn J, Barron LL, Abrams ZB, Majewski T, Bondaruk JE, Bahlo J, Fischer K, Hallek M, Stilgenbauer S, Czerniak BA, Oakes CC, Ferrajoli A, Keating MJ, Abruzzo LV. Time-to-progression after front-line fludarabine, cyclophosphamide, and rituximab chemoimmunotherapy for chronic lymphocytic leukaemia: a retrospective, multicohort study. Lancet Oncol. 2019;20(11):1576-86. Epub 20190930. doi: 10.1016/s1470-2045(19)30503-0. PubMed PMID: 31582354; PMCID: PMC7147008.

340. Juliusson G, Christiansen I, Hansen MM, Johnson S, Kimby E, Elmhorn-Rosenborg A, Liliemark J. Oral cladribine as primary therapy for patients with B-cell chronic lymphocytic leukemia. J Clin Oncol. 1996;14(7):2160-6. doi: 10.1200/jco.1996.14.7.2160. PubMed PMID: 8683250.

341. Faderl S, Wetzler M, Rizzieri D, Schiller G, Jagasia M, Stuart R, Ganguly S, Avigan D, Craig M, Collins R, Maris M, Kovacsovics T, Goldberg S, Seiter K, Hari P, Greiner J, Vey N, Recher C, Ravandi F, Wang ES, Vasconcelles M, Huebner D, Kantarjian HM. Clofarabine plus cytarabine compared with cytarabine alone in older patients with relapsed or refractory acute myelogenous leukemia: results from the CLASSIC I Trial. J Clin Oncol. 2012;30(20):2492-9. Epub 20120514. doi: 10.1200/jco.2011.37.9743. PubMed PMID: 22585697; PMCID: PMC4874149.

342. Earl HM, Hiller L, Howard HC, Dunn JA, Young J, Bowden SJ, McDermaid M, Waterhouse AK, Wilson G, Agrawal R, O'Reilly S, Bowman A, Ritchie DM, Goodman A, Hickish T, McAdam K, Cameron D, Dodwell D, Rea DW, Caldas C, Provenzano E, Abraham JE, Canney P, Crown JP, Kennedy MJ, Coleman R, Leonard RC, Carmichael JA, Wardley AM, Poole CJ. Addition of gemcitabine to paclitaxel, epirubicin, and cyclophosphamide adjuvant chemotherapy for women with early-stage breast cancer (tAnGo): final 10-year follow-up of an open-label, randomised, phase 3 trial. Lancet Oncol. 2017;18(6):755-69. Epub 20170504. doi: 10.1016/s1470-2045(17)30319-4. PubMed PMID: 28479233.

343. Lorusso D, Di Stefano A, Fanfani F, Scambia G. Role of gemcitabine in ovarian cancer treatment. Ann Oncol. 2006;17 Suppl 5:v188-94. doi: 10.1093/annonc/mdj979. PubMed PMID: 16807454.

344. Hayashi H, Kurata T, Nakagawa K. Gemcitabine: efficacy in the treatment of advanced stage nonsquamous non-small cell lung cancer. Clin Med Insights Oncol. 2011;5:177-84. Epub 20110529. doi: 10.4137/cmo.S6252. PubMed PMID: 21695043; PMCID: PMC3117632.

345. Stathopoulos GP, Syrigos K, Polyzos A, Fountzilas G, Rigatos SK, Ziras N, Potamiannou A, Tsiakopoulos I, Androulakis N, Aravantinos G, Athanasiadis A, Papakotoulas P, Georgoulias V. Front-line treatment of inoperable or metastatic pancreatic cancer with gemcitabine and capecitabine: an intergroup, multicenter, phase II study. Ann Oncol. 2004;15(2):224-9. doi: 10.1093/annonc/mdh065. PubMed PMID: 14760113.

346. Magaway C, Kim E, Jacinto E. Targeting mTOR and Metabolism in Cancer: Lessons and Innovations. Cells. 2019;8(12). Epub 20191206. doi: 10.3390/cells8121584. PubMed PMID: 31817676; PMCID: PMC6952948.

347. Xie Y, Wang Y, Xu Z, Lu Y, Song D, Gao L, Yu D, Li B, Chen G, Zhang H, Feng Q, Zhang Y, Hu K, Huang C, Peng Y, Wu X, Mao Z, Shao J, Zhu W, Shi J. Preclinical validation and phase I trial of 4-hydroxysalicylanilide, targeting ribonucleotide reductase mediated dNTP synthesis in multiple myeloma. J Biomed Sci. 2022;29(1):32. Epub 20220512. doi: 10.1186/s12929-022-00813-2. PubMed PMID: 35546402; PMCID: PMC9097096.

348. Banerjee S, Michalarea V, Ang JE, Ingles Garces A, Biondo A, Funingana IG, Little M, Ruddle R, Raynaud F, Riisnaes R, Gurel B, Chua S, Tunariu N, Porter JC, Prout T, Parmar M, Zachariou A, Turner A, Jenkins B, McIntosh S, Ainscow E, Minchom A, Lopez J, de Bono J, Jones R, Hall E, Cook N, Basu B, Banerji U. A Phase I Trial of CT900, a Novel α-Folate Receptor-Mediated Thymidylate Synthase Inhibitor, in Patients with Solid Tumors with Expansion Cohorts in Patients with High-Grade Serous Ovarian Cancer. Clin Cancer Res. 2022;28(21):4634-41. doi: 10.1158/1078-0432.Ccr-22-1268. PubMed PMID: 35984704; PMCID: PMC9623233.

349. Felip E, Gutiérrez-Chamorro L, Gómez M, Garcia-Vidal E, Romeo M, Morán T, Layos L, Pérez-Roca L, Riveira-Muñoz E, Clotet B, Fernandez PL, Mesía R, Martínez-Cardús A, Ballana E, Margelí M. Modulation of DNA Damage Response by SAM and HD Domain Containing Deoxynucleoside Triphosphate Triphosphohydrolase (SAMHD1) Determines Prognosis and Treatment Efficacy in Different Solid Tumor Types. Cancers (Basel). 2022;14(3). Epub 20220127. doi: 10.3390/cancers14030641. PubMed PMID: 35158911; PMCID: PMC8833711.

350. Woods D, Turchi JJ. Chemotherapy induced DNA damage response: convergence of drugs and pathways. Cancer Biol Ther. 2013;14(5):379-89. Epub 20130204. doi: 10.4161/cbt.23761. PubMed PMID: 23380594; PMCID: PMC3672181.

351. Schuh A, Becq J, Humphray S, Alexa A, Burns A, Clifford R, Feller SM, Grocock R, Henderson S, Khrebtukova I, Kingsbury Z, Luo S, McBride D, Murray L, Menju T, Timbs A, Ross M, Taylor J, Bentley D. Monitoring chronic lymphocytic leukemia progression by whole genome sequencing reveals heterogeneous clonal evolution patterns. Blood. 2012;120(20):4191-6. Epub 2012/08/24. doi: 10.1182/blood-2012-05-433540. PubMed PMID: 22915640.

352. Guieze R, Robbe P, Clifford R, de Guibert S, Pereira B, Timbs A, Dilhuydy MS, Cabes M, Ysebaert L, Burns A, Nguyen-Khac F, Davi F, Veronese L, Combes P, Le Garff-Tavernier M, Leblond V, Merle-Beral H, Alsolami R, Hamblin A, Mason J, Pettitt A, Hillmen P, Taylor J, Knight SJ, Tournilhac O, Schuh A. Presence of multiple recurrent mutations confers poor trial outcome of relapsed/refractory CLL. Blood. 2015;126(18):2110-7. Epub 2015/09/01. doi: 10.1182/blood-2015-05-647578. PubMed PMID: 26316624.

353. Burns A, Alsolami R, Becq J, Stamatopoulos B, Timbs A, Bruce D, Robbe P, Vavoulis D, Clifford R, Cabes M, Dreau H, Taylor J, Knight SJL, Mansson R, Bentley D, Beekman R, Martín-Subero JI, Campo E, Houlston RS, Ridout KE, Schuh A. Whole-genome sequencing of chronic lymphocytic leukaemia reveals distinct differences in the mutational landscape between IgHV(mut) and IgHV(unmut) subgroups. Leukemia. 2018;32(2):332-42. Epub 20170606. doi: 10.1038/leu.2017.177. PubMed PMID: 28584254; PMCID: PMC5808074.

354. Wu Y, Niu Y, Wu Y, Chen X, Shen X, Gao W. SAMHD1 can suppress lung adenocarcinoma progression through the negative regulation of STING. J Thorac Dis. 2021;13(1):189-201. doi: 10.21037/jtd-20-1889. PubMed PMID: 33569199; PMCID: PMC7867844.

355. Chen W, Cheng P, Jiang J, Ren Y, Wu D, Xue D. Epigenomic and genomic analysis of transcriptome modulation in skin cutaneous melanoma. Aging (Albany NY). 2020;12(13):12703-25. Epub 20200707. doi: 10.18632/aging.103115. PubMed PMID: 32639949; PMCID: PMC7377867.

356. Baylin SB, Jones PA. A decade of exploring the cancer epigenome - biological and translational implications. Nat Rev Cancer. 2011;11(10):726-34. Epub 20110923. doi: 10.1038/nrc3130. PubMed PMID: 21941284; PMCID: PMC3307543.

357. Pon JR, Marra MA. Driver and passenger mutations in cancer. Annu Rev Pathol. 2015;10:25-50. Epub 20141017. doi: 10.1146/annurev-pathol-012414-040312. PubMed PMID: 25340638.

358. Landau DA, Carter SL, Stojanov P, McKenna A, Stevenson K, Lawrence MS, Sougnez C, Stewart C, Sivachenko A, Wang L, Wan Y, Zhang W, Shukla SA, Vartanov A, Fernandes SM, Saksena G, Cibulskis K, Tesar B, Gabriel S, Hacohen N, Meyerson M, Lander ES, Neuberg D, Brown JR, Getz G, Wu CJ. Evolution and impact of subclonal mutations in chronic lymphocytic leukemia. Cell. 2013;152(4):714-26. doi: 10.1016/j.cell.2013.01.019. PubMed PMID: 23415222; PMCID: PMC3575604.

359. Castro-Giner F, Ratcliffe P, Tomlinson I. The mini-driver model of polygenic cancer evolution. Nat Rev Cancer. 2015;15(11):680-5. Epub 20151012. doi: 10.1038/nrc3999. PubMed PMID: 26456849.